Novel Tridentate N,S,N-Metal Compounds of Zinc, Germanium and Phosphorus

John Lortie, BSc

Chemistry

Supervisor: Dr. G. Nikonov

Department of Chemistry

Faculty of Mathematics and Science

Brock University

St. Catharines, Ontario

Thesis submitted in partial requirement for the

degree of Master of Science

Abstract

A novel ligand based on a flexible NSN tridentate framework, and main group compounds of the general formula M(NSN) were prepared on zinc, germanium, and phosphorus. The compound ZnNSN(dimethylaminopyridine) (**III-45a**) is fluxional with **III-46a** in tetrahydrofuran, and its exchange parameters were calculated from NMR measurements. An X-ray structure was obtained for GeNSN (**III-47a**) crystals isolated from diethylether and exhibits an envelope-like geometry with coordination of the soft sulfur donor to the germanium centre. **III-47a** was not reactive with CH_3I but showed reactivity with 3,6-di-*tert*-butyl-o-benzoquinone. ClPNSN (**III-53**) was prepared both by transmetallation of **III-46a** and by a reaction of an *in situ* generated Li_2NSN and PCl_3. HPNSN (**III-52**) was prepared by halogen exchange of **III-53** and L-selectride.

Acknowledgements

First and foremost, my most sincere appreciation goes to my supervisor Dr. Georgii Nikonov who has been a monumental influence on me. His passion and excitement for research is inspiring, and I am grateful for being fortunate enough to work with such a creative and innovative professor over the past several years. Thank you for your patience, and for providing an environment which fosters creativity and the opportunity to grow.

Thank you to my committee members Dr. Martin Lemaire, Dr. Art Van der Est, and Dr. John Corrigan from Western for their time and valuable feedback in the preparation of this dissertation. Also, the support by the excellent staff at Brock, including Jennifer Roberts, Marie Harris, Irene Palumbo, Alison Moffat, glassblower Jordan Vandenhoff, and technical assistance for NMR experiments by Razvan Simionescu have been invaluable for bringing this project to fruition.

I must also thank my friends and colleagues whom I was fortunate to spend time with in the Nikonov group. Thank you to Dr. Van Hung Mai, Dr. Terry Chu, Dr. Minh Tho Nguyen, and Dr. Iryna Alshakova for demonstrating true excellence, and to Josh Clarke, Jan-Willem Lamberink, Joseph Cartwright, Anton Dmitrienko, Aisha Kassymbek, Aliona Baradzenka, Brandon Corbett, and Billy Petrushko for all your encouragement and the great times together. It was a pleasure to learn alongside such talented researchers. Acknowledgements extend to the other graduate students in the chemistry department, especially to the groups of Drs. Dudding, Metallinos, Hudlicky, Lemaire, Yan, Atkinson, Zelisko and Pilkington for their friendship over the years.

Thank you to my girlfriend Jen who has been with me through long nights of writing and drinking too much coffee, and for our relaxing evenings out which also often involved winding up

at that same coffee shop. Her ambition is as contagious as her laughter, and I can always count on her positivity to brighten up a room. I could not have asked for a better partner and I am excited for our future together.

Finally, I could have not accomplished this without my family. I will forever be in their debt for the sacrifices made which helped me reach this point. To my mom and grandma, thank you for your continuous love and support throughout my entire education, even during difficult times and when it required moving away. I would like to thank my dad and the rest of my family for their support and encouragement in my decision to pursue further education. I hope that I have made my late Papa and all of you proud.

Table of Contents

List of Schemes

List of Figures

List of Abbreviations

{^{1}H}	Proton-Decoupled
1-D	One-Dimensional
2-D	Two-Dimensional
aAAc	Acylic Alkyl Amino Carbene
acac	Acetylacetonate
ADPnO	3,7-Di-Tert.-Butyl-5-Aza-2,8-Dioxa-1-(Pnictogen)Bicyclo[3.3.0]Octa-2,4,6-Triene
ADPO	3,7-Di-Tert.-Butyl-5-Aza-2,8-Dioxa-1-Phosphabicyclo[3.3.0]Octa-2,4,6-Triene
Ar	Aromatic
Bn	Benzyl
Bu	Butyl
cAAC	Cyclic Alkyl Amino Carbene
Cp*	Pentamethylcyclopentadienyl
CV	Cyclic Voltammetry
DABCO	1,4-Diazabicyclo[2.2.2]Octane
DCM	Dichloromethane
DEPT	Distortionless Enhancement By Polarization Transfer
DFT	Density Functional Theory
DIPP	2,6-Diisopropylphenyl
DMAP	4-Dimethylaminopyridine
DMEDA	N,N-Dimethylethylenediamine
DMF	N,N-Dimethylformamide
E	Electrophile
e-	Electron
EPR	Electron Paramagnetic Resonance
Et	Ethyl

ET	Electron Transfer
Et_2O	Diethylether
eV	Electron Volt
EXSY	Exchange Spectroscopy
FLP	Frustrated Lewis Pair
HBPin	Pinacolborane
HMBC	Heteronuclear Multiple Bond Correlation
HOMO	Highest Occupied Molecular Orbital
HSQC	Heteronuclear Single Quantum Coherence
HSQCed	Heteronuclear Single Quantum Coherence - Edited
IDipp	1,3-Bis-(2,6-Diisopropylphenyl)-Imidazol-2-Ylidene
*i*Pr	Isopropyl
ItBu	1,3-Bis-(Tert-Butyl)-Imidazol-2-Ylidene
KHMDS	Potassium Bis(Trimethylsilyl)Amide
L	Two-Electron Donor Ligand
LDA	Lithium Diisopropylamide
LUMO	Lowest Unoccupied Molecular Orbital
m	Meta
Me	Methyl
MeCN	Acetonitrile
Mes	Mesityl
n	Normal
NAcNAc	β-Diketiminate (Nitrogen Analogue Of Acetylacetonate Ligand)
$NAcNAcAl^{I}$	NAcNAc = $[ArNC(Me)CHC(Me)NAr]^{-}$, where Ar = 2,6-*i*$Pr_2(C_6H_3)$
NHC	N-Heterocyclic Carbene
NHGe	N-Heterocyclic Germylene
NMR	Nuclear Magnetic Resonance
NOE	Nuclear Overhauser Effect

o	Ortho
OTf	Triflate
p	Para
Pd/C	Palladium On Carbon
Ph	Phenyl
ppm	Parts Per Million
Pr	Propyl
p-tol	Para-Tolyl
pTsOH	Para-Toluene Sulfonic Acid
py	Pyridine
RT	Room Temperature
S	Spin
SET	Single Electron Transfer
SIMes	1,3-Bis(2,4,6-Trimethylphenyl)Imidazolidin-2-Ylidene
t	Tertiary
TEMPO	(2,2,6,6-Tetramethylpiperidin-1-Yl)Oxyl
Tf_2O	Triflic Anhydride
THF	Tetrahydrofuran
VT	Variable Temperature
X	Single-Electron Donor Ligand
α	Alpha
β	Beta
Δ	Delta
δ	Sigma
$\Delta H^{\ddagger}$	Activation Enthalpy
$\Delta S^{\ddagger}$	Activation Entropy
π	Pi
π*	Pi Antibonding

σ	Sigma
σ*	Sigma Antibonding

I. Introduction

Transition metal complexes have been utilized for activations of small molecules for decades but unfortunately are often quite expensive and toxic. Alternatively, solutions can be found within the developments of main group chemistry, due to the high abundance and thus lower costs of main group metals, and their often relatively more benign nature (this is not always the case, as there is no "general toxicity" for an element, but rather toxicities depend on factors such as the oxidation state or ligands bound to a metal complex[1]). The development of main group compounds amenable to activations of small molecules and the cleavage of strong bonds is very important and has been rapidly advancing in recent years. Since Spikes, Fettinger, & Power presented the first example of hydrogen activation facilitated by a germanium analogue of an alkyne (**I-1**) at ambient conditions in 2005 (Scheme 1), our understanding of how to manipulate reactive main group compounds has developed extensively.[2] This example relies on heavier group 14 analogues of alkenes and alkynes, which show increased distortions from linear to trans-bent, and that either one or two of the π bonds (respectively) are converted into non-bonding pairs of electrons.[3,4] From an orbital perspective, this ambiphilic (containing both donor and acceptor) character resembles carbenoids and transition metals.

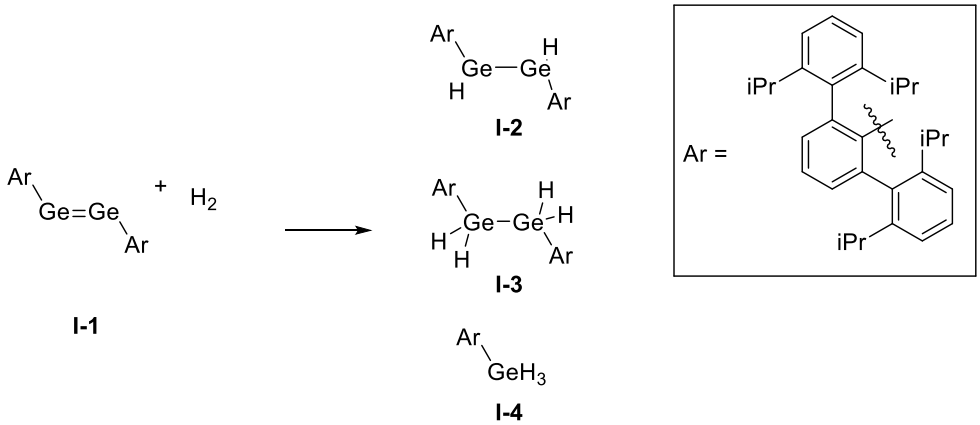

Scheme 1. Activation of dihydrogen by a germanium analogue of an alkyne.

Today, there are examples of compounds from groups 2, 13, and 14 which are capable of activation of H_2, and there are even more examples across the periodic table capable of activating other sigma bonds. Nevertheless, examples are still limited and reactivity can stand to be improved.[5]

Another intriguing avenue in main group chemistry is the development of new nucleophilic species, akin to Grignard and related metal alkyl and aryl reagents, which may find utility in cross coupling reactions. Organozinc reagents were among the first organometallic reagents to be discovered and have been known since the mid 1800's to be useful in alkylation reactions[6,7]. They are pyrophoric for small R groups but are notably less reactive than the alternative Grignard or organolithium reagents. This makes their application slightly easier, as milder conditions may be used, but also comes at the expense of requiring stoichiometric amounts of reagent. This problem may be alleviated if the organozinc reagent can be regenerated *in situ* by a simple, yet non-trivial procedure. Unfortunately, preparations of organozinc reagents typically require an activated form of zinc, such as a zinc-copper couple alloy, or the reduction of $ZnCl_2$ by an alkali metal to react with an alkyl halide. Alternatively, inactivated zinc species such as $ZnCl_2$ should require the use of highly reactive organolithium reagents. Since the motivation was to use less reactive reagents, regeneration of organozincs under these conditions in the presence of other sensitive functionalities would be problematic. Instead, if a zinc compound were able to activate a C-X bond to produce an organozincate, it may be possible to extend this application to coupling reactions if cleavage of the Zn-C bond was facile enough.

Both issues above may be addressed by the application of a non-innocent ligand to a main group compound. A non-innocent ligand is one which is either capable of stabilizing multiple oxidation states by an internal charge compensation or distribution, or may participate by

transferring or accepting an atom or a group.[8] A redox active ligand may affect the Lewis acidity or basicity of the metal, stabilize various oxidation states by functioning as an electron reservoir, or it may participate in outer sphere mechanisms[9]. Milstein described this theme as metal-ligand cooperation. In a broad sense, these are compounds which either bear a redox-active ligand, contain non-coordinated Lewis bases which behave similarly to frustrated Lewis pairs, and/or ligands whose role in catalysis is their lability and ability to create a coordinatively unsaturated reactive intermediate.[10] Complexes bearing non-innocent ligands thus may have an enhanced ability to undergo oxidative additions and the reverse, reductive eliminations, or participate in ring opening and expansions.[11]

Finally, whereas classic examples of Lewis acid catalysts of aluminum, boron and zinc (e.g. Friedel-Crafts alkylation and acylation with $AlCl_3$ and $ZnCl_2$) have been used for decades, inversion of their polarity of these main group centres, such that they become nucleophilic, would have massive repercussions in main group chemistry. In 2006, an anionic boron-based nucleophile (**I-5**) by Segawa, Yamashita, and Nozaki was reported[12], but an aluminum analogue (**I-8**)was not prepared until 2018 by Aldridge and coworkers (Scheme 2). The aluminyl anion **I-8** was stabilized by a bulky, dianionic NON-tridentate ligand based on a dimethyl-xanthene derivative at ambient temperature. These precedents suggest that other bulky, dianionic tridentate pincer ligands may be successful in stabilization of anionic main group species, which may then be envisioned to be effective for main group catalyzed reactions.

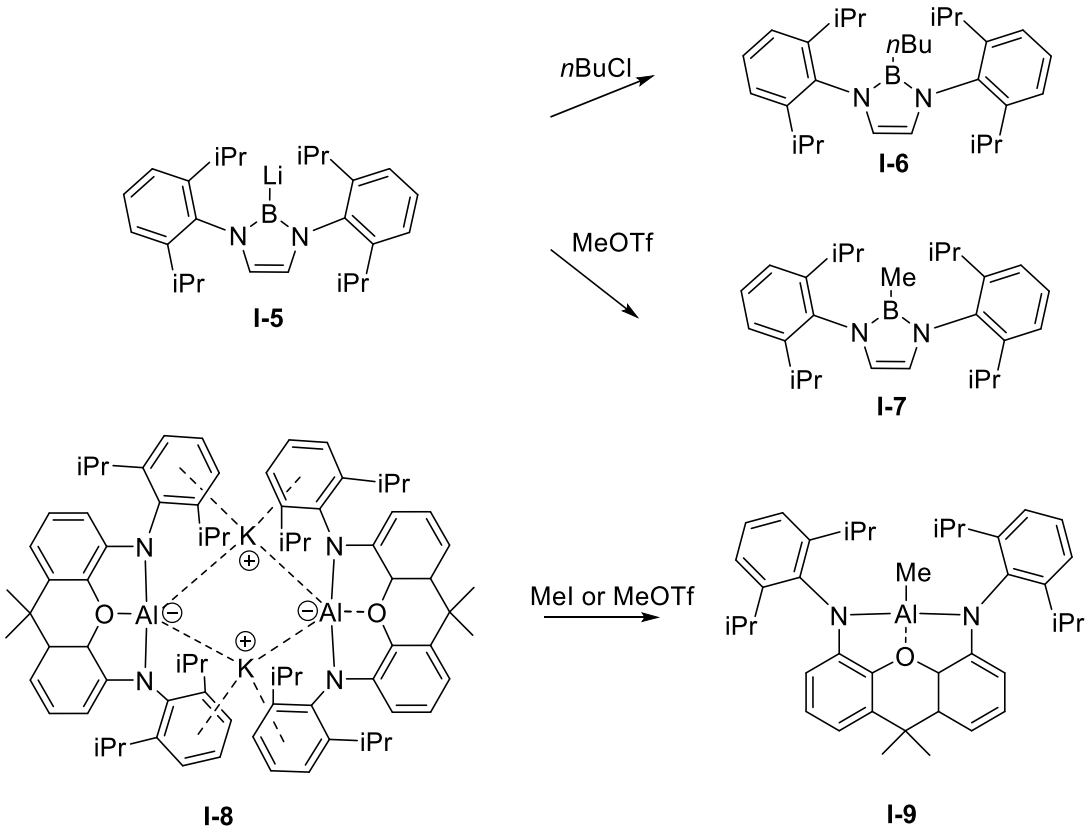

Scheme 2. First examples of boryl anion and aluminyl anions and reactions.[12,13]

This aim of this research was to enabling unique reactivity modes (such as C-X bond activation and function as a cross-coupling catalyst) with an anionic zinc compound stabilized by a non-innocent ligand, and for enabling/comparing reactivity of various main group compounds (groups 12-15) bearing the same ligand. While the goal was not reached, novel compounds of zinc, germanium, and phosphorus bearing a tridentate will be discussed. The following background review will be divided into two sections. The first part will discuss activation of small molecules by main group compounds (group 12-15), with an emphasis on non-innocent ligands. The second part will be related to a discussion of zinc catalyzed cross-coupling.

II. Background Review

II.1 Small Molecule Activation

One of the main goals in organometallic chemistry is to develop highly selective and efficient catalysts for an otherwise challenging synthetic step. For reasons of efficiency, a robust catalyst attainable via a simple synthesis with cheap, and non-toxic reagents, and that can operate under mild conditions is desired. While expensive late transition metal catalysts based on Ru, Rh, Ir, and Pd are commonly used in industrial processes today, academics are pursuing the development of main group catalysis. Many of these elements are relatively inexpensive due to their abundance in the Earth's crust (e.g. silicon, aluminium, calcium), and equally importantly have greatly reduced toxicities (e.g. sodium, magnesium, calcium, aluminum, zinc etc.).

To demonstrate the potential ability of a main group species to be used for catalysis, a key step is the activation of small molecules, as it may lead to a means for utilization of cheap and simple feedstocks for atom economical reactions. The phrase "activation of small molecules" generally implicates the cleavage of an E-H bond, or can also describe cleavage of other strong bonds (e.g. C=C) from small molecules such as C_2H_4. The difficulty with main group compounds, however, is that they do not possess empty energetically accessible d orbitals as transition metals do. Instead, main group compounds tend to have large HOMO-LUMO gaps, which renders some critical steps, such as oxidative addition, energetically inaccessible.[3] Thus, either isolobal relationships are used to design compounds which may behave similarly to other known systems, and/or specially designed ligands are employed to lower the energy gap. As such, there are three ways in which to induce transition metal-like chemistry in main group compounds: carbenoids, frustrated Lewis pairs (FLP), and low-valent metals stabilized by strong donor-ligands (which includes non-innocent ligands[14]). This discussion will highlight some examples of group 12, 13,

14, and 15 element compounds for bond activations, as well as highlight a few common frameworks of non-innocent ligands. Simply, non-innocent ligands may be redox active, or facilitate reactions by outer-sphere mechanisms.[9,15]

In 2005, the first activation of dihydrogen (H_2) was reported by a germanium analogue of an alkyne **I-1**. The reactivity of heavy alkyne analogues towards activation of relies on the distortions experienced by heavier analogues, of which a change from linear to trans-bent lowers the symmetry from $D_{\infty h}$ to C_{2h}. Thus, symmetry allowed mixing of in-plane π and σ*, and in-plane π* and σ orbitals occurs via second-order Jahn-Teller effect, and results in a non-bonding electron pair orbital and a low-lying vacant non-bonding orbital (LUMO), respectively.[3,4] Subsequently, a side-on approach of H_2 to the ambiphilic germanium compound allows for orbital overlap akin to the frontier orbitals of transition metals. (Figure 1**Error! Reference source not found.**)

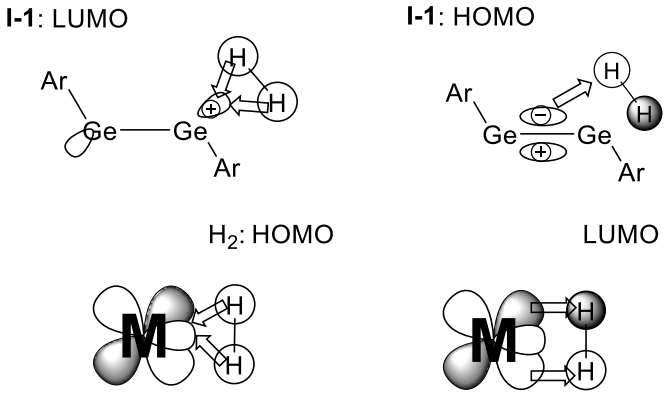

Figure 1. Frontier orbital of heavy alkyne analogue and comparison to transition metal frontier orbitals for the activation of H_2.

Carbenes are another class of very reactive compounds that may act as nucleophiles or electrophiles, due to their high-lying lone pairs and low-lying antibonding orbital. Both stable carbenes and metal compounds bearing carbene ligands have been used for activations of small

molecules. A comparison of the frontier orbital depictions of carbenes to transition metals, and the similarities of the HOMO and LUMO of H_2 and alkenes reveals why they are successful for activations (see Figure 2. Top: Orbital overlaps of metal complexes with H_2, comparable to carbene activation of alkenes. Bottom left: concerted [2+1] cycloaddition orbital overlap from an angled approach of singlet carbene with an alkene. Bottom right: cartoons of HOMO and LUMO of H_2 and an alkene (left)). An electrophilic carbene can coordinate to the HOMO and simultaneously populate the LUMO, destabilizing the bonding interaction until the bond breaks and the substrate is added oxidatively to the centre atom.

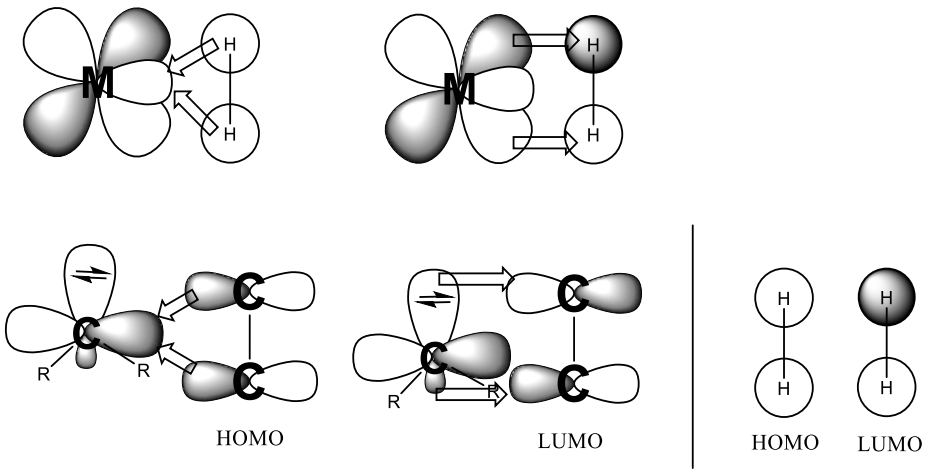

Figure 2. Comparison of frontier orbitals of transition metals and carbenoids.

Although traditional, stable cyclic-di(amino)carbenes, commonly called Arduengo carbenes, do not react to activate H_2 or CO, Bertrand demonstrated the first example of activation of H_2 by singlet carbenes in 2007, using cyclic and acyclic alkyl amino carbenes (cAAC and aAAC). (Figure 3)[16] Notably, the reaction of these carbenes with NH_3 led to oxidative addition of N-H to carbon (**II-3**), which is a challenging transformation in transition metal chemistry due to the usual formation of stable Lewis-acid-base adducts.[16] The success of this transformation was due to both an increase in the nucleophilic character, and significantly increased electron

withdrawing ability of carbon. Compared to the diamino carbene, the lack of a second lone pair in cAAC, capable of donating to the vacant p orbital of carbene, results in the decrease of the HOMO-LUMO gap. This approach may apply for other substrates and carbenoid compounds, and as such led to stable singlet carbenes proving to be active for P_4 activation and stabilization of highly reactive species, including radicals.[17]

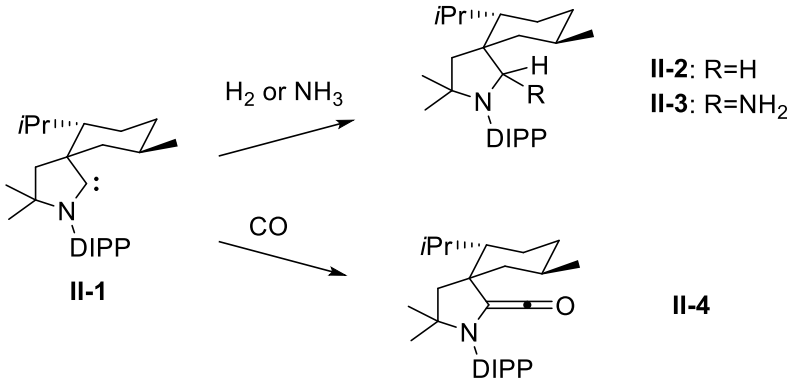

Figure 3. cAAC activation of small molecules.

Main group carbenoids are effective for small molecule activations. These compounds can be seen in examples of group 13 to group 15, such as but not limited to Al^{I} (eg. NacNacAl; NAcNAc = $[ArNC(Me)CHC(Me)NAr]^{-}$, where Ar = 2,6-*i*$Pr_2(C_6H_3)$)[18], its gallium analogue[19], silylenes[20], germylenes (Scheme 3) [21], nitrenes[22], and phosphinidenes.[23]

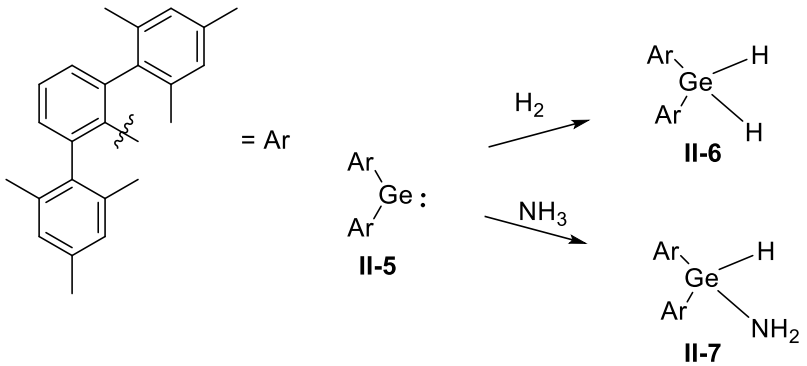

Scheme 3. Example of germylene reactivity for activation of H_2 and NH_3 by Power.[21]

Combinations of Lewis acids and bases have also been shown to be active species in bond activations. While normally Lewis acids and bases form strong adducts with each other, a bulky Lewis acid and a bulky Lewis base cannot form strong adducts because steric repulsion prevents their quenching. Such Lewis pairs were termed by Stephan, frustrated Lewis pairs (FLP), and show unique reactivity.[24] In a sense, the previously mentioned carbenoids may also be considered a type of FLP, as the Lewis acidic and basic orbitals are located at the same metal centre, but are unable to quench each other due to their orthogonal orientation. However, the term "FLP" is generally used for pairs of Lewis acidic and basic partners which are located on different atoms.

FLPs were a major breakthrough in main group chemistry because of their ability to activate small molecules[25]. Common FLP systems tend to use a very electron deficient Lewis acid, such as tris(pentafluorophenylborane) (**II-8**), combined with a bulky Lewis base of phosphorus or nitrogen.[26] Similarly, the closely related work done by Piers was trending toward FLP activity but was limited towards activation of silanes, when Stephan reported the first FLP system in 2006[27]. As an example, Piers *et al*. discovered that hydrosilylation of carbonyl compounds could be catalyzed by the very Lewis acidic **II-8**, and provided evidence that it functions by polarizing the Si-H-BR_3 bond, thus enabling a nucleophilic attack at silicon.[28]

In the design of the original FLP system (Scheme 4), for the starting compound, a resonance structure can be drawn with a dearomatized phenyl ring (**II-8'**), which was exploited in a reaction with a very bulky phosphine (Bis(2,4,6-trimethylphenyl)phosphine), enacting a fluorine transfer to boron. This zwitterionic species **II-9** was modified by fluoride abstraction form boron, and a subsequent hydride transfer from a hydrosilane furnishes the phosphonium borate **II-10,** which was then shown to liberate H_2 under heating to yield **II-11**. Remarkably, the reaction can

be reversed so that the phosphine-borane product is able to activate H_2 heterolytically at 1 atm and room temperature.[27]

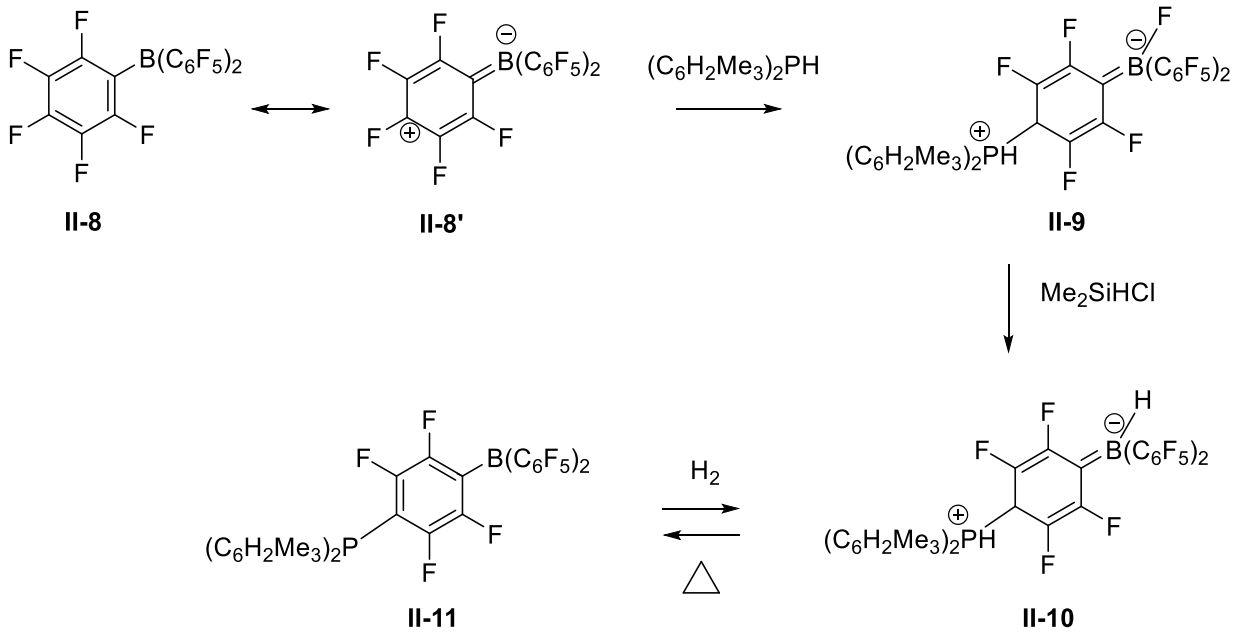

Scheme 4. Synthesis and reactivity of the first FLP to demonstrate reversible hydrogen splitting.

Since then, examples have been demonstrated with separated phosphine/borane pairs, or as functionalities on the same molecule. The heterolytic cleavage ascribed for transition metals is now known for main groups, and thus FLPs have found utility in a multitude of reactions. Early examples of FLP demonstrated poor air and moisture tolerance. **II-8** is a very electron deficient borane, and thus is very sensitive to moisture[29]. Parkin calculated that the Bronsted acidity of $H_2O*B(C_6F_5)_3$ adduct is comparable to that of HCl in acetonitrile. Stephan also developed alcohol and water tolerant FLPs which were capable of hydrogenating aldehydes and ketones which do not poison the catalyst.[30] It was realized that careful tuning of Lewis acidity allows for hydrosilylations, even in the presence of Lewis basic water or alkylamines. [29]

Lastly, apart from other group 14 metallenes, other low valent main group compounds may also be used for small molecule activations. Due to their low oxidation state and resulting electron density and isolobal orbitals, they may react via oxidative addition of the substrate to the metal centre as seen before. A well-studied example of this is NacNacAl^{I}, which was found to activate H_2, silanes, boranes, allanes, phosphines, amines, alcohols, Cp*H[31], and C-F bonds.[32,33]

II.1.1 Non-Innocent Ligands

If an oxidative addition process produces an element in a very unfavourable oxidation state, the reaction will not proceed. Thus, it should be noted that there are still only a few examples of aluminum (+1) and zinc (0) compounds, and that zinc (+3) are (+4) states are not possible. To circumvent this restriction of unusual oxidation states, the activation may be accomplished by a binuclear species, or by the application of a non-innocent ligand may help by stabilizing charges on the ligand instead of at the metal centre, or by participating cooperatively in bond forming or breaking processes. A ligand is non-innocent if it may either i) be oxidized or reduced, thus affecting the Lewis acidity or basicity of the metal, or ii) function as electron reservoirs with resonance forms having different oxidation states at the metal centre. Alternatively, the ligand may cooperate with the metal for activation of a substrate, either by, iii) facilitating a radical reaction of the substrate on the ligand, or iv) an asymmetric bond forming or cleavage step.

Traditionally, ligands in Werner coordination compounds function as spectators while a reaction proceeds at the metal centre. However, non-innocent ligands pose a problem when discussing oxidation states. The interaction of a ligand with a metal may be interpreted by structural changes in their geometry, but a change of electron density of a ligand is not enough to distinguish discrete electron transfer from a back-bonding event. This prefaces a discussion of the term “oxidation state”, which is a convenient method to predict and describe behaviour of

compounds, while simultaneously being a fiction with a flawed definition. Correct assignment of oxidation state is difficult as the definition still has not been agreed upon. The IUPAC definition says that "oxidation state" is *the charge an atom might be imagined to have when electrons are counted according to an agreed-upon set of rules*[34]. The formalism is based on counting bonds and charges of ligands around a naked metal atom, but this general method fails to account for the extent a ligand redistributes electron density. This works well for traditional Werner complexes, but its systematic application to determine the oxidation state of a metal fails when a ligand may be ambivalent[35], a non-ambiguous σ donor, or is redox active. Redox-active ligands are found in the fields of biochemistry and pure chemistry, and examples such as O_2, NO, porphyrins and quinones are common for discussion of non-innocence.[36] Similarly, ambiguity of resonance forms of compounds stabilized by an N-heterocyclic carbene (NHC) in Figure 4, leads to two resonance interpretations of the oxidation state of phosphorus, +3 or +1.

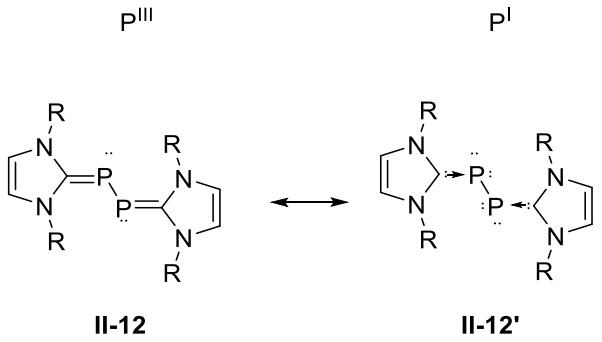

Figure 4. NHC stabilized diphosphorus with two resonance structures.[37]

Ligand non-innocence can arise when a ligand is ambivalent, and a ligand-to-metal electron transfer (or vice versa) may occur. Catechols, semiquinones, and quinones are examples of a ligand framework which is redox active, and have been studied extensively for both oxygen, N-H, and

sulfur substituted analogues. As shown in Scheme 5, a bidentate redox active ligand may adopt different bonding motifs to the metal. A one electron donor (representative of a covalent bond) is considered an X-type ligand, whereas coordination via a dative interaction of a two-electron donor is described as an L-type ligand. The ligand of structure A is functioning as an X_2 ligand (two X-type bonding interactions) and increases the oxidation state of the metal by +2, whereas the of structure C is an L_2 ligand which does not affect the calculation of oxidation state at the metal.

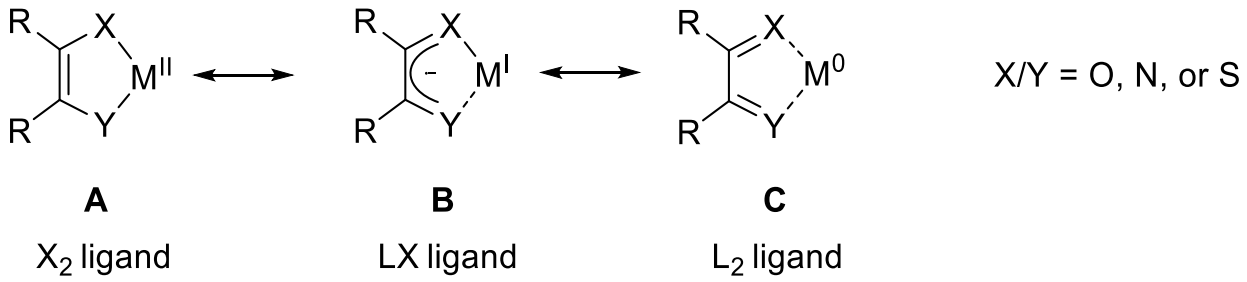

Scheme 5. Representative structures of 1,2-chelating species as X_2, LX, or L_2 ligands.

A very versatile class of ligands in organometallic chemistry that belongs in this family are the β-diketiminates (often referred to as NacNac). Ligands of this type are relatively easy to prepare and functionalize, and many species bearing NacNac ligand frameworks have been used in catalysis due to their ability to stabilize low valent and monomeric metal complexes.[18,38] Furthermore, they have been used extensively for main group,[39] transition metal,[39] and lanthanide compounds.[40] The NacNac ligand may adopt different bonding modes,[39] and it may act cooperatively in bond activations. For a long time, the NacNac framework was regarded as an LX spectator ligand, and the role of the metal included facilitating bond activations[31,41] and undergoing redox reactions.[42,43] Contrary to those reactions bearing "innocent" NacNac ligands, NacNac complexes may sometimes contain "hidden non-innocence". The challenge of detecting redox activity of the framework is that, due to the symmetry of the 5 atoms in the backbone of the

bidentate ligand, the intra-ligand bond distances are not affected by reduction of the ligand. To prove oxidation on the ligand, $Ni(NacNac)_2$ (**II-13**) and $Zn(NacNac)_2$ (**II-14**) were prepared and subjected to cyclic voltammetry (CV).[44] EPR analysis of the first oxidation (reversible) of **II-13** shows a *S*=½ species, and orbital population analysis calculated spin density on the metal of only +1.58. A metal centered oxidation of **II-13** if tetrahedral would be expected to give rise to a Ni^{III} d^7complex and exhibit *S*=3/2 (in contradiction to EPR analysis), whereas a square planar complex would be *S*=1/2 due to the splitting of the t_2 orbitals. Calculations suggest that this oxidized species although twisted (α=78°), is closer to tetrahedral geometry(α=90°) than square planar (α=0°). Thus, this situation was explained by a ligand centered radical which is antiferromagnetically coupled to *S*=1 Ni^{II}, thus matching the EPR *S*=½. Examining the proposed ligand-based radical further, the authors oxidized the zinc species, which shows two irreversible oxidations. As zinc is unable to undergo metal centred oxidation, the spin densities for the two oxidized species are mainly located on the ligands. Single electron reduction of NacNac complexes were also verified by magnetic susceptibility experiments.

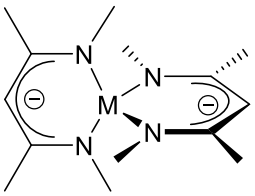

M= Ni^{II} (**II-13**) and Zn^{II} (**II-14**)

*Figure 5. Bis(NacNac)metal complexes **II-13** and **II-14**.*

A non-innocent derivative of NacNac was also reported and used to prepare complexes of cobalt and zinc, which demonstrated multiple possible electron transfers (two of which being fully

reversible) when subjected to cyclic voltammetry. These reversible ETs were present in both species and attributed to ligand centered oxidations (Scheme 6). [45]

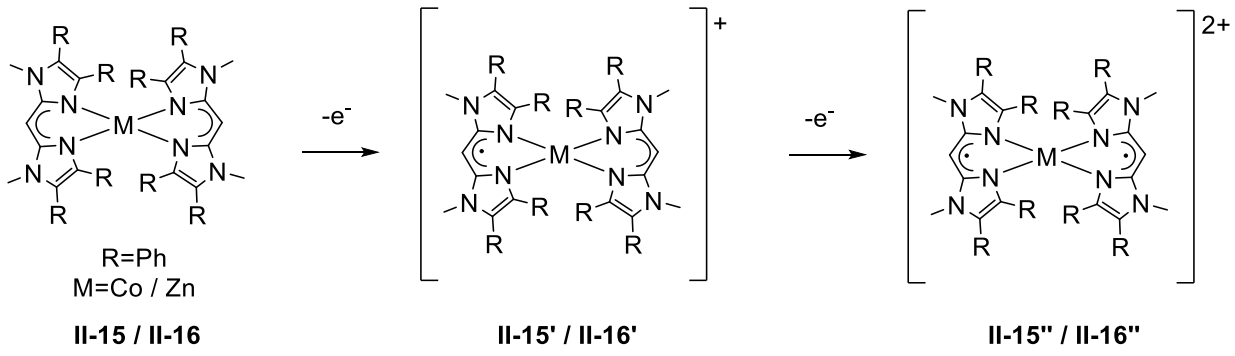

II-15 / II-16 **II-15' / II-16'** **II-15'' / II-16''**

Scheme 6. Redox non innocent β-diketiminate ligand on zinc and cobalt.[45]

Diiminopyridine ligands have been shown to exhibit both redox non-innocence, and have been used to stabilize low-valent main group complexes, such as Ge^0.[14] Interestingly, diiminopyridine bound to iron can function as an electron reservoir, which was exploited for [2+2] cycloadditions[46]. Furthermore, because the ligand is redox active and the electron storage capacity of the ligand is significant, oxidation and reduction can occur on the ligand during the course of a cycloaddition, allowing iron in to reside in the more stable Fe^{II} state, as opposed to Fe^0.[9] This functionality was similarly exploited for catalytic applications with cobalt: hydrogenation and hydrosilylation of alkenes, and as well as for hydroboration of both alkenes and alkynes. Calculations of this ligand system were extended to ZnNNN(DMAP), which also showed that redox events occurred at the ligand, as the closed shell zinc ion would be incapable of undergoing redox activity.[47] Related species formed by reduction of the dichloride to monochloride (**II-17**) and the subsequent DMAP adduct (**II-18**) revealed strong interaction of the unpaired electron delocalized over the ligand, and thus reduced species can be represented by de-aromatized ring systems. This is noted by EPR evidence for a highly delocalized radical, tending

toward Zn in an oxidation state of +2, as there was significant hyperfine coupling with nuclei in the backbone, with spin density primarily at the nitrogen and para position on the pyridine ring.[48] Further reduction by KC_8 in the presence of another equivalent of DMAP gives rise to another species (**II-19**) with a ligand based LUMO and minimal Zn character in the HOMO and HOMO-1, as there is more metal-to-ligand backdonation. (Figure 6) Interestingly, when contrasting this to other main group compounds involving the same diiminopyridine ligand, there is variability in the electronic nature of the ligand, and thus inconsistency may arise in the assignment of oxidation states to metals coupled to a redox active ligand. For a discussion on this, see references [48,49].

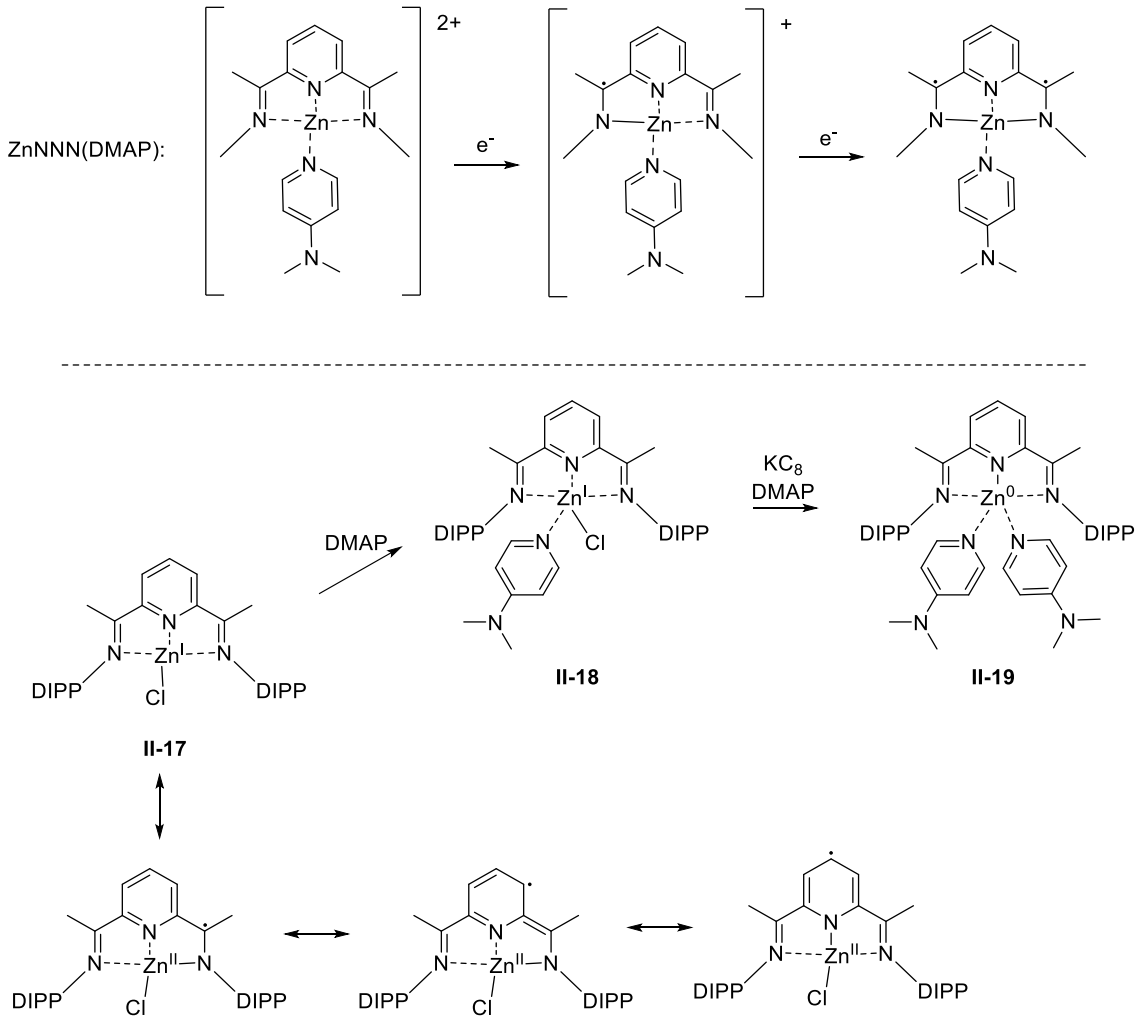

Figure 6. Diiminopyridine compounds of zinc.

Similar redox non-innocence can be observed in many systems, and an asymmetric (regarding the pendant arms at 2 and 6 of the centre pyridine) example is Milstein's iron P,N,N-complexes (eg. **II-20**). Structural characteristics of diiminopyridine complexes cause discrepancies in the assignment of oxidation state of the metal by ±2, and thus are a point of contention. The P,N,N-Fe complexes only contend with a ±1, thus simplifying the argument slightly. (Scheme 7) To understand the electronic framework of these systems, combinations of structural parameters, magnetic susceptibilities, Mössbauer spectroscopy, and DFT calculations can be used in conjunction with one another to evaluate the extent of electron transfer versus backdonation from a metal. As demonstrated, structural evaluations were proven to be insufficient and led to erroneously defined oxidation states, thus probing by multiple spectroscopic methods should be considered. For an example of the arduous process of attempting to define oxidation states of iron complexes bearing a redox-active ligand, see Butschke *et al*. [50]

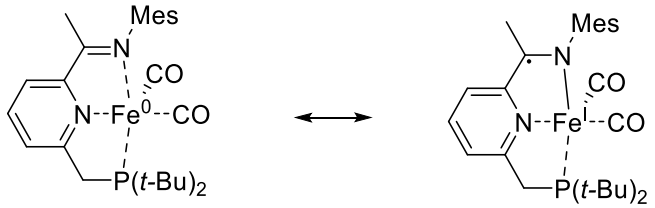

II-20 **II-20'**

Scheme 7. Fe(PNN) complex with two canonical forms.[50]

For a further reviews on metal-ligand cooperation or non-innocent ligands, see reviews by Milstein *et al*.[10] or de Bruin *et al*.[9]

II.1.2 Small Molecule Activations by Group 12 Compounds

While often described as a transition metal, zinc is more closely related to main group due to the fully occupied d-orbitals, and the subsequent lack of redox activity. Thus, its reactivity would

be governed by the accessibility of the LUMO, and by extension, by its Lewis acidity. Furthermore, while there are both Zn^{I} and Zn^{II} complexes, oxidative addition to zinc is not likely to happen, as Zn^{III} and Zn^{IV} are inaccessible. These systems instead usually react by concerted mechanisms or by insertions[51] as to preserve the stable Zn^{II}. Most zinc enzymes react by deprotonation of a coordinated H_2O, by displacement, or by polarizations of bonds.[52] Organozinc reagents react violently with water, but their dihalides are much easier to handle, and thus many isolable zinc catalysts are produced by substitution reactions of halides by anionic ligands. There have been many catalytic zinc species reported for reduction of unsaturated substrates, including ketones, aldehydes, α,β-unsaturated ketones, alkenes, CO_2, amides, imines, phosphaimines, and nitriles, and alkynes.[51,53] These reactions operate exclusively on Zn(II) centres, primarily by insertion/ metathesis or FLP pathways and will not be described here. For a review on zinc catalyzed reductions, see Junge and Beller [51].

An example of activation by a zinc compound which was not solely a consequence of changing the Lewis acidity at zinc, was demonstrated by Roesky *et al*. in 2010. A NacNac analogue, bis(phosphimino) ligand reacts with $ZnCl_2$ or $ZnPh_2$ to yield tetra- and tri-coordinate zinc species respectively. The Ph substituted species **II-21** has a delocalized negative charge (Figure 7). This species was found to react with a ketene, generating a new ring and tetracoordinate zinc, with similarity to tripodal ligands.[54] This non-innocence also contrasts the geometry of other examples of species with this ligand, in which the ligand acts as a spectator instead of forming a bicyclic structure with early transition metals and lanthanides via the backbone carbon with a carbene-like character.[55]

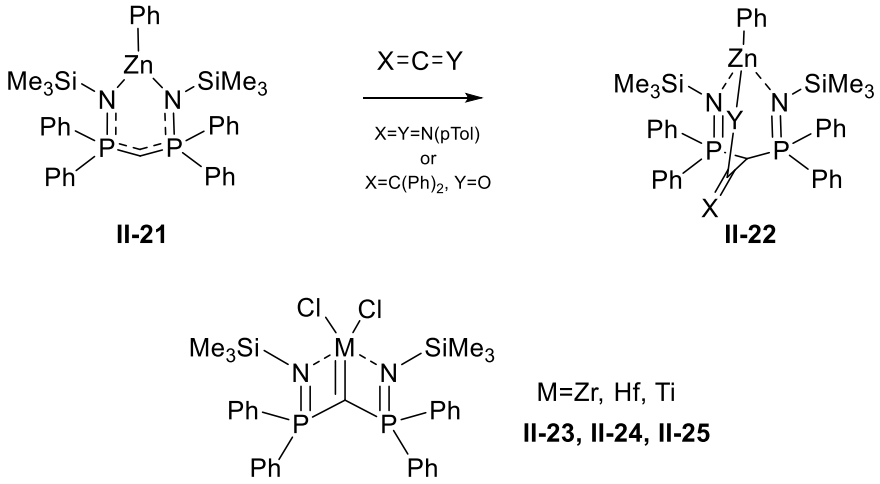

Figure 7. Contrasting reactivity modes of bis(phosphimino) complexes.

In 2013, Stephan reported reaction of H_2 with $(Cp^*)_2Zn$ (**II-26**) in conjunction with various carbene ligands.[56] Reactivity of this compound was screened with various carbenes, and while SIMes (**II-30a**) and IDipp (**II-30b**) showed no reaction, I*t*Bu (**II-30c**) generated a coordination complex with zinc. Furthermore, SIMes and IDipp and I*t*Bu all reacted in the presence of H_2 as well (**II-27a-c**). While in the presence of **II-26** and H_2, both I*t*Bu or SIMes facilitated loss of Cp*H, and the latter would unequivocally concurrently generate a zinc hydride species (**II-29a** characterized by X-ray crystallography). Notably, this found utility for the hydrogenation of imines, in which hydrogenolysis of **II-26** yields a zinc hydride that could insert into the C=N bond (Scheme 8).

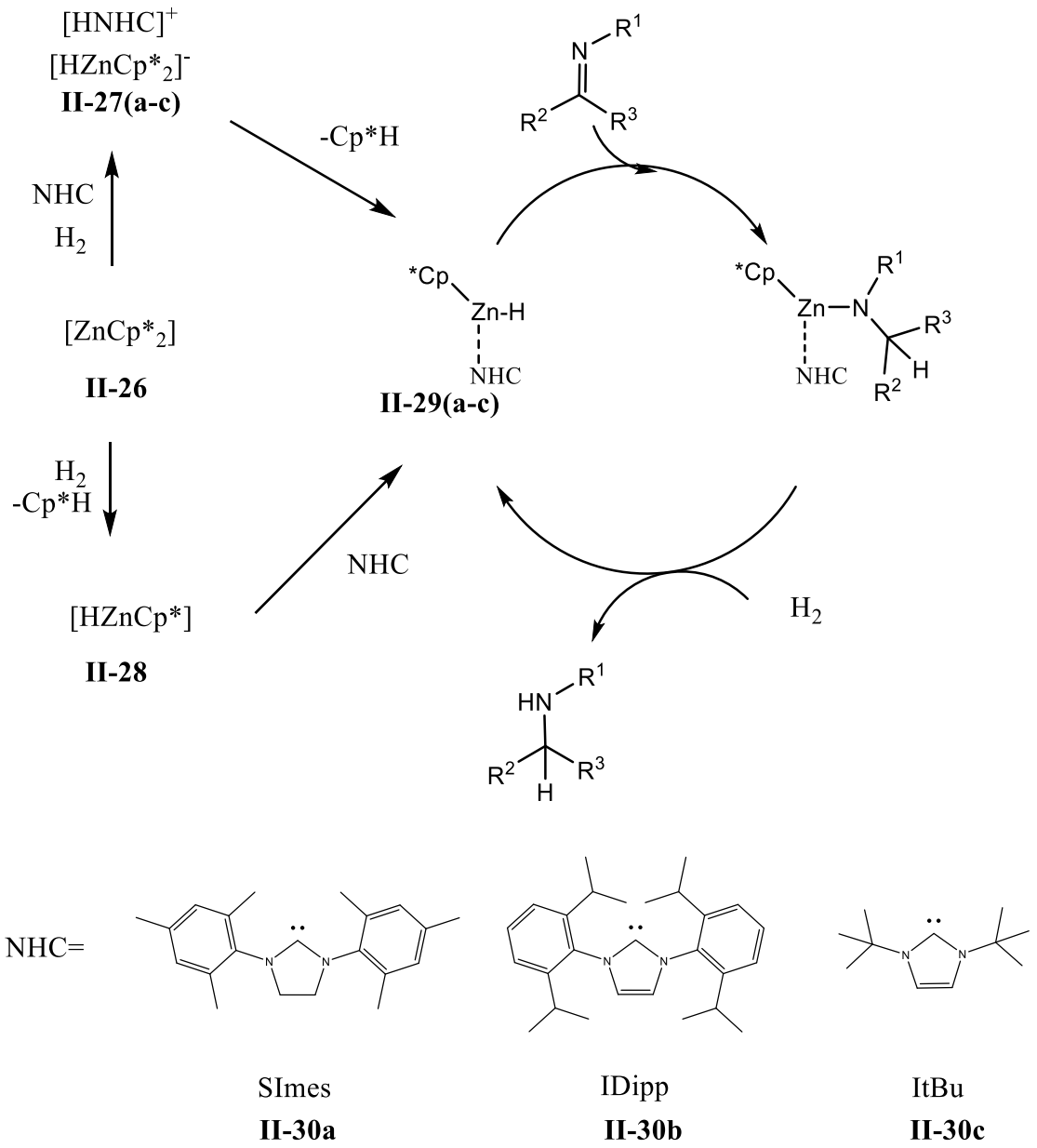

Scheme 8. Mechanism for hydrogenation of imines catalyzed by an in situ generated zinc hydride, following hydrogenolysis.[56]

II.1.3 Small Molecule Activations by Group 13 Compounds

As mentioned earlier, group 13 FLP chemistry has been successful for activation of small molecules and has found catalytic applications for metal free hydrogenations. As a discussion of FLP chemistry is beyond the scope of this historical, see a review by Stephan and Erker[24].

Formazanate ligands feature an NNCNN backbone which is redox active (Figure 8). A boron complex bearing this ligand ($M=B(OAc)_2$)[57]. When $M=B(Ph)_2$, the complex may undergo two-electron reduction, followed by a reaction with an electrophile which proceeds by addition to the ligand backbone nitrogen, followed by a homolytic N-E cleavage step facilitated by TEMPO.[58] Similarly, boron difluoride formazanate prepared by transmetallation from a bis(formazanate) zinc species could also undergo stepwise one-electron reductions. CV shows two quasi reversible redox processes, with accessible and stable reductions. An interesting feature for the proposed mechanism of transmetallation is ring contraction from six-membered to five-membered chelated rings, accompanied by the slippage of a nitrogen atom which can serve to bind to boron[59].

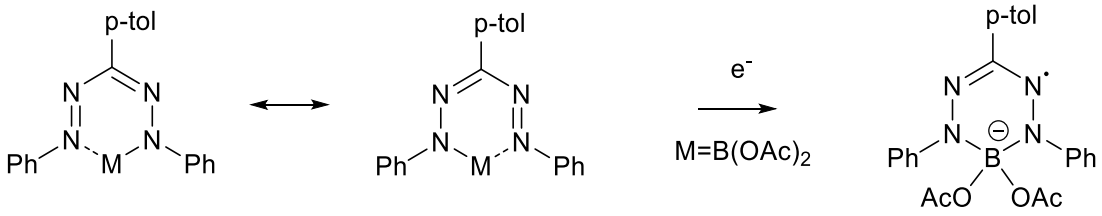

Figure 8. General structure for formazanate complexes

As mentioned before, the challenge of facilitating catalysis at a main group centre is the ability to stabilize low oxidation states, which is generally inaccessible or unstable, so synthesis and protection of these highly reactive species are usually performed using bulky ligands. Furthermore, in order to achieve reactivity of main group compounds, analogies may be drawn from carbenes. For a review of group 13 and 14 as NHC analogues see Asay, Jones, and Driess[60]. An example of a low valent aluminum (I) species bearing a DIPPNacNac ligand was reported in 2000 by Roesky *et al.* [18] Aluminum hydride compounds have been used for activation of unsaturated substrates including CO_2[61](not catalytic), ketones, aldehydes, alkynes[62], whereas

this species was later discovered to be capable of activating H-X bonds[31]. For a discussion of carbene analogue character and supporting calculations, see Schoeller and Frey. [63].

Similar to the aforementioned NacNacAl^{I}, NacNacGa^{I} was also able to activate H_2, alcohols, amines, phosphines , hydrostannane, and water.[64] In contrast though, (**II-31**) with an unsaturated backbone was also able to activate H_2 by a non-innocent ligand to accept a proton and generate a four-coordinate gallium hydride (**II-33**). (Scheme 9) As an extension of this, the authors showed how this could be used for catalytic reduction of CO_2. Hydrogallation of CO_2 (**II-36**) occurs at room temperature under 1 atmosphere of CO_2 that proved to be pivotal to hydroboration of CO_2 with pinacolborane.[65] This system thus demonstrates a cooperation with the metal for activation of H_2, SiH_4, NH_3, and SH_2. H_2 activation is believed to proceed via a concerted mechanism by 1,4-addition, but acidic ammonia activation is believed to proceed via pre-coordination followed by intermolecular deprotonation.[65]

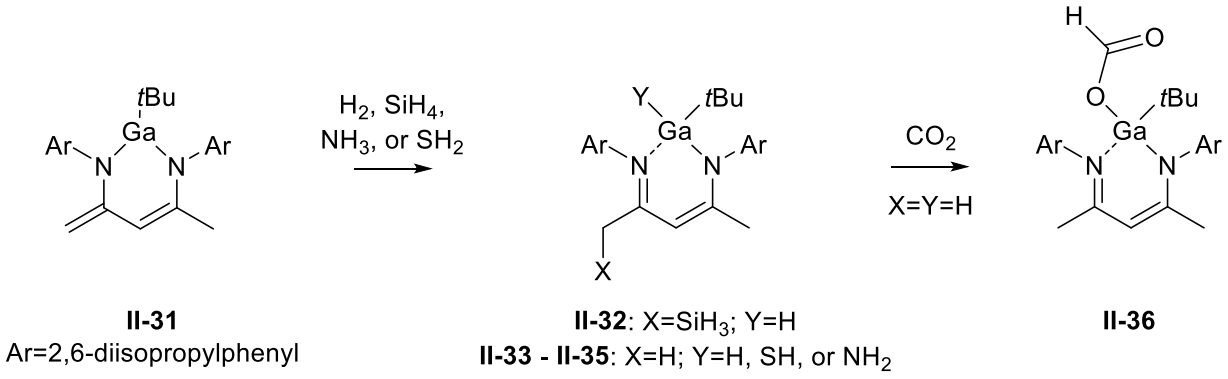

II-31
Ar=2,6-diisopropylphenyl

II-32: X=SiH_3; Y=H
II-33 - II-35: X=H; Y=H, SH, or NH_2

II-36

Scheme 9. Non-innocence of bis(amine) ligand.

Another common ligand design is one which contains a hard nitrogen donor at the centre of the ligand. The benefit is the stabilizing effect of the resonance forms of an oxidized ligand, which enhances the ability for these ligand frameworks to participate as non-innocent ligands. One example of a species containing a central pyrrole is presented here. Aluminum dihydride

compounds stabilized by either symmetrical or asymmetrical tridentate ligands have been reported (Scheme 10). The species reacted by deprotonation of two equivalents of an acetylacetone derivative, along with dissociation of one of the pendant amines to yield (**II-40** and **II-40'**). Similarly, the dihydride (**II-37**) was able to undergo hydroalumination of phenylthioisocyanide (**II-41**), also accompanied by dissociation of the labile amine group. [66]

VT-NMR spectroscopy showed that there is a fast exchange of the coordinated amine. For **II-40** and **II-40'**, the difference in $\Delta H^{\ddagger}$ is only 0.2 kcal/mol, and the $\Delta G^{\ddagger}$ is 15.0 kcal/mol.[67] Similarly, deprotonation and reaction with $AlCl_3$ could be used to generate the dichloro species (**II-38**), whereas a direct reaction with $AlMe_3$ could generate the dimethyl derivative. From the dichloride species, *tert*-butyl amide was strong enough to facilitate deprotonation of the pendant NH*t*Bu arm, which led to the displacement of the NMe_2 arm (**II-43**), whereas the same procedure using LiNMePh resulted only in displacement of a chloride (**II-42**). For the dimethyl aluminum species, reaction with phenol generated aluminum phenoxide with liberation of methane, but a reaction with ketene instead afforded insertion into the C-N bond of the pendant arm of the ligand instead. [66]

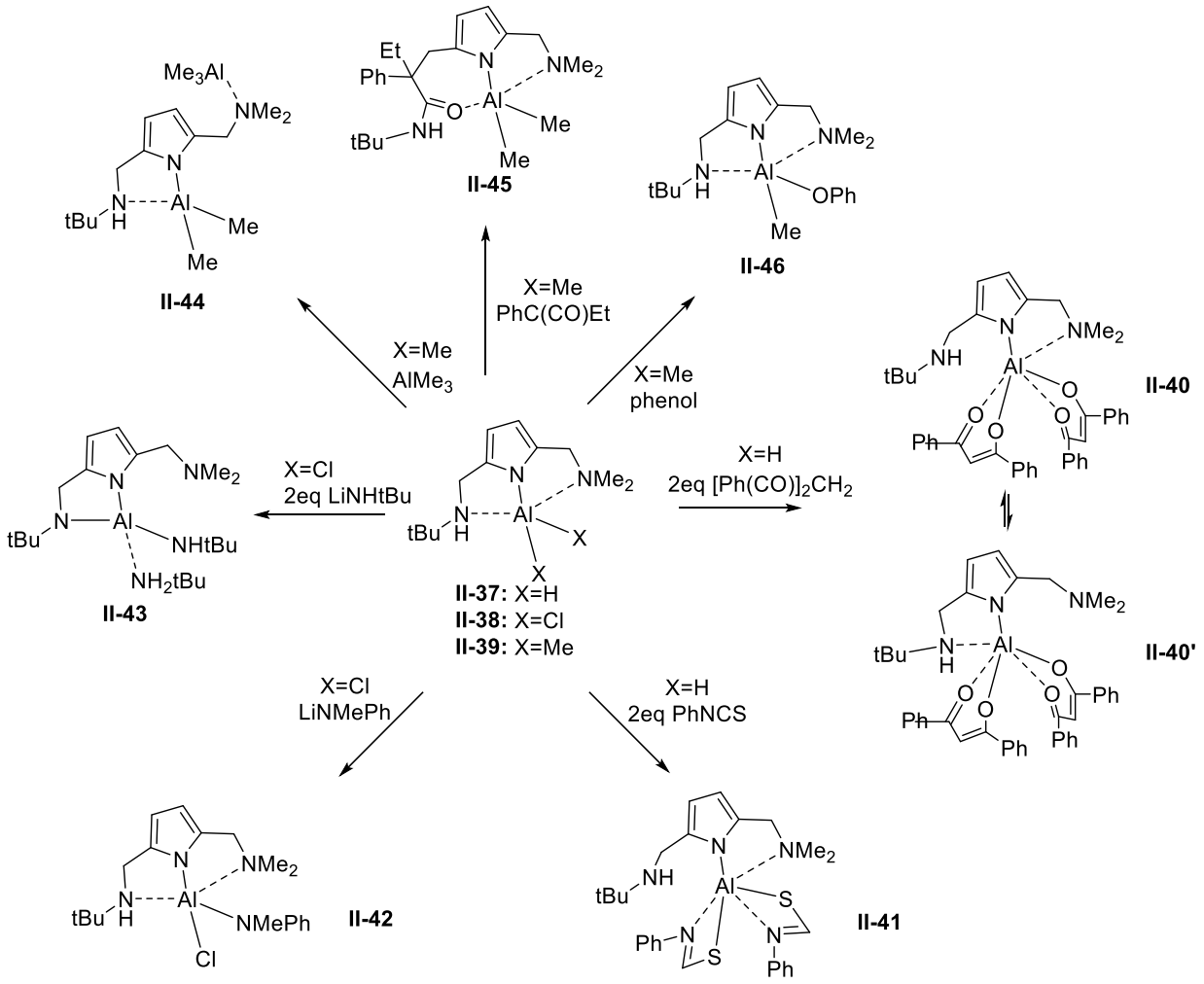

Scheme 10. Reactivity of aluminum complex stabilized by a pyrazole functionalized ligand.

Recently, Aldridge reported a new aluminate **I-8** which could be used as a nucleophile for nucleophilic substitution reactions. Although aluminates of $[AlR_4]^-$ are known, an Al^I species of this type has not been prepared. This resulted in a species which can undergo a variety of nucleophilic reactions with HX (**II.47**), methyliodide or methyltriflate (**I-9**), NacNacMgI(Et_2O) (**II.48**), and the parent Al-I, as well as activation of H_2 (**II.49**) and sp^2-C-H activation of benzene (**II.50**). The ligand dimethylxanthene provides a three-ring, flexible backbone for two secondary aniline groups. While not a novel ligand, the chemistry presented is significant. Deprotonation with KHMDS followed by substitution of AlI_3 gives the iodoaluminum (III) species (**II.51**), which

can then be reduced by KC_8. With an excess of reducing agent, the product is dimeric with two potassium counter anions (**I-8**). The identity of I-8 was confirmed by an independent synthesis of the possible aluminum (III) dihydride (**II-49**) (due to the difficulty with locating hydrogens in X-ray structures, and the tendency for aluminum to be in the +3 oxidation state) which has distinctly different ^{1}H NMR resonances (Scheme 11).[68]

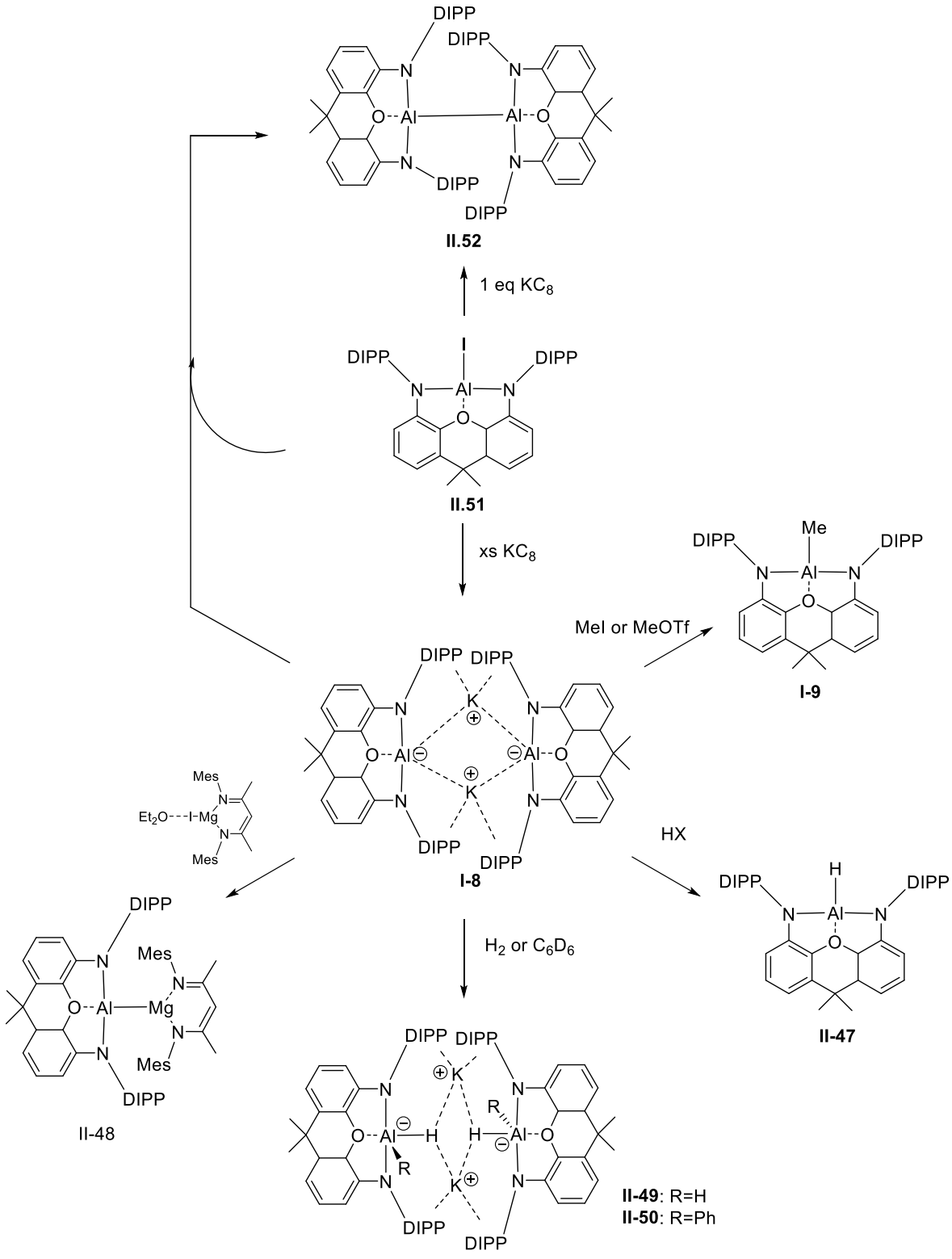

Scheme 11. Various nucleophilic reactivities of aluminyl anion ***I-8****.*

II.1.4 Small Molecule Activations by Group 14 Compounds

As mentioned above, carbene complexes have strong donor and acceptor properties, which can be exploited in bond activation. Notably, they find utility in cyclopropanation and insertion reactions. While some carbenes have historically been regarded as highly reactive, fleeting intermediates, which were originally only formed *in situ* by photolysis (e.g. from diazomethane[69]), α-elimination, or by deprotonation of a cation (e.g. NHCs), stable carbenes have also been reported. In recent years, the popularity of NHC frameworks has skyrocketed, which also reflects the synthetic application of these useful and reactive compounds.

The first example of a free carbene was reported Bertrand in 1988 (**II-52**)[70]. This species utilized the stabilizing effect of a trimethylsilyl group and a phosphorus flanked by bulky diisopropylamines, and undoubtedly bore some C-P multiple bond character. Despite this stabilization, the species demonstrated a carbene-like reactivity, evidenced for example, by carbene insertion into the C-H bond of an *i*Pr substituent upon pyrolysis (**II-53**, Scheme 12).[70] Following this work, the first example of an NHC was reported by Arduengo in 1991, bearing adamantyl amino groups on an aromatic five-membered ring.[71] Whereas NHCs are often singlet spin, dialkyl carbenes tend to be triplet due to the small HOMO-LUMO gap of these complexes with strong donor and acceptor properties, and demonstrate a radical type reactivity as a biradical species. A gap of 2 eV is enough to stabilize a singlet state, as in NHC, whereas a gap of about 1.5eV may lead to a triplet carbene.[72,73]

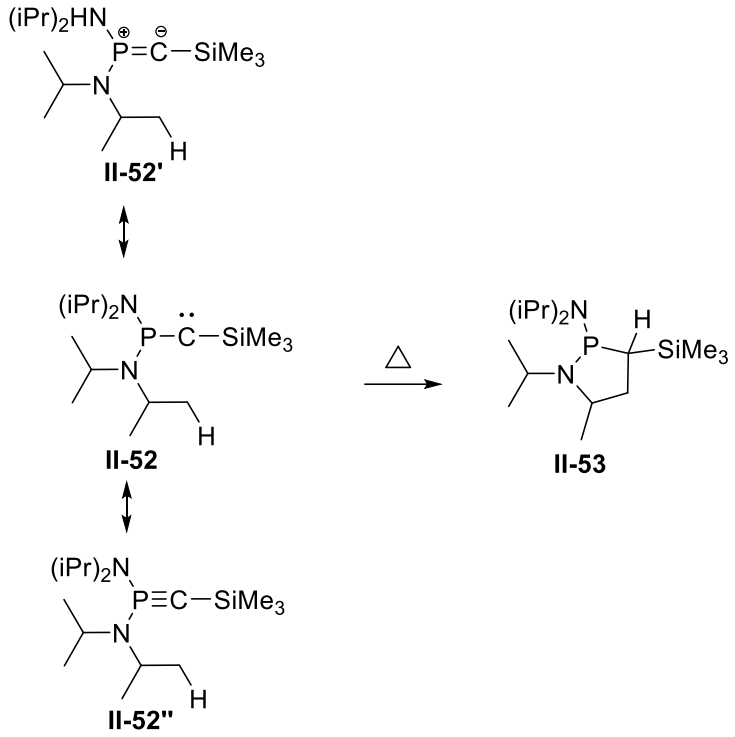

Scheme 12. Phosphino carbene prepared by Bertrand.[70]

While activations of stable bonds of H_2 and NH_3 were historically limited to reactions by transition metals, stable carbenes have also been shown to activate small molecules CO, H_2, NH_3, and P_4[17]. Unfortunately, early examples of stable NHCs or acyclic diaminocarbenes do not show the ability to activate H_2, NH_3, nor CO. Additionally, Arduengo reported in 1995 that imidazol-2-ylidene could not react with CO and would only lead to a weakly coordinated, non-bonded species.[74] Despite this, replacing one of the electronegative, π donating nitrogen atoms for an alkyl group yields a cyclic or acyclic alkylaminocarbene, which is reactive enough to proceed (Scheme 13). This reactivity is due to the difference in the inductive effects of N versus C, and the decreased π-donation to the carbene atom from the flanking groups, which lowers the energy of the LUMO. As a result, the energy gap of cAACs reported by Bertrand was calculated to be 46 kcal/mol versus 68 kcal/mol for the related NHC complexes.

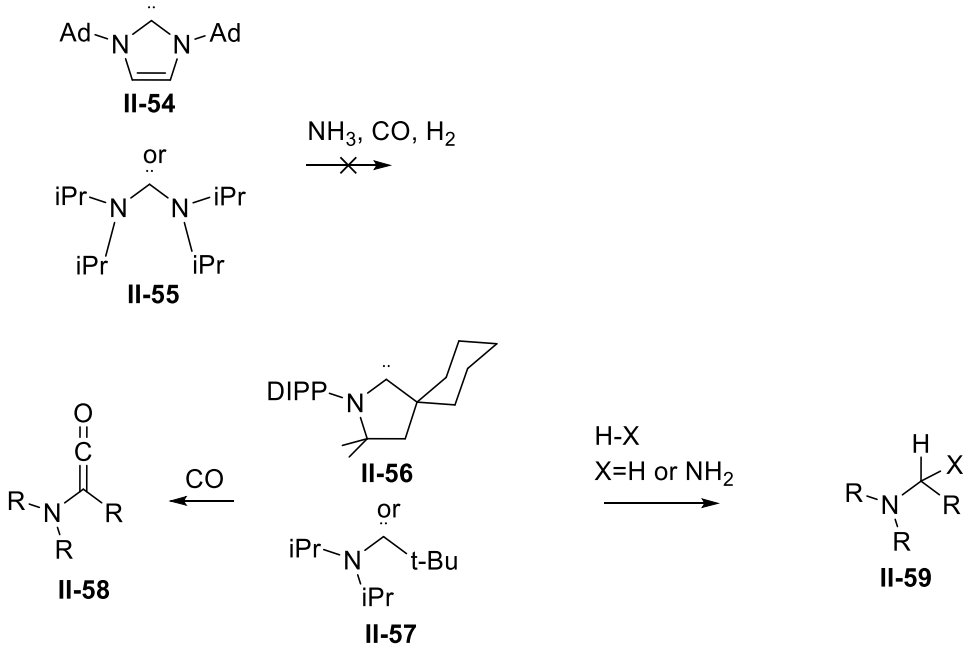

Scheme 13. Diaminocarbene and alkylaminocarbene reactions.[17]

Although NHCs do not activate H_2, oxidative addition of Si-H of phenylsilane at room temperature does occur, and a similar reaction proceeds for cAAC as well. At elevated temperatures though, phenylsilane reacts to bring about expansion of the carbene ring (**II-60a** or **II-60b**) by presumed insertion into the Si-H bond and migration, to yield a six-membered ring (**II-61a** or **II-61b**, respectively). The reaction was proposed to go through the product of oxidative addition, however such an intermediate was not observed, and only the ring expansion product was isolated.[75] Similarly, at room temperature, insertion into the P-H bond of phenylphosphine occurred (**II-63a/b**), but reactions with pinacolborane led to a ring opened dimerization product (**II.46b**).[76] (Scheme 14) Under identical conditions, reaction of cAAC with pinacol borane gave the oxidative addition product, whereas a reaction with more acidic BH_3 resulted in a Lewis acid-base adduct.

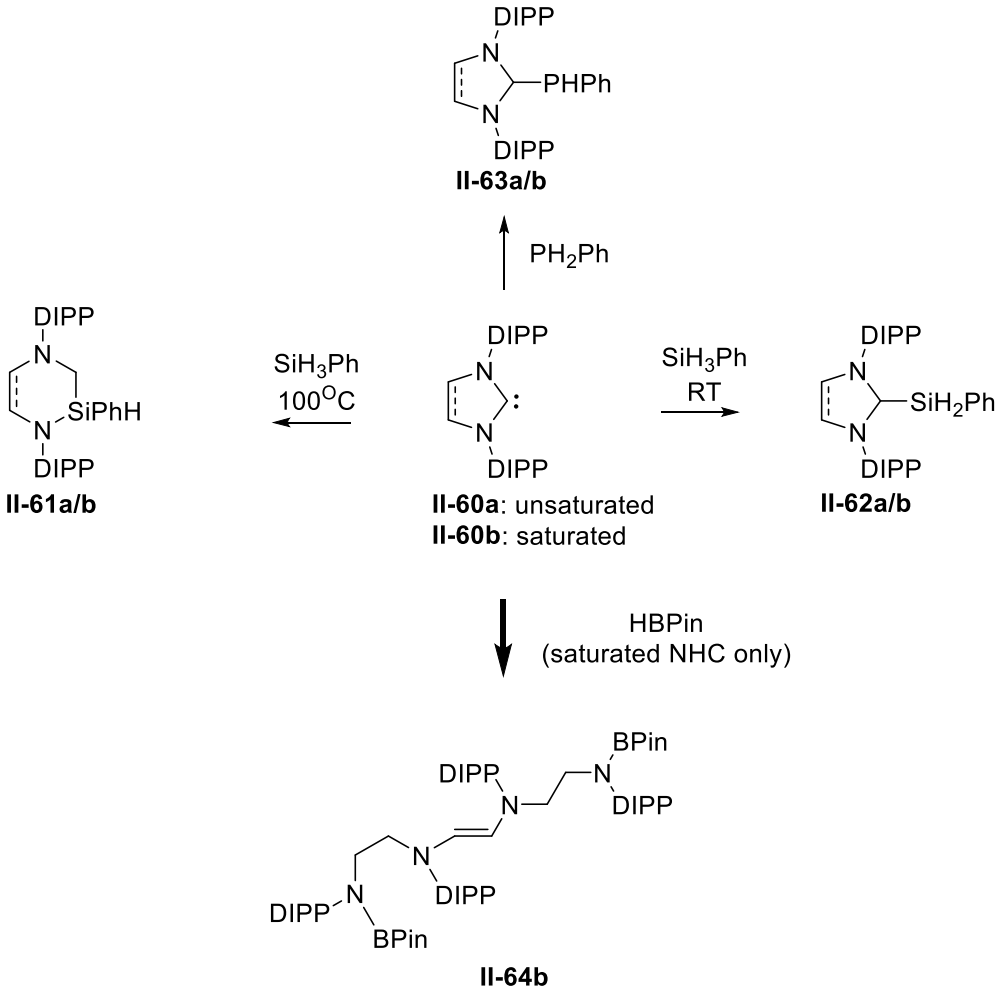

Scheme 14. Silane, borane, and P-H activation by NHCs.[75,76] *Reactions reported for both saturated and unsaturated NHCs, except where bolded.*

Due to their lower basicity, NHC compounds have been successful as organocatalysts, with triazolylidene carbenes being particularly common. For a review on NHC-mediated organocatalysis, see Flanigan *et al.*[77] While (alkyl)(amino) carbenes are more nucleophilic and more electrophilic than their bis(amino)-carbene counterparts, cAACs have not been used yet in catalytic applications and only found application in stoichiometric reactions. Alternatively, both NHCs and cAACs have become prominent in transition metal catalysis, for stabilization of unusual oxidation state transition metals and main group complexes. Among unusual main group

complexes, there are a multitude of carbene-phosphinidene adducts, which gave rise to a controversy on the nature of the P-C bond.[78] Possible descriptions of such species are presented in Scheme 15.

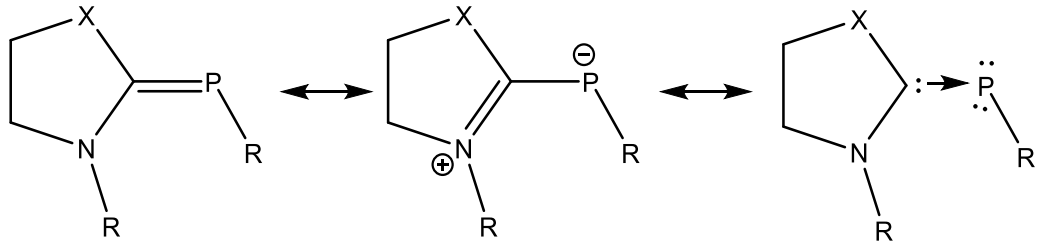

Scheme 15. Resonance structures and representations for carbene-phosphinidene adducts.

With this in mind, results by Roy *et al*. provided support for stabilized phosphinidene by a reaction of cAAC (**II-65**) with PCl_3 to yield two isomers of phosphinidenes (**II-66** and **II-66'**, Scheme 16). These two conformational isomers bore different C-P bonds in chlorophosphinidene,[79] characterized by X-ray crystallography, mass spec, and NMR, and both retain the singlet ground state.

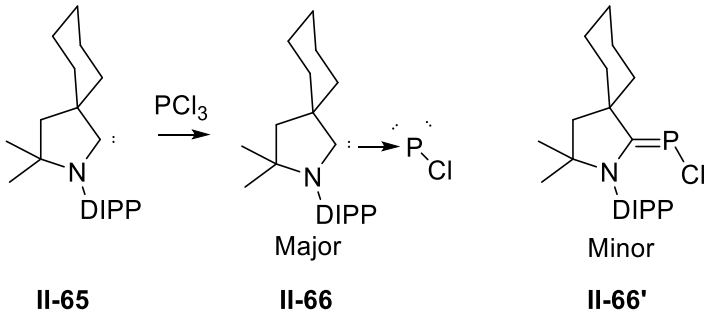

Scheme 16. Isomers of chlorophosphinidenes.[79]

The reactivity of germylenes and stanylene has been well researched over the past 40 years, whereas stable lighter analogues were only reported in the 1990s. Dialkyl(aryl) substituted silylenes and germylenes both tend to dimerize. Silylenes form strong Si=Si bonds and require

external stimuli for cleavage to the silylene, whereas germylenes may exist in an equilibrium with the dimer, which speaks to the relative stabilization of the lone pair and can be explained by a couple factors. Dimerization of these carbene analogues is affected by the size of the singlet-triplet gap of the carbene, and the dissociation energy of the E=E bond. The singlet-triplet gap of group 14 carbenoids is dependant on the substituents and the electronic factors. For example, Arduengo type- carbenes, silylenes, and germylenes were calculated to have singlet-triplet gaps in the order of GC<Si<Ge, which is the opposite trend of the calculated energies for H_2X: or $(NH_3)_2X$: (where X=C<Si<Ge). [80] The choice of substituent of ERR' also has a dramatic effect on the dissociation energy and lowering of the singlet-triplet gap by widening the R-E-R' angle. As already shown earlier, a germylene disubstituted with bulky σ-donor ligands was successful in activating H_2 and NH_3 (Scheme 3).[21] The heavier tin analogue, however, was not amenable to H_2 activation, while ammonia underwent N-H activation and elimination of the proteo-aryl ligand. [21] Another use of a bulky bis(aryl) germylene was seen in the activation of Zn-C bond of $ZnMe_2$, which exemplifies the carbene-like nature of this species. This would afford a Ge(IV) by insertion into the Zn-C bond of $ZnMe_2$.[81]

The first NHGe which reacted with an organic reagent (in this example, two equivalents of silylazide) produced a five-membered tetra-azo germanium compound. [82] Other germanium (II) compounds may react by substitution of labile groups by other bases, insertions as seen for carbenes, coordination as bases themselves, and di-germylene complexes may act cooperatively to facilitate addition reactions, such as reaction with diazo compounds, which undergoes concomitant cleavage to yield a 1,2-digermylene hydrazine. For a review of group 13 and 14 heterocyclic carbene analogues and their reactivity, see reference [60], and for a review of aluminum (I) , silicon (II), and germanium (II), see reference. [83].

Reactions of NacNacGe complexes are also of interest, as it applies to non-innocent ligands. The germylene chloride **II-67**b reacts with 3,5-di-tert-butylorthoquinone to yield a germanium (IV) (**II-68**)[84], whereas reductions of the chloride are dependent on the ligand framework, and tuning the ligand may facilitate N-H activation of NH_3 (see references from Scheme 17). Similarly, the silylene analogue with an unsaturated backbone also reacts with NH_3 and P_4.[17]

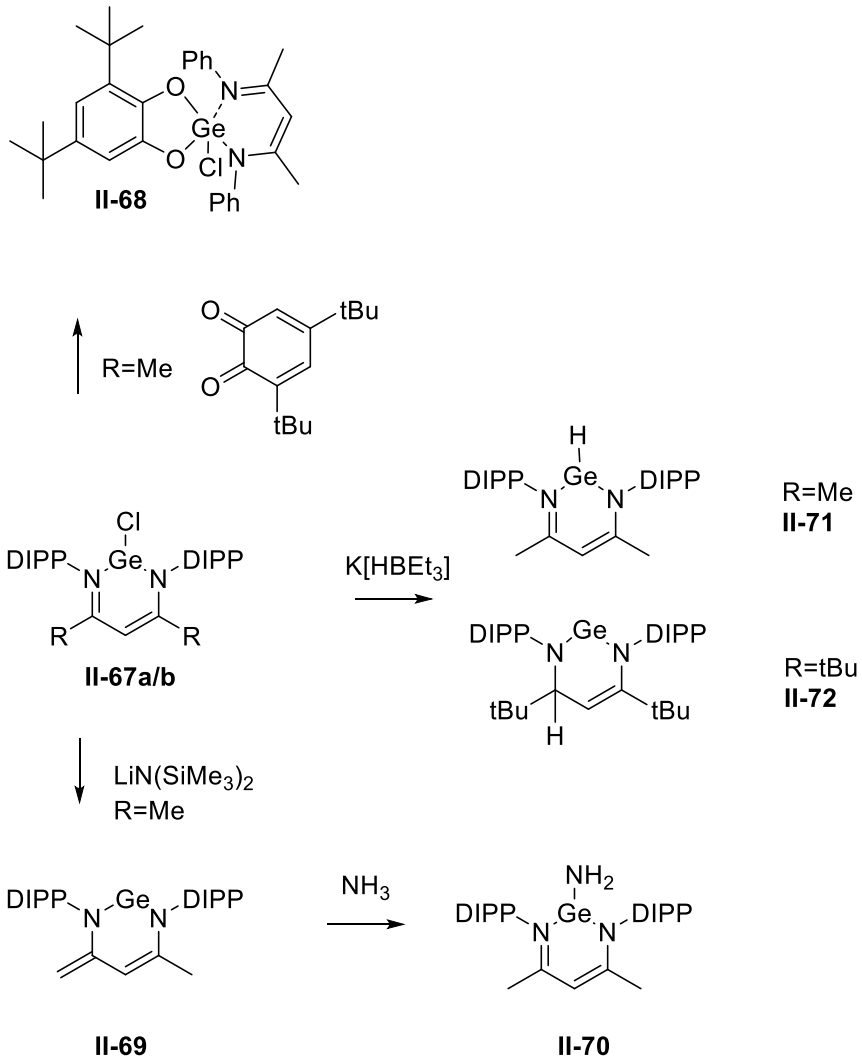

Scheme 17. Various NacNacGe chemistries.[84–87]

Another unprecedented reaction was reported by Driess, by using a bis(NHC) silylone (0) stabilized by $GaCl_3$ (**II-73**, Scheme 18). This compound reacted with Se_8 and was used to prepare a trapped form of a heavy analogue of CO based on silicon (**II-74**). Previously, the only examples of heavier congeners of CO required cryogenic matrices at low temperature or dilution in the gas phase at high temperature. Similarly, changing the stoichiometry of Se_8 as well as a reaction with $TeP(nBu)_3$, yielded heavy CO_2 analogues **II-75** and **II-76** respectively.[88] This same framework was successful for producing germylones as well. While reactions of metallones is outside the scope of this historical, an interesting example of the reactivity of these compounds is their ability to function as bases in forming strong donor-acceptor adducts. With this in mind, a bis(N-heterocyclic silylene)pyridine was able to stabilize a germylone with $FeCl_4$ adduct, and insertion of $GeCl_2$ to this species yields a push-pull Ge(0)→Ge(II)→$Fe(CO_4)$.[89,90]

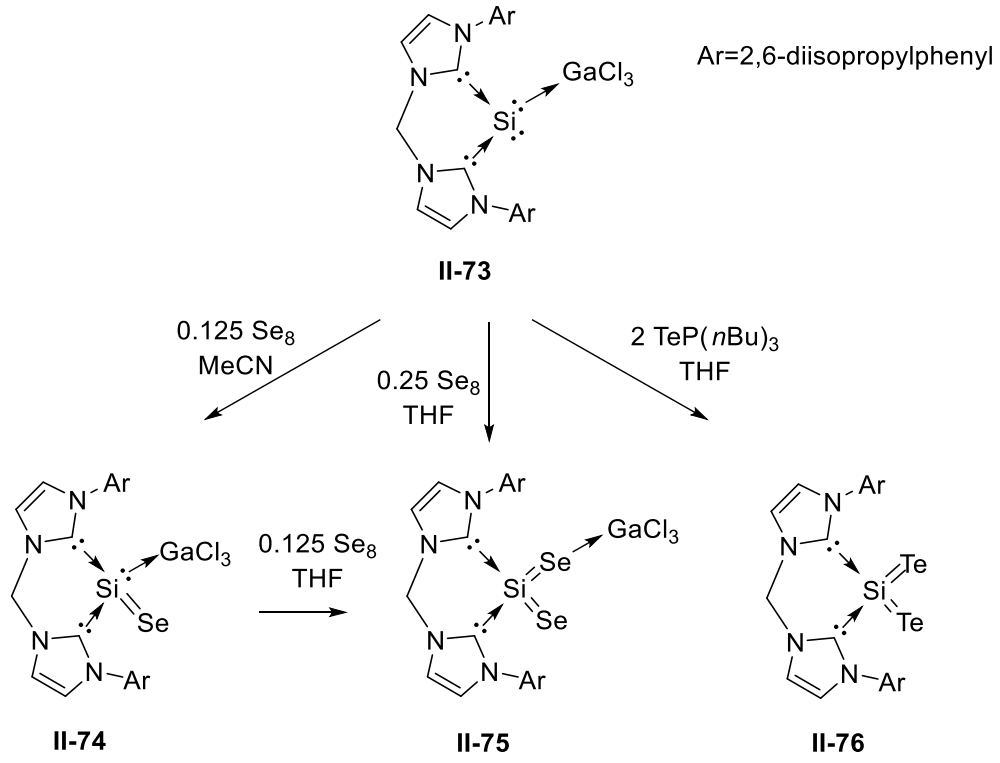

Scheme 18. Preparation of stabilized heavy analogues of CO and CO_2.

II.1.5 Small Molecule Activations by Group 15 Compounds

The first example of bicyclic 10-P-3 (meaning formally 10 electron, 3-coordinate phosphorus) compound (5-aza-2,8-dioxa-3,7-di-*tert*-butyl-1-phosphabicyclo[3.3.0]octa-3,6-diene, ADPO, **II-77**) was reported by Culley and Arduengo.[91] Assignment of an oxidation state of phosphorus in this compound presents a challenge, and the ambiguity was originally termed electromorphism. A typical phosphine with three donor ligands and one lone pair would be expected to have eight valence electrons and have a tetrahedral geometry as P^{III}, while a two-electron reduction will yield a formally dianionic P^{I} complex (phosphinidene) with a T-shaped geometry. A tridentate ligand in this case should occupy the meridional position. The ONO ligand framework presented here may act to stabilize charges internally, and thus may be planar or bent in different phosphorus complexes. The electromorphism is thus another manifestation of ligand non-innocence and demonstrates a ligand's ability for internal charge compensation[92]. Therefore, compounds able to adopt different geometries may be envisioned to also participate in electron density transfer and undergo charge delocalizations. The unsaturated ONO ligand was applied to various main group metals, and an interesting consequence of this framework is the ability to form a hypervalent, three-membered four-electron bonds when the system is planar. Thus, this description of a T-shaped phosphorus bears ten electrons here, while the bent geometry bears eight electrons.

Due to symmetry incompatibilities of an out-of-plane empty p-orbital (associated with a neutral, zero-charged species), known three-centre-four-electron bonds, and the in-plane N-P and phosphorus lone pair utilizing s-orbital and in plane p-orbital, the zero-formal charge planar representation for 10-P-3 is not compatible. Other remaining representations (Scheme 19) further highlight the P^{I} character for a planar structure, and P^{III} for the bent electromorph. Furthermore,

the planar structure bearing ten electrons should be considered for greater ability to activate small molecules based on the increased electron density. (Scheme 20) This is an example of the second class of non-innocent ligands mentioned above, but again, while the term oxidation state is poorly defined, the utility of this electron rich species should not be discounted.

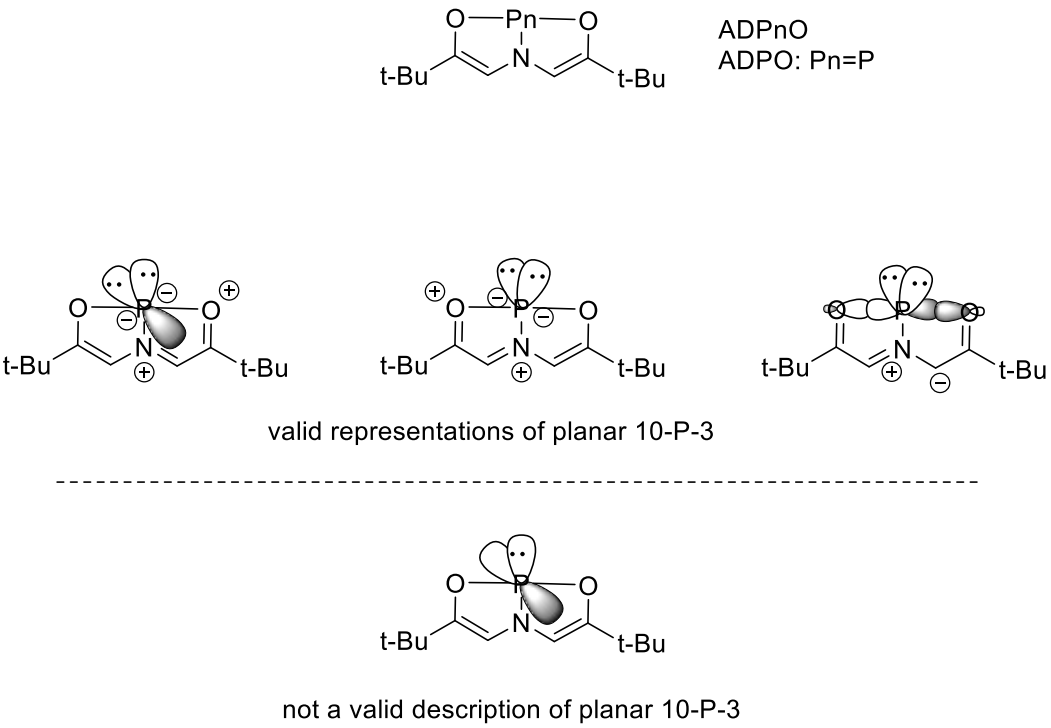

*Scheme 19. Best descriptions of orbitals in ADPO (**II-77**).*[92]

Furthermore, as these structures will have different ground state energies, the barrier for inversion may be measured. It is believed that the neutral ONO ligand species of the ADPO system would likely be a transition state for inversion as it would be unstable if planar.[92]

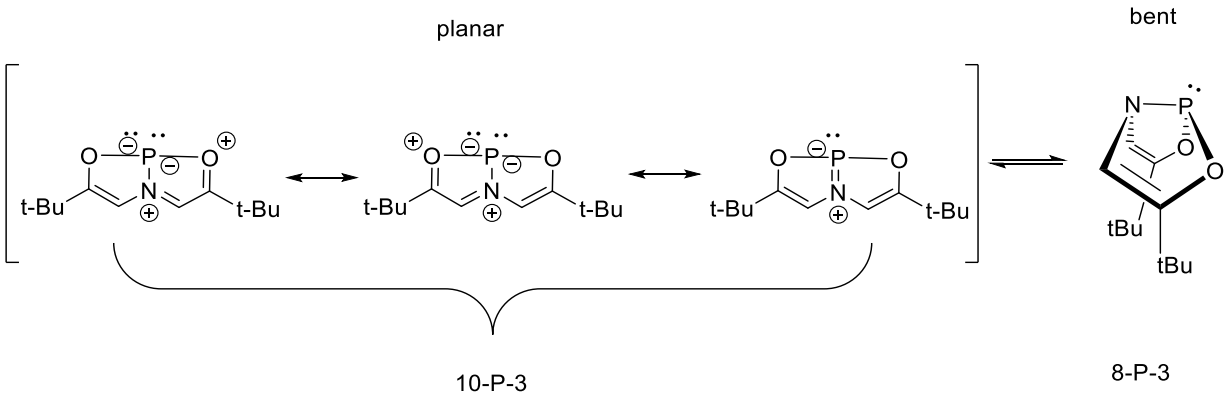

*Scheme 20. Electromorphic representations for ADPO (**II-77**) by Arduengo III.*[91]

The ***II-77*** system reported by Arduengo is planar, but there are other reported three-coordinate phosphorus compounds which adopt a bent geometry such as saturated analogues by Wolf[93]. Similarly, instead of observing planar, bicyclic phosphine structure analogues when the ligand is a modified to bis(phenoxlyamine), bridged dimer coordinated to two boranes is observed (Scheme 21). While many saturated P(ONO) systems undergo oligomerization quite rapidly[94] (slow-reversible dimerization for unsaturated ADPO by Arduengo[92]), stable analogues have been reported[95].

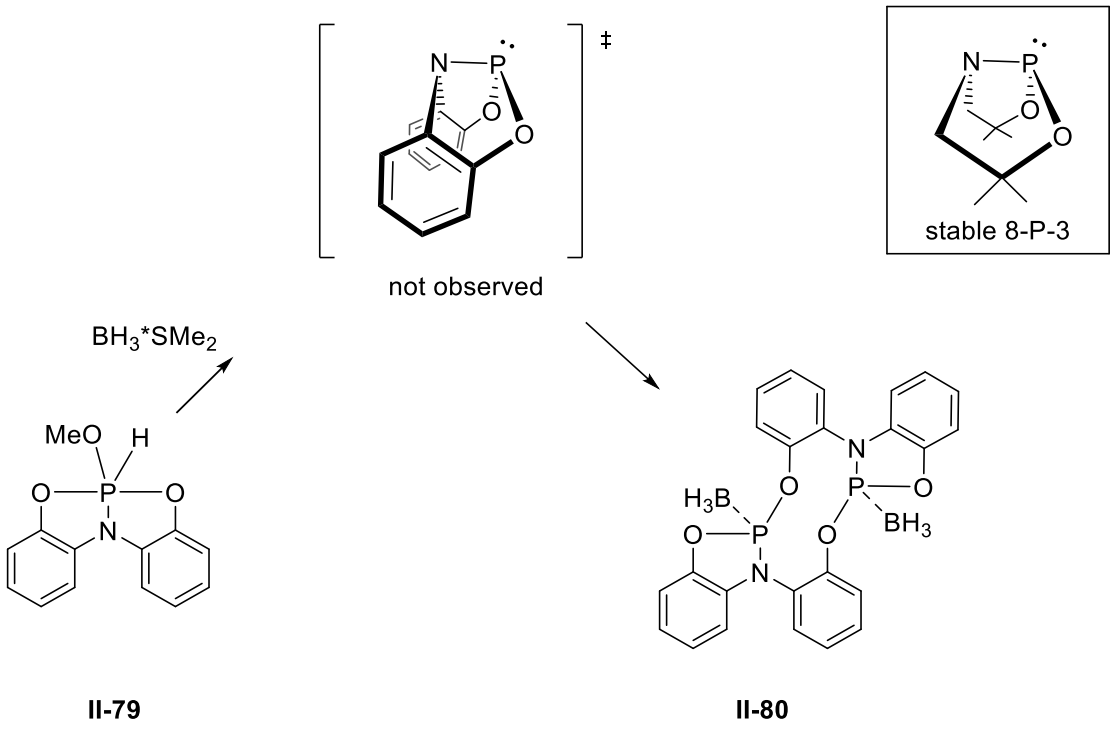

Scheme 21. Bent 8-P-3 implicated as transition state in dimerization.

This compound was then re-examined roughly 20 years later by Radosevich *et al*. to demonstrate the utility of this fascinating system. Transfer hydrogenation by P^{III}/P^{V} with ammonia borane for catalytic transfer hydrogenation of PhNNPh to PhNHNHPh was developed (Scheme 22). This reaction does not seem to have any other measurable intermediate, except for the **II-81** species. The authors only observed the formation of the P^{III} species by time lapsed NMR, which implies that a reductive mechanism is not a simple reductive elimination where the substrate inserts followed by a reductive elimination. [96].

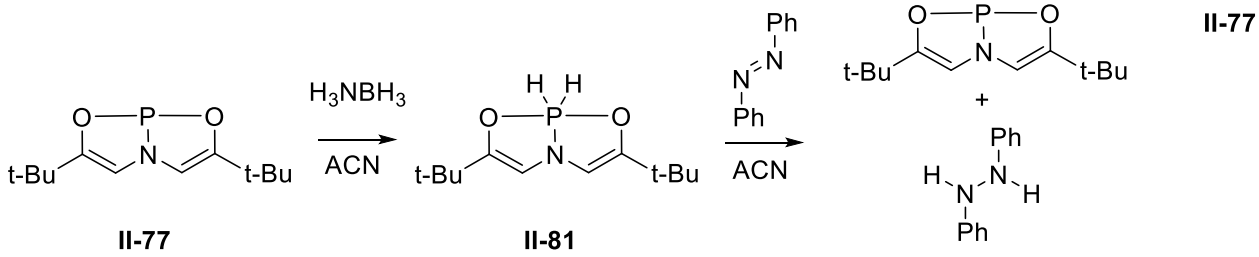

Scheme 22. Transfer hydrogenation with ONO P^{III}/P^{V}.

Later, this was also found to activate ammonia, alkyl amines, and aryl amines by N-H oxidative additions.[97] The ***II-77*** system was able to react with various dicarbonyls (**II-82** and **II-83**), and activate the sp^3 C-F bond of a strained perfluoroepoxide.[98] These systems are quite susceptible to hydrolysis to give the neutral ligand (**II-86**). Protonation of the **II-77** system by one equivalent of acid would selectively open one arm, as the reverse reaction to the saturated ketone. Similarly, reaction with an alcohol proceeds via a five-coordinate P^{V} intermediate (**II-88**), which then rearranges to yield the P^{III} compound with a transfer of proton (**II-89**). Oxidative cyclization of **II-77** with an orthoquinone leaves the ONO ligand in a bent geometry. Furthermore, biacetyl

effectively undergoes addition to the ligand backbone to produce an 8-P-3 system with a bent geometry (Scheme 23).[96,99]

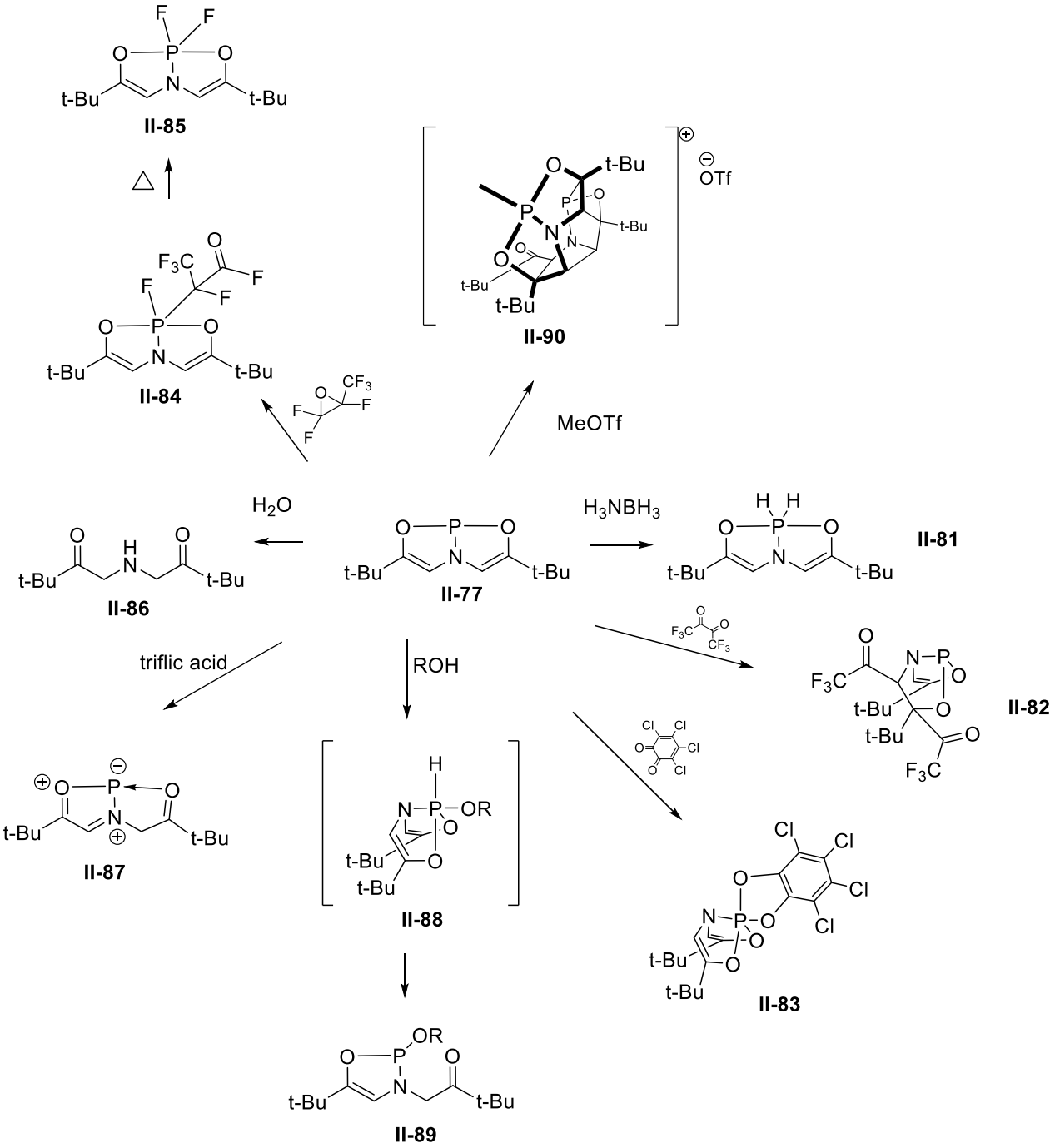

Scheme 23. Various reactions of ADPO complex.

Driess *et al*. showed that if methyl triflate was used instead of triflic acid, a methylated phosphonium could be formed, but undergoes a domino cyclization with another equivalent of ADPO to yield a pentacyclic, caged, methylated phosphonium species **II-90**. [100] This is due to the nucleophilic nature of the starting phosphinidene and the delocalization of charge, which makes the backbone susceptible to C-C bond formation at the expense of the double bond.

This system also proved to be nucleophilic for stabilization of transition metal complexes. **II-77** binds to silver in a new coordination mode, [101] as well as to manganese and iron carbonyl complexes. The IR spectrum of ADPO-Fe(CO)$_4$ showed the CO bands at higher stretching frequencies than for trimethylphosphite, indicating the decreased accepting ability of the bent ligand. [102]

Similarly, this same ligand was used to stabilize related pnictogen compounds (ADPnO) 20-Bi-9 (**II-91**)[103], as well as the first 10-As-3 (**II-93**).[104] However, moving up the group, the nitrogen coordinated ONO could not be obtained, but the related N-nitroso has been isolated. Thus, with size, the ability to undergo disproportionation increases, and bismuth may adopt such a high coordination number, even following the same procedure as the lighter analogues. (Scheme 24)[99]

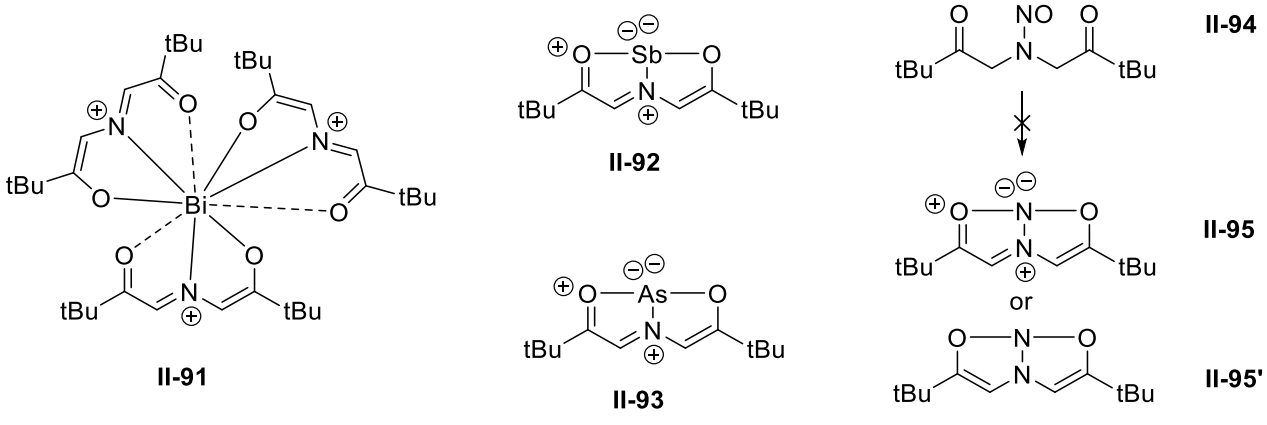

Scheme 24. Various ADPnO compounds.

Another report from Arduengo was a neutral tricoordinate phosphorus with a NNN pincer ligand (**II-96**). This C_s symmetric species was able to undergo oxidative addition with alcohols, phenols, carboxylic acids, amines, anilines, which was proven to be reversible at elevated temperatures for volatile alcohols and amines. (Scheme 25) Since the ground state here also has a bent ligand, the inversion energy was measured to be ($\Delta G^{\ddagger exptl}_{298}$ =10.7(5) kcal/mol) by variable temperature NMR. Furthermore, DFT calculations found a metastable C_2-symmetric intermediate for inversion. [105]

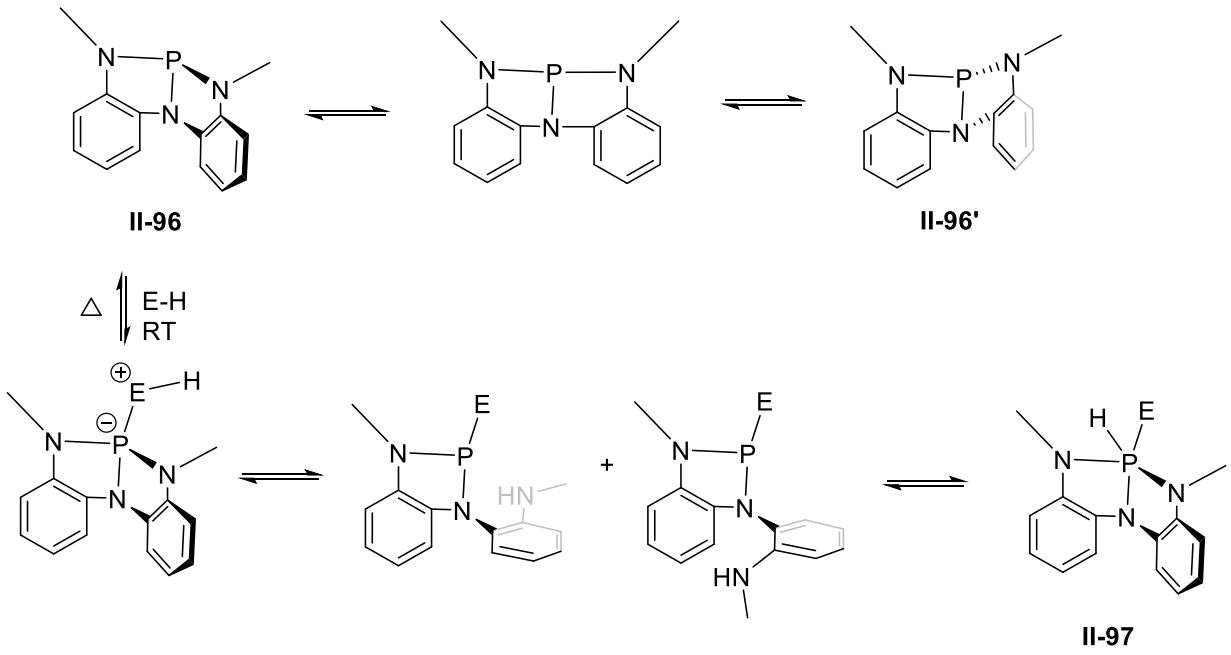

Scheme 25. Proposed pathway for oxidative addition of O-H and N-H bonds at phosphorus.

An NPN system akin to **II-77** by Arduengo, was reported by the Kinjo group. This species has two tricoordinate phosphorus atoms and demonstrates catalytic activity (Scheme 26). Uniquely though, the donor atoms were replaced by stronger nitrogen donors, and the apical position were replaced by phosphorus. [106,107] This also facilitates a bent geometry with sp^3 hybridized

phosphorus atoms in the starting compound. As a common theme for these systems, this compound was shown to activate NH_3 at room temperature (**II-99**, Scheme 26).[106] Kinjo *et al.* also investigated coordination, photoisomerization, ammoniaborane activation (**II-100**), and oxidation of this complex (**II-102**).[107] Furthermore, activation by cooperative interaction with the ligand backbone, where one amido arm becomes protonated and dissociates, while generating an aza-phosphane, and subsequent ligand isomerization to the imine-substituted P,N bidentate complexes, is seen in Scheme 26.[107]

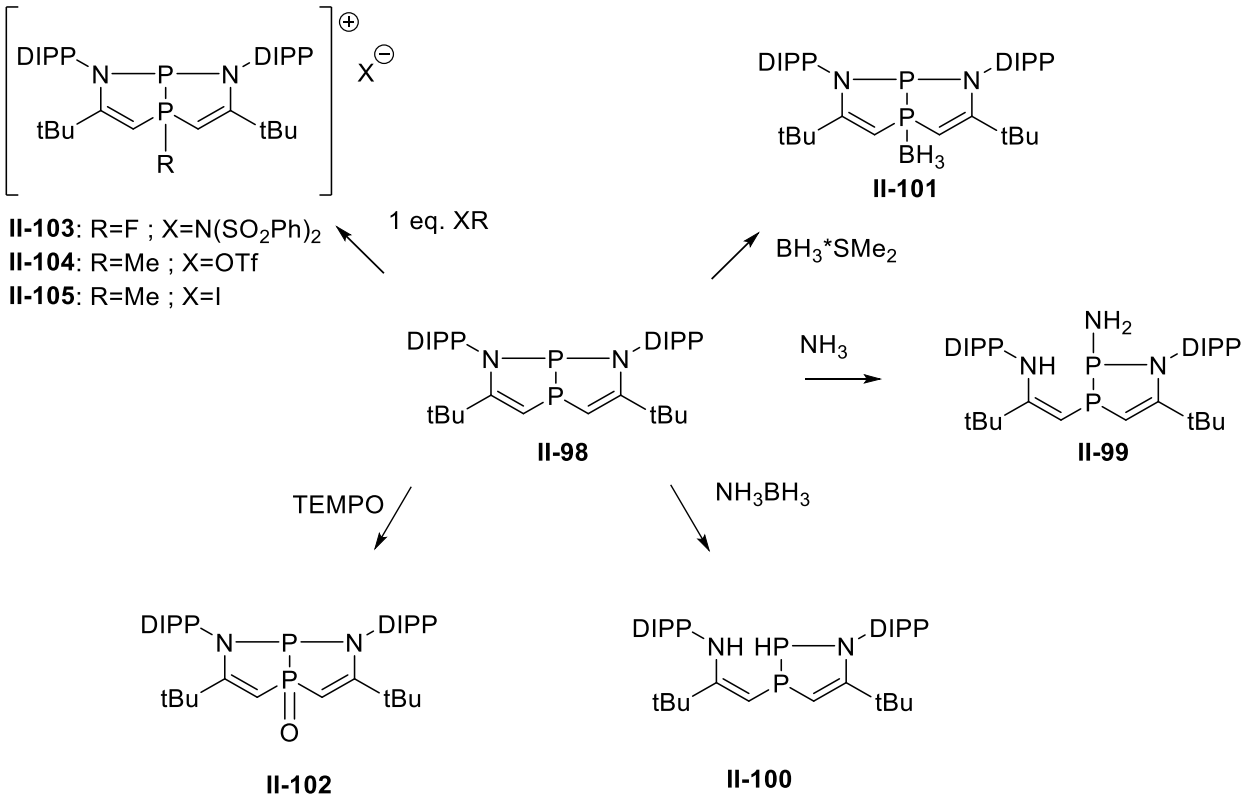

Scheme 26. Kinjo system- metal-ligand cooperative activation of ammonia.[106,107]

On iron, work was done with a redox active bis(di-*tert*-butylphenoxyl)amine ligand **II-106**, which enabled coupling and reductive elimination of di-*tert*-butyldisulfide. Reactions of o-

chloranil could also be performed. While remaining planar in all cases, this ligand serves to maintain a formal +3 oxidation state at iron (Scheme 27 left). [108] The same ligand on phosphorus, (**II-108**) presented by Aldridge, was used for activation of water and NH_3 by oxidative addition at phosphorus. Unlike the ADPO systems, the inability of proton transfer from phosphorus leaves the pentacoordinate phosphorus intact. Upon heating however, dehydrocoupling can occur to generate the dimeric species (Scheme 27, right).[109]

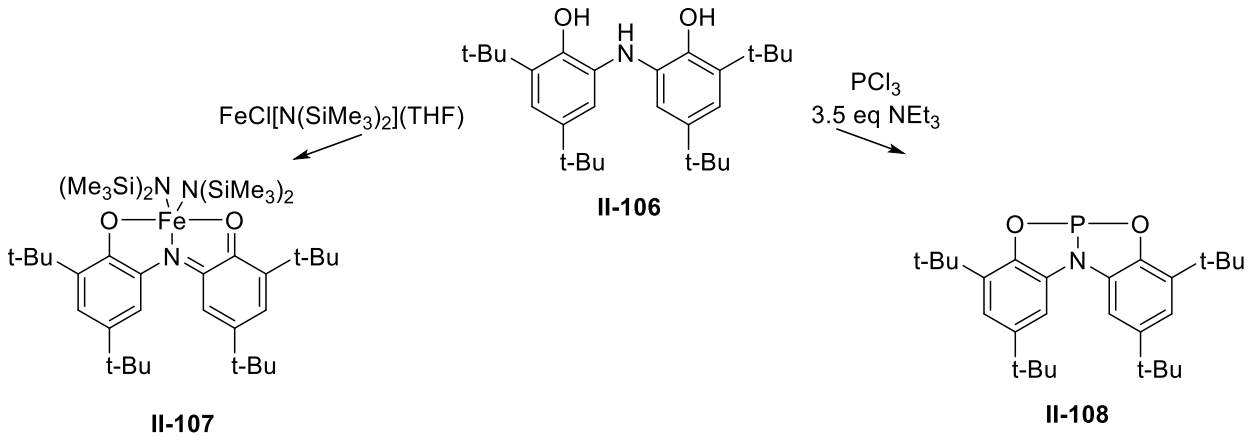

Scheme 27. Compounds of redox-active ligand bis(3,5-di-tert-butyl-2-phenol)amine.

Another planar phosphorus compound, a rigid CCC ligated phosphorus **II-109**, protected by bulky silanes also showed similar electronic delocalization. A bimetallic gallium compound was reacted with excess n-BuLi then reacted with PCl_3. [110] The phosphorus centre could act as a nucleophile to AuCl or $PdBr_2$(NHC), or could be oxidized by $SOCl_2$ or Br_2, which would provide access to a cationic phosphorus species upon treatment with Lewis base. The species was also able to react with sulfur and selenium generating a cationic phosphorus and ring expansion by insertion of one of the chalcogens to the P-C bond. The structure did not deviate much from its parent

compound when coordinated to gold or sulfur, however. Reaction with XeF_2 generates a difluorophosphorus compound **II-110** (Figure 9).[110]

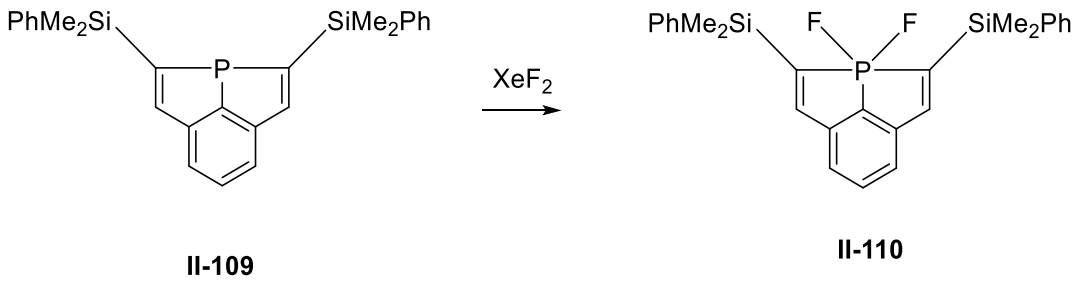

II-109 **II-110**

Figure 9. Rigid CCC ligated phosphorus.

For a very recent review of three-coordinate phosphorus systems with geometrically constrained ligands, see reference [11]

II.2 Zinc Catalyzed Cross-Coupling

In organic syntheses, chemoselective reactions of substrates bearing specific functionalities mediated by a metal catalyst are quite invaluable. The coupling reactions developed by Suzuki, Heck, and Negishi resulted in the shared winning of the 2010 Nobel Prize in Chemistry. These pioneering reactions involved palladium (0) catalysts with either an aryl or alkyl halide. Negishi coupling arose in efforts to amend the poor functional group tolerances and chemoselectivity of reactive Grignard reagents in Kumada-Corriu coupling, and instead of organozirconium or organoaluminum reagents, even less reactive organozinc reagents were used.

Organozinc reagents have also been known for decades to be useful reagents for alkylation and arylations, and require milder conditions than Grignard and organolithium compounds. These reagents have commonly been employed for their ability to undergo transmetallation, and thus have been used in the Negishi cross couplings. The downside to these reagents is that stoichiometric or greater amounts are often required, and thus the reactions produce a lot of waste. While cross couplings on palladium have been studied extensively, zinc catalyzed cross coupling reactions remain scarce. The requirements for coupling reactions catalyzed by zinc should be a nucleophilic R group, and the ability to regenerate the group. As mentioned, organozinc reagents have been readily used for alkylation and arylation reactions, but regeneration with cheap reagents for catalytic application remains problematic.

The application of zinc as a catalyst for cross-coupling reactions has not developed much. Papers from 2010-2016 related to generation and reactivity of organozinc reagents, including their role in cross-coupling, have been briefly reviewed.[111] A recent, more tailored use of zinc catalysts for synthesis of heterocycles has been discussed.[112] A review on zinc-catalyzed bond-forming reactions is also available.[113]

Common pathways for zinc-mediated coupling reactions involve single electron transfer (SET) reactions or could proceed by nucleophilic aromatic substitution mechanisms. Despite the large amount of zinc reagents required, there are also many examples of C-C bond forming reactions utilizing catalytic zinc agents, although their role tends to be as a Lewis acid catalyst. There are plenty of examples of zinc Lewis acid catalyzed reactions, such as aldol and lactone polymerization, but the discussion of those largely remain outside the scope of this historical.

Selective activation of C-I bonds by zincate was shown to be useful, as the chemistry is related to Grignard and lithium reagents but has higher thermal stability. While there is no reaction of $ZnEt_2$ with aryl iodides, the reaction was proven to be solvent dependant, as a mixture of Et_2O and N-methylpyrrolidinone allowed conversion at room temperature. The authors also had conversion of pentafluoroiodobenzene to pentafluorobenzene and iodomethane with the use of $ZnMe_2$ and LiCl, and noted how the reaction fails to proceed in the absence of salt, thus highlighting the requirement of stoichiometric zincate with catalytic lithium(acac).[114] The mechanism proposed involved the *in situ* generation of a zincate after the first zinc-iodine exchange, which increases the reactivity and thus speeds up the conversion (Scheme 28). This was successful for aryliodides containing both electron donor and acceptor functionalities, as well as heteroaromatics.

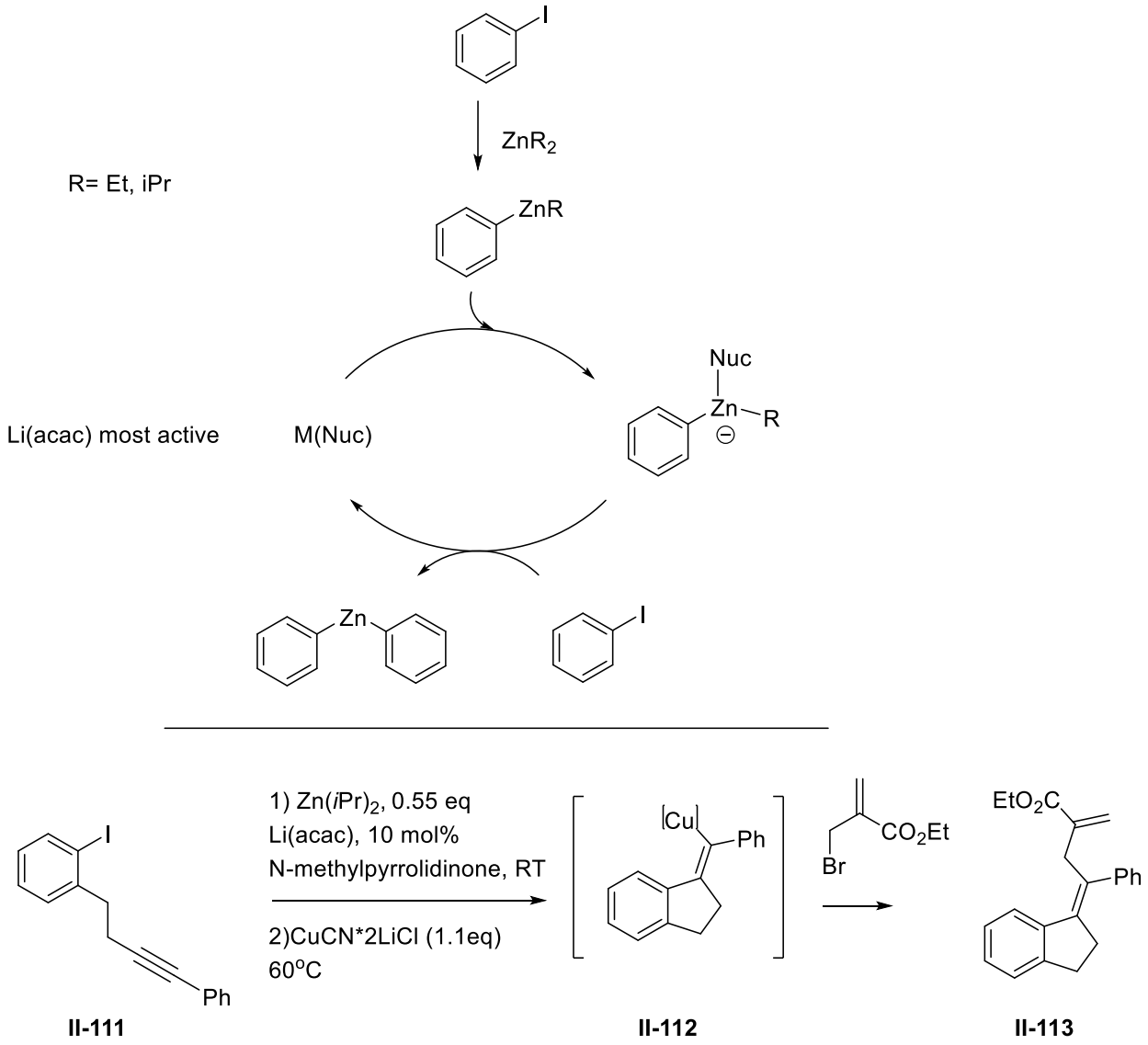

Scheme 28. First example of nucleophilic catalysis of the iodine-zinc exchange reaction, and example of a reaction utilizing zinc-halogen exchange.

Other examples of organozinc reagents undergoing coupling reactions without a transition metal catalyst involve activation via single electron transfer (SET). Alkylzinc reagents have been demonstrated to undergo coupling with aryliodides[115], and alkynylzinc reagents couple with aryl and alkenyliodides via SET.[115] These reactions proceeded with the use of a sub-stoichiometric

amount of $ZnEt_2$ pre-catalyst. The suggested plausible catalytic system proceeds via the mono- or bis- alkynylzinc complex with a phosphine activator. (Scheme 29)

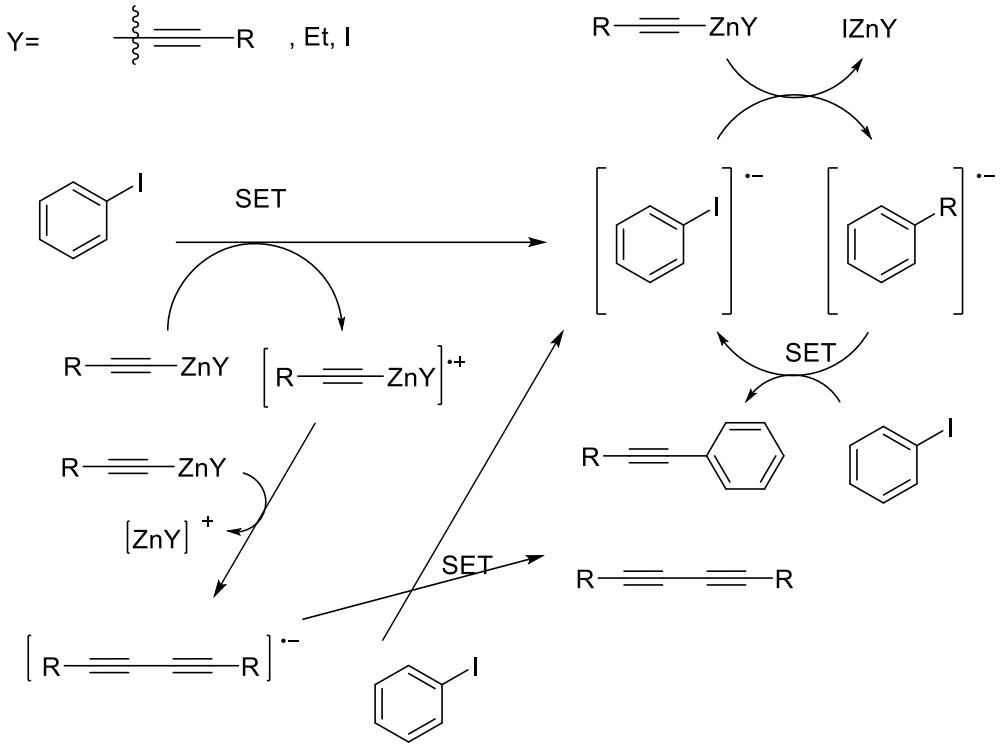

Scheme 29. Mechanism for coupling of alkynylzinc reagents by single electron transfer.[116]

A simple system of 5% Et_2Zn in the presence of 10% DMEDA (dimethylethylenediame) was successful in Sonogashira type coupling of phenoliodides and terminal alkynes to yield the benzofuran derivative. A mechanism was suggested but not backed by any evidence, and thus further studies are required. The authors believe that the catalyst forms by reduction of $ZnEt_2$, i.e. a Zn^{II} species, with two equivalents DMEDA to Zn^0, which then reacts with aryl-iodide by oxidative addition to zinc, substitution by deprotonated alkyne, followed by reductive elimination to a species that spontaneously cyclizes. This system by Anilkumar *et al*. manifests the first example of $C(sp^2)$-C(sp) cross coupling catalyzed by zinc, coupling of an aryliodide or aryl bromide with a terminal alkyne proceeding in moderate yields at 125°C in 24 hours.[117] They also

reported a similar reaction of terminal alkynes with 1-bromo-alkynes to yield C(sp)-C(sp) coupled diacetylenes[118].

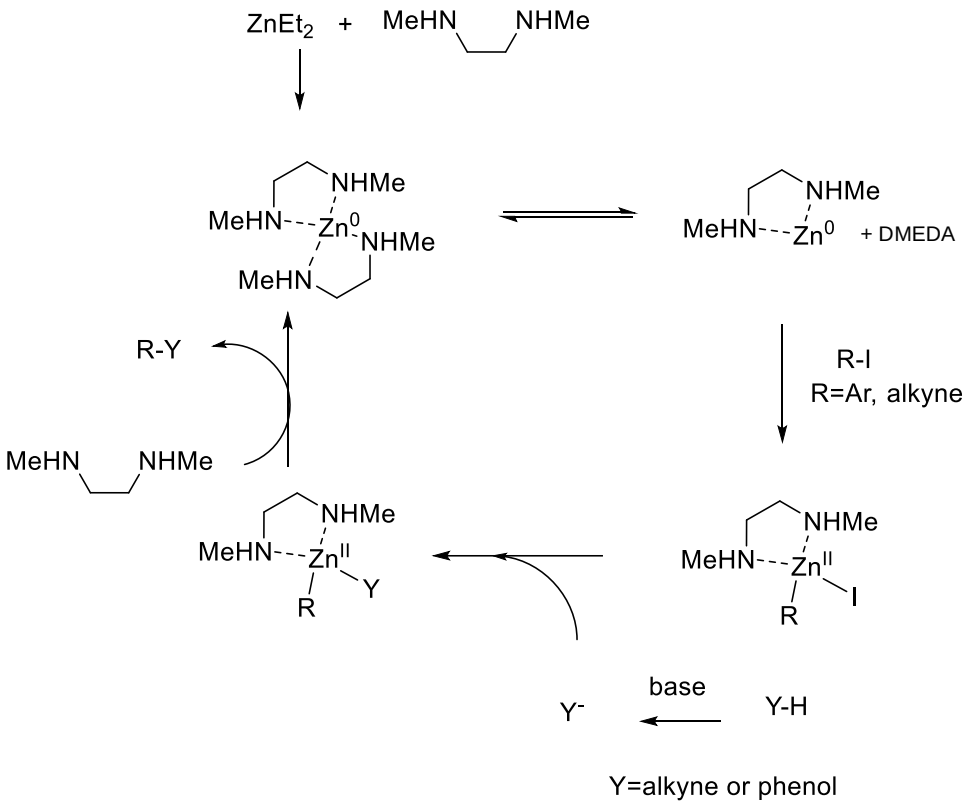

Scheme 30. The proposed mechanism for coupling reactions of aryl iodides/alkynes with terminal alkynes/phenols.[118–120]

Problems with this proposed mechanism include the following: a) Zn^0 compounds are rare and difficult to stabilize; b) Zn^{II} catalysts are understood to proceed through mechanisms which do not involve oxidative addition of a substrate to zinc; and c) the charge balance is not met, as an Et^- fragment could be susceptible to protonation. To demonstrate the difficulty in generating Zn^0, Roesky reported $(cAAC)_2M$ complexes, and showed that even $(cAAC)_2Zn$ bearing strong donor/acceptor cAAC ligands (often used to stabilize low oxidation state compounds due to their

small HOMO-LUMO gap) remained in the +2 oxidation state over +0. This was confirmed by EPR, magnetic susceptibility, and supported by theoretical calculations.[121] Next, while thermal decomposition of diethyl zinc is possible, thus study showed that decomposition does not occur below 230°C while under He or H_2 atmosphere.[122] The conditions utilized by Anilkumar of 145°C under N_2 does not seem sufficient to warrant thermal decomposition to zinc (0). Thus, the proposed mechanisms, which describes zinc 0/2 cycling, seems unlikely.

II.3 Project Goals

The goals of this project were to i) synthesize a novel tridentate non-innocent ligand framework, which may participate in charge stabilization; ii) apply the ligand to prepare novel main group compounds (ie. zinc, germanium, and phosphorus); iii) functionalize the compounds to species which could potentially be used for bond activations and cross-coupling reactions, and screen reactivity.

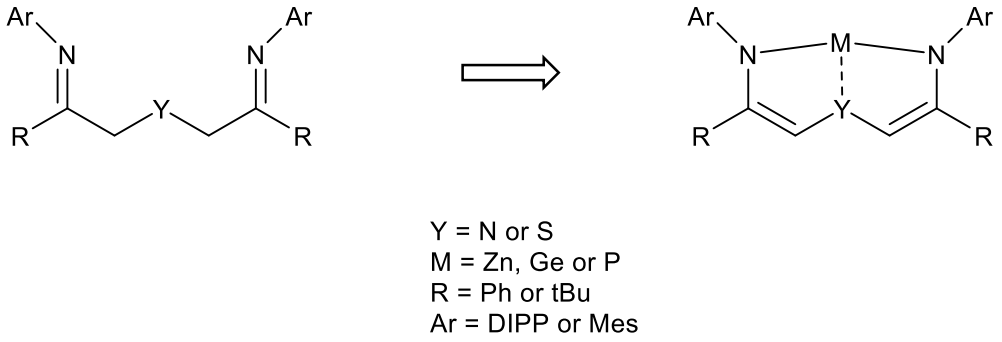

Scheme 31. Target ligands and main group compounds.

III. Results and Discussion

III.1 Ligand Synthesis

The main objective of our work was to design new NYN ligands, where Y is a donor atom, to stabilize main group elements in unusual oxidation states and/or geometries that would make them active in catalysis. The well-known ADPO species developed by Arduengo *et al*., and the pioneering work of the Radosevich group with **II-77** on the application of this phosphorus complex in the activation of small molecules and catalysis, as well as a small library of ZnOSO of catalysts for hydrosilylation of ketones served as inspiration for this project.

Surprisingly, no examples with stronger acyclic σ-donors replacing oxygens could be found in a literature search, except for a patent filed by Tohi, Matsui, and Fujita on Nov 6, 2001 of Waki-Cho (JP), which does describe a library of NYN (where Y is from Group 16) complexes of Group 8-11 metals, developed for applications in olefin polymerizations.[123] The use of a stronger σ-donating ligand may lead to increased activity at the metal centre for oxidative additions, or for increasing hydridicity of M-H bonds in the case of a metal hydride complex. Further, the ligand may also help to promote a possible reductive elimination step in a catalytic cycle by weakening the M-R bond or by stabilizing a lower coordination-number species produced by reductive elimination. Similarly, stabilization may occur by reorganization of the relatively flexible ligand framework, or by internal charge compensation of a potentially redox active ligand.

As an aside, it is worth mentioning that related complexes of the ONO ligand have been used for many main group metals. One example revealed a unique process which a silicon complex bearing a sterically demanding Si(*t*Bu)$_3$ group attached to a silicon centre, dimerized at low temperature by radical proton abstraction of THF. (Scheme 32)[124] With this in mind, it is also

possible that protonation of these novel NYN complexes could be considered if unusual decomposition occurs in THF.

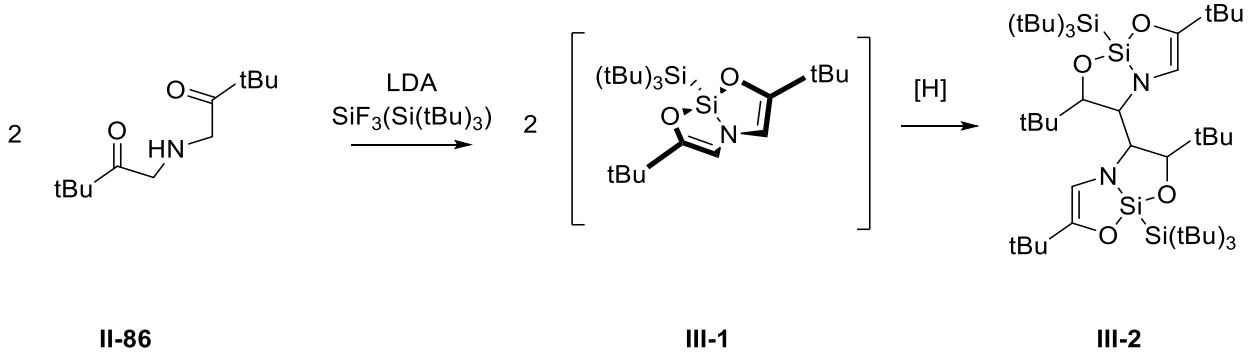

II-86 **III-1** **III-2**

Scheme 32. Dimerization of SiONO species.[124]

III.1.1 Attempts to Synthesize the NNN ligands

As stated above, one of the goals of the project was to create bulky, tridentate chelating ligands with strong donors which would be capable of internal charge stabilization and thus have a potential use in bond activations and catalysis (Figure 10). As seen earlier, bulky groups on β-diketiminate ligands have served to maintain monomeric metal complexes, and so a similar approach was to install the N-Aryl functionality. Based on analogy with the Arduengo ONO (**II-86)** framework, we envisioned the strategy schematically presented in Scheme 33.

Ar= a) 2,6-diisopropylphenyl, b) 2,4,6-trimethylphenyl

R= tBu:	**III-3(a/b)**	**III-5(a/b)**
R= Ph:	**III-4(a/b)**	**III-6(a/b)**

Figure 10. Target ligands.

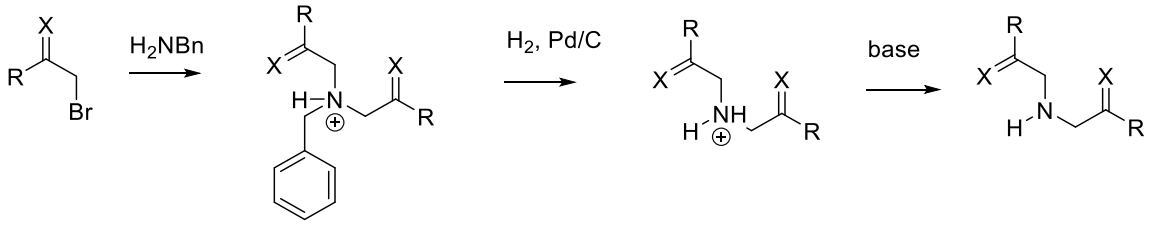

X=O				
R=tBu	**III-7**	**III-9**	**III-11**	**II-86**
R=Ph	**III-8**	**III-10**	**III-12**	**III-13**
X=N-Ar				
R=tBu	**III-14(a/b)**	**III-16(a/b)**	**III-18(a/b)**	**III-3(a/b)**
R=Ph	**III-15(a/b)**	**III-17(a/b)**	**III-19(a/b)**	**III-4(a/b)**

Scheme 33. Ideal route for synthesis of XNX based ligands.

As seen in Scheme 33, the crux for the synthesis is the α-brominated carbonyl compound. The initial plan was to form the corresponding imine followed by selective alpha-bromination. As there were no reports in the literature for the direct, selective α-bromination of methyl-imines, analogies were drawn from ketone chemistry.

The main challenges of the brominations were over-bromination (chemoselectivity) and regioselectivity. While a multitude of conditions were attempted (Scheme 35), a common issue was that the bromination at the para position of the N-Ar ring was preferable to the designed mono-bromination of the methyl group. Thus, the imine Mes-N=C(Me)(Ph), which has the para-position

blocked by methyl, was targeted to circumvent the para-bromination. This imine appeared to be easily prepared by direct condensation with acetophenone. While NMR analysis suggested that bromination was successful, the isolation was troublesome as the compound decomposed during vacuum distillation with the Kügelrohr at high temperatures.

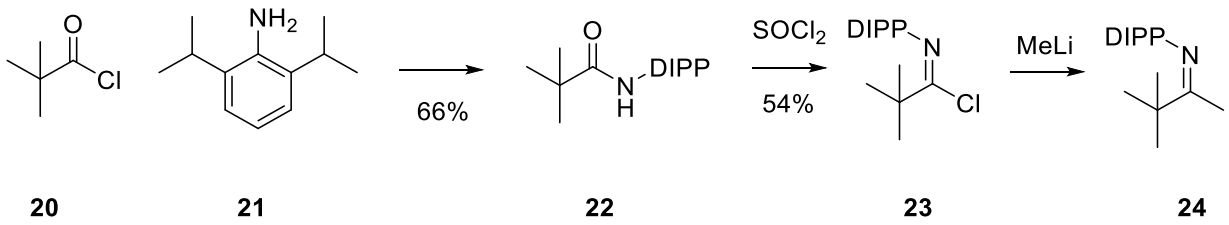

20 **21** **22** **23** **24**

Scheme 34. Synthesis of bulky tBuC(=N-DIPP)Me.

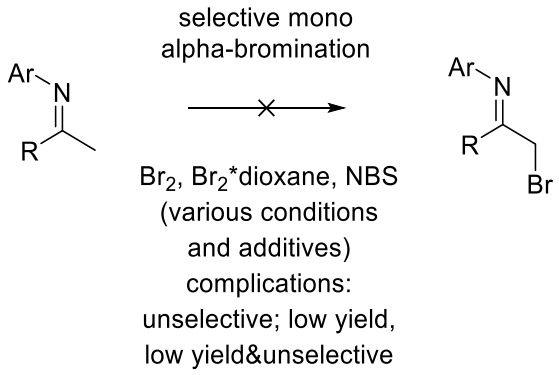

Scheme 35. Attempted unsuccessful brominations of the imine.

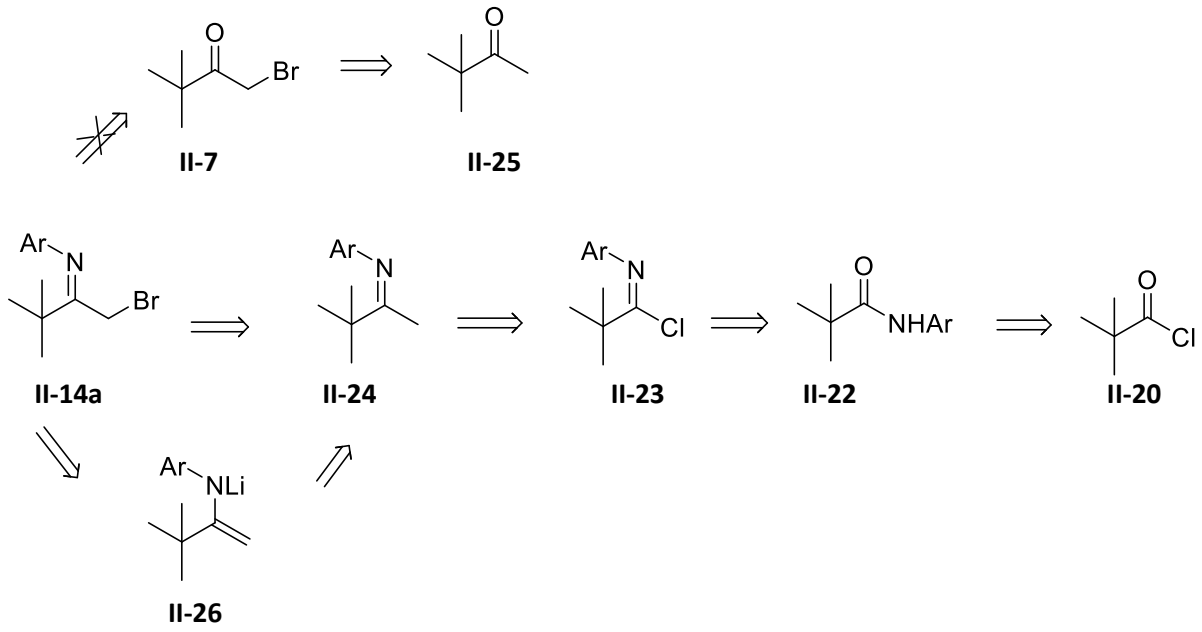

Scheme 36. Retrosynthetic pathways for t-butyl substituted α-bromoimine.

Another attempt was made by first deprotonating the imine with LDA, followed by bromination. The idea behind this approach was to concentrate the negative charge on the carbon atom which was the desired center for bromination. This route also proved to be unsuccessful as a mixture of products was obtained that was difficult to separate.

To circumvent unselective α-brominations, it was also envisioned that congers of the bis(ketoamine) species reported by Arduengo could be functionalized by a late-stage imination. For this, however, the *t*Bu substituted backbone was believed to be too hindered for imine condensation, thus a phenyl substituted system was pursued.

However, we were unable to perform selective α-brominations of acetophenone with bromine (with and without additives), as the product did not match the ^{1}H NMR literature data of this known species, and the product of recrystallization of the green sludge-consistency (inconsistent of the off-white/colourless **III-8**) material was also inconsistent with literature data. It is possible that the brominated species produced were products of multiple brominations,

including the substitution in the aromatic ring. However, the bromination of pinacolone was successful via this procedure of Br_2 as the brominating agent, and the product **III-7** was isolated by vacuum distillation. Thankfully, α-bromination of acetophenone to yield **III-8** was eventually successful by means of using the bromine-dioxane adduct.[125] Preparation of this reagent was scalable up to 50 g.

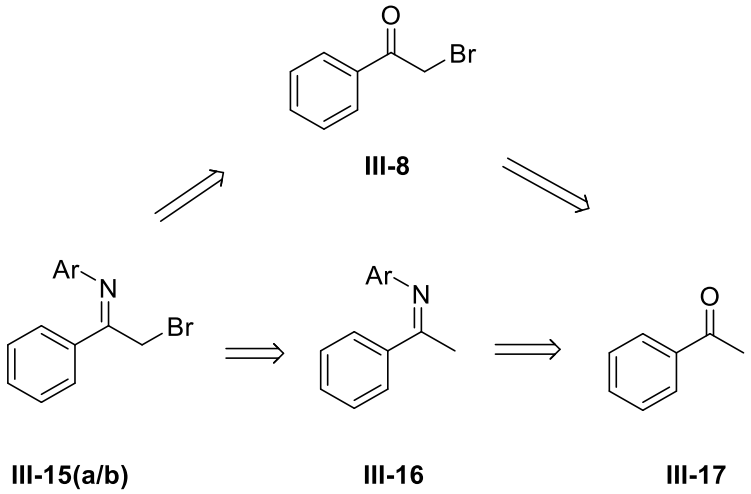

Scheme 37. Synthetic pathways to phenyl-substituted α-bromoketimines.

To allow for late-stage functionalization and tuning of bulky groups on the nitrogen donor atoms, it was envisioned that imine formation could be performed from various stages of ONO: from the benzylated salt, debenzylated salt, or neutral compound. This would require **III-7** or **III-8** as starting material, and likely harsh conditions to perform imination on the *t*Bu substituted group, if it were even possible to form via this route. Alternatively, for the **III-14a**, the reaction would need to go through the amide **III-22** before further functionalization. (see Scheme 36 & Scheme 38).

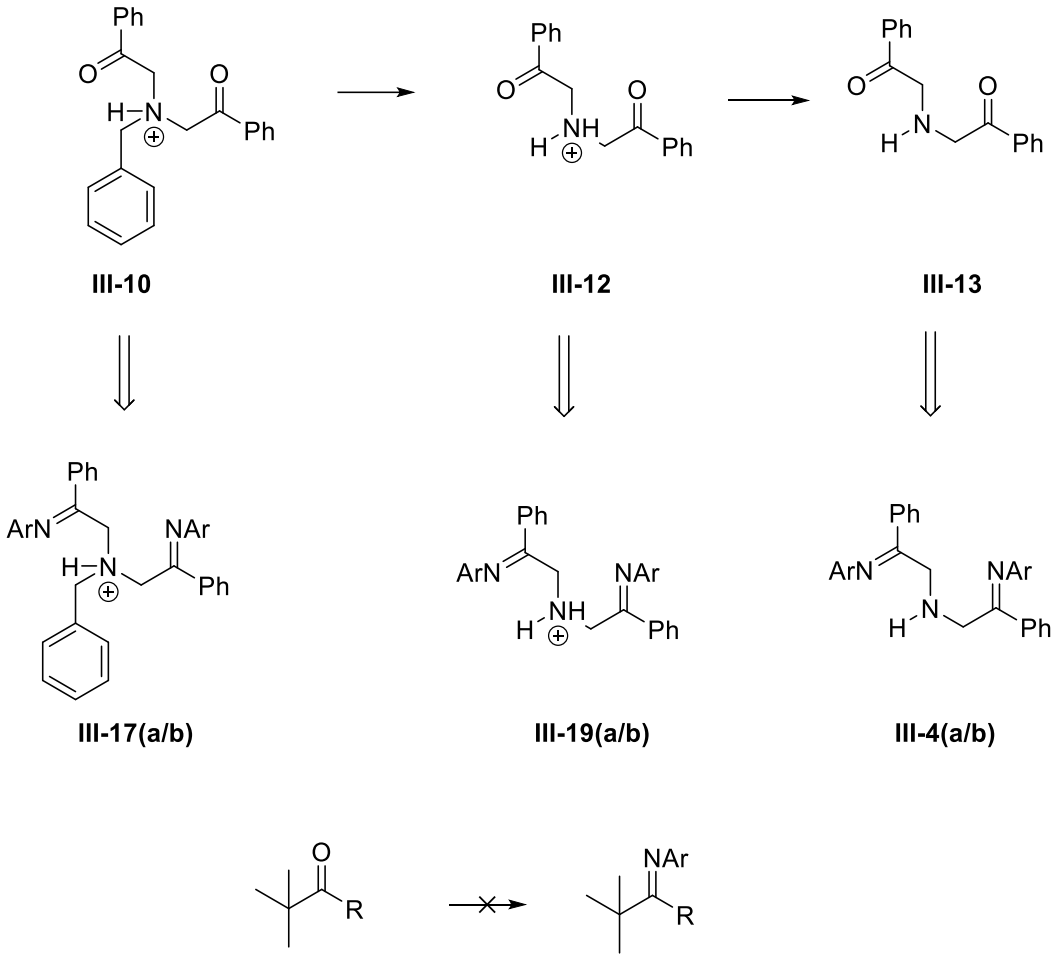

Scheme 38. Potential iminations envisioned from various states of ONO.

Attempts to replicate the synthesis of ONO (**II-86** and **III-13**) by the groups of Arduengo and Radosevich via S_N2 substitution of benzylamine with the **III-7** or **III-8** remained challenging (Scheme 33), as the compound would often fail to form and isolation was hindered by very fine precipitation of the ammonium salt **III-9** or **III-10** from either toluene or benzene. The yield for the reaction was improved slightly by first distilling the benzylamine, which produced enough for debenzylation and deprotonation, but proved not to be a viable route in our hands. As the problematic step was with the preparation of **III-9**/**III-10** salt, a solution of NH_3 was used, but as expected failed to react due to the poor nucleophilicity of nitrogen, and the inertness of NH_3.

In summary, attempted reproduction of the Arduengo/Radosevich procedures for production of ONO by a reaction of benzylamine with bromoketone resulted in dismally low yields. Reproduction in benzene instead of toluene lead to a better performance and a compound in high enough yield to work up by hydrogenation and treatment of base, but again the yields of this final neutral bis(keto)amine were too low to continue further attempts of imination.

The plan was to try various acidic and dehydrating conditions to directly generate the imine from **III-13** by condensation with an amine, but the low yields of **III-13** were too prohibitive. Another route to potentially obtain the NNN ligand could be envisioned through an aza-Wittig type reaction of the Arduengo ONO compound with the corresponding iminophosphorane. It is worth noting that an undergraduate colleague Brandon Corbett, visiting from Cardiff University, attempted the aza-Wittig reaction of Ph_3P=N-(mes) with $(PhC(O)CH_2)_2NH_2^+$ in C_6D_6 with in-situ deprotonation, but was unsuccessful. The traditional method for generating the Arduengo ONO ligand faces the problem of debenzylation with Pd/C and H_2 in the final step. It is unclear whether these conditions would be compatible with an imine analogue, thus imination may have to occur post hydrogenation.

Another route envisioned was that either the diketone or diimine would be to proceed though α-haloketone or imine, followed by a Gabriel synthesis or Depline reaction to generate the α-aminoketone or -imine, and subsequent reaction with another equivalent of halo-carbonyl. (Scheme 39) This route could potentially be a way for generating an asymmetric ligand and would avoid the need for hydrogenation/debenzylation as per the old procedure, but at the risk of over-substitution to higher order amines upon a reaction with another equivalent of an α-halocarbonyl substrate. To further complicate matters, α-aminoketones are known to undergo self-condensations to generate dihydropyrazines under basic conditions, which may then aromatize to pyrazines. A

way to mitigate this problem could be to protect the amine with a boc group followed by condensation of the ketone with an aniline, however the deprotection again suffers due to the acidic conditions required which could then potentially facilitate hydrolysis of the imine.

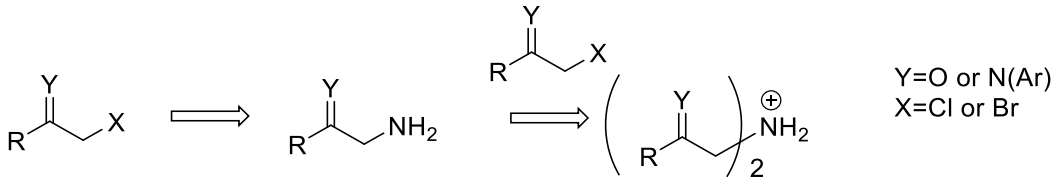

Scheme 39. Potential alternative route to YNY ligand, where Y=O/N.

III.1.2 Synthesis of the NSN Ligand

As the synthesis of **III-4** were unsuccessful after multiple attempts, attention was directed to installing a different substituent in the flexible centre position of the ligand. Nitrogen is a hard donor ligand and has been shown to be effective in this position (i.e. in the chemistry of diiminopyridines) for hard metals, but a softer donor may serve to stabilize the amphoteric nature of zinc. In fact, in 2010 Driess *et al*. reported zinc complexes (**III-27** and **III-28**) bearing hard oxygen donors and a soft sulfur atom which proved to be effective for hydrosilylation of ketones. Wanting to exploit better the donor ability of nitrogen, attention was directed to developing novel NSN complexes. (Scheme 40).

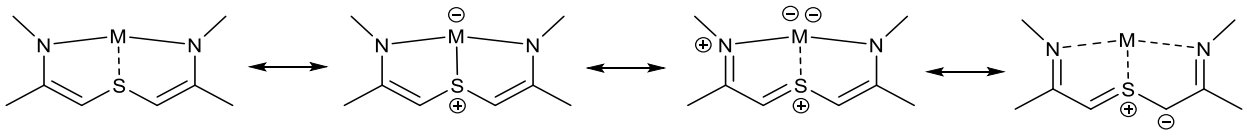

Scheme 40. Resonance forms of metal NSN complexes, akin to metal ONO and NNN complexes.

As a notable catalyst, the use of the OSO ligand is based on the use of mixed hard and soft donor atoms. Procedures for the preparation of OSO compounds (**III-29** & **III-30**) are well known due to their application in production of thiophenes.[126,127] Due to their ease of preparation, Driess reported catalytic hydrosilylation of ketones with this hard/soft OSO ligand. Utilizing various diamines as Lewis bases, a library of catalysts was created. While the hydrosilylation was able to proceed marginally with $ZnEt_2$ as a catalyst, and failed in the absence of a zinc catalyst, TMEDA coordinated **III-27a** was found to be the most active. In comparison, replacing *t*Bu for Ph (**III-28**) in the ligand backbone was detrimental, only yielding conversions of 54% compared to stoichiometric conversions with **III-27a** due to negative induction effects of the phenyl substituents. It appears that the rate is increased when a hemilabile group is attached, as the final step in the mechanism is the elimination of the silylether. This is also supported by a decreased rate when a rigid phenanthroline (45% conversion) is used as a coordinating diamine, as well as when an equivalent of monodentate DABCO (67% conversion) is used. [128] (Figure 11)

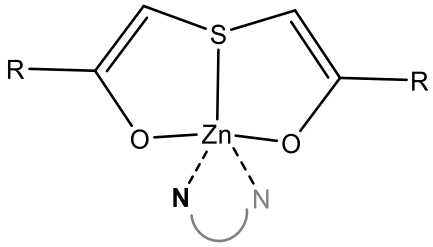

III-27(a-c): R=tBu ; N,N=TMEDA, bpy, phen
III-27d: R=tBu ; N=DABCO
III-28: R=Ph ; N,N=TMEDA

Figure 11. ZnOSO species reported for hydrosilylation of ketones.

Analogous to the report above, a projected outcome by the utilization of this ligand with harder metals is the possibility for both internal charge stabilization, to stabilize different oxidation states involved in a potential catalytic system, and the hemilability of sulfur may allow for steric

relief and to play a role in making a coordination site available. The backbone of this ligand would not likely bear a rigid structure, thus further allowing for distortions arising from excess charges, and hemilability of sulfur serving to facilitate addition to zinc and providing a force for elimination of substrates after. Furthermore, kinetics and reactivity studies of a zinc bearing an ambiguous oxidation state ligand would be interesting due to the limitation of oxidation states of zinc.[129]

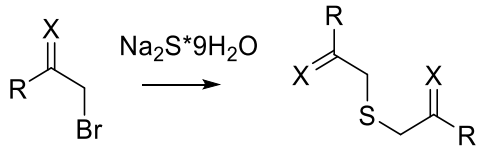

X=O		
R=tBu	**III-7**	**III-29**
R=Ph	**III-8**	**III-30**
X=N-Ar		
R=tBu	**III-14(a/b)**	**III-5(a/b)**
R=Ph	**III-15(a/b)**	**III-6(a/b)**

Scheme 41. General scheme for tridentate sulfur-containing ligands.

From **III-7**/**III-8**, one route was to form **III-29**/**III-30** with a late-stage imination to **III-5**/**III-6**. As mentioned in the previous section, preparation of various sulfur-diketone species is known and used in the syntheses of thiophenes. This project mainly consisted of reactions involving **III-30**, as crystallization of this compound was relatively easy and more reproducible than with **III-29** analogue. Preparation of **III-30** was performed in acetone as reported.[130]

With **III-30** in hand, imination was tried next. Since nitrogen is a poor nucleophile, activations of the carbonyls were attempted via analogies from the syntheses of bulky NacNac species. Various acidic and dehydrating conditions were used but to no avail. Dehydrating conditions with only molecular sieves in benzene were attempted, as well as an unusual apparatus for drying refluxing ethanol solution over molecular sieves (Figure 12),[131] analogous to the

imination of a non-bulky ketone with non-substituted aniline, but no reaction was observed. Amounts of HCl or pTsOH from 10% to stoichiometric were used with either Dean-Stark traps or Hickman head device on small scales, but again, no conversions of **III-30** were observed, even following a procedure adapted for the challenging imination of indigo.[132]

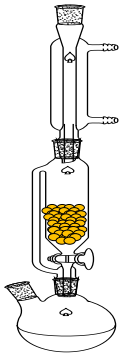

Attempts:
-stoich. HCl
-cat-stoich pTsOH, toluene
-benzene/mol sieves
-$TiCl_4$, DABCO
-$TiCl_4$, NEt_3
-dehydration refluxing EtOH w/ mol sieves (figure)
-$Ti(OiPr)_4$, MeOH

Figure 12. Apparatus used for drying conditions with a volatile solvent.

Activating an acyclic carbonyl should be quite easy, however with two other Lewis basic atoms present in a fashion which could chelate proton(s) (Figure 13), the angle of attack of the carbonyl carbon may be hindered. It may also be possible to try two equivalents of acid to prevent a pseudo tridentate organization around a hydrogen, at the risk of protonating the aniline.

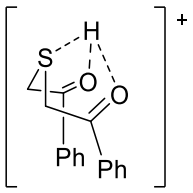

Figure 13. Possible proton chelation during imination attempts.

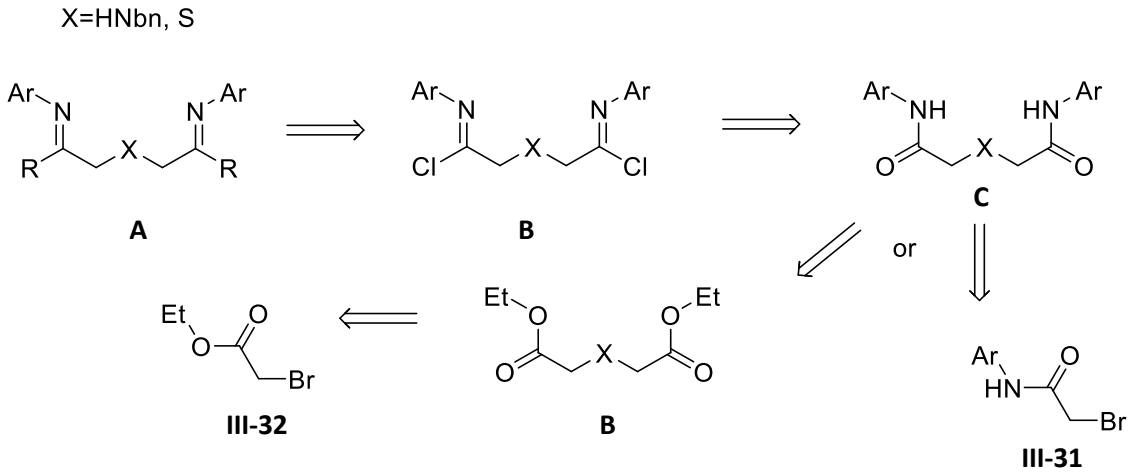

Scheme 42. Route to ligands utilizing α-bromoester or α-bromoamide starting material.

Following the idea of late-stage imination, another route was envisioned to convert a bis(amide)- substituted sulfur compound "**C**" to the bis(imine) "**A**" (Scheme 42). This compound was envisioned to be produced either directly from an α-bromoamide (**III-31**) or from an α-bromoester(**III-32**) (Scheme 43) with subsequent conversion of the functional group. Firstly, **III-32** was reacted with sodium sulfide according to literature procedure to generate **III-33**. Conversion of the ester functional group was also attempted but no conditions to yield a clean product were discovered. Similar results were found for the N-benzyl-diester (Scheme 44).

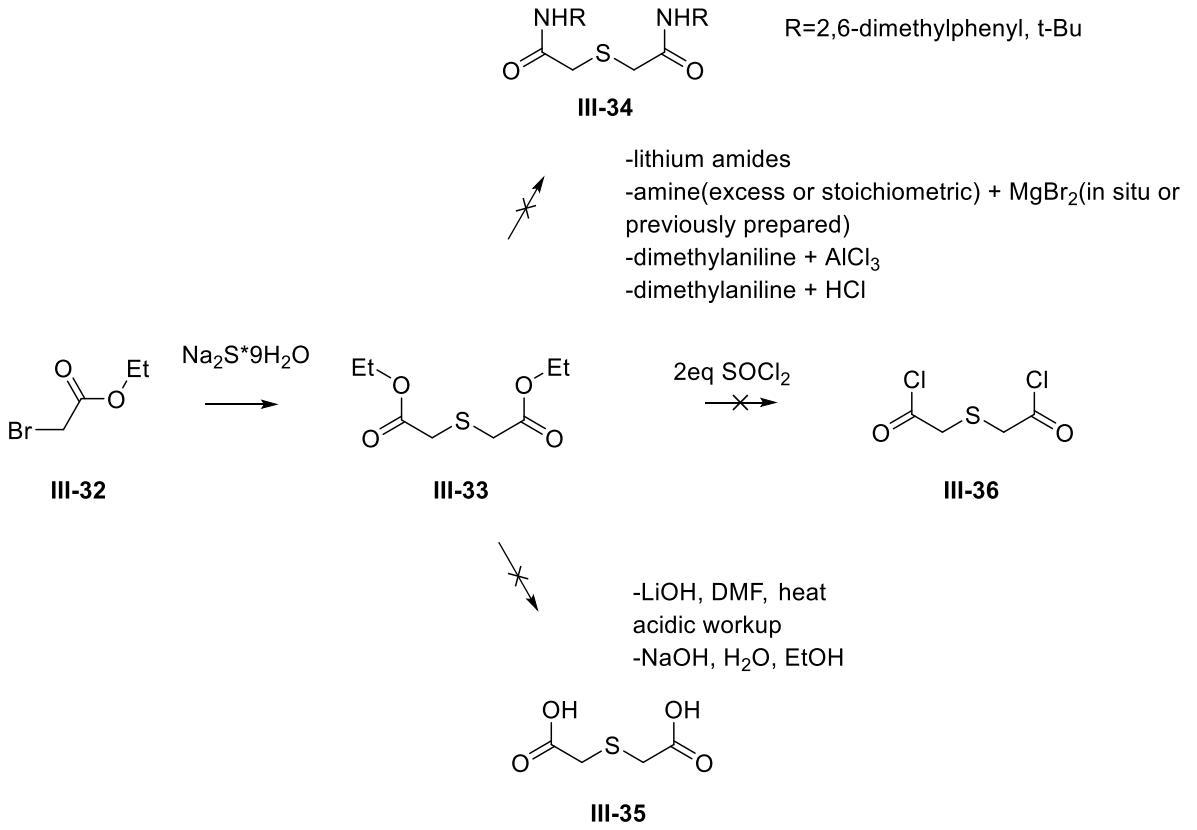

Scheme 43. Attempts to functionalize sulfur-diester compound.

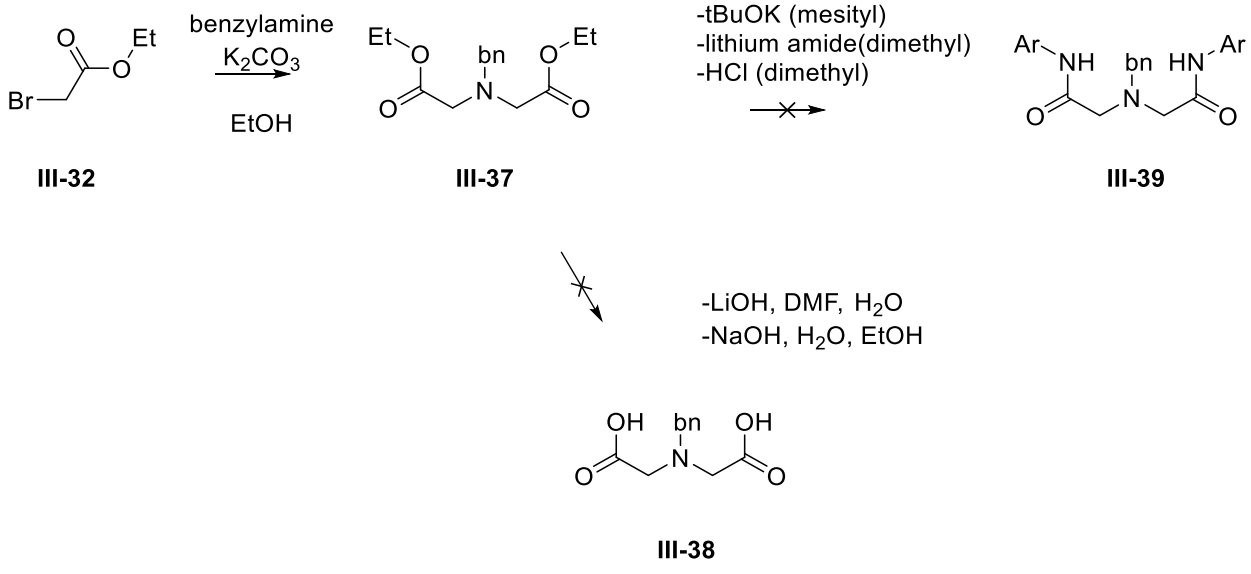

Scheme 44. Other attempts to generate the NNN ligand from the diester analogue.

Bromoacetylbromide (**III-40**) was reacted with 2,4,6-trimethylaniline to form the α-bromoamide(**III-31**) (Scheme 45), which was then reacted with sodium sulfide to generate **III-34**. Unfortunately, conversion of **III-34** to **III-41** was not a viable route. Attempts were made utilizing either two equivalents of PCl_5 or excess to two equivalents of $SOCl_2$, but this method led to unselective chlorinations at the methylene positions.

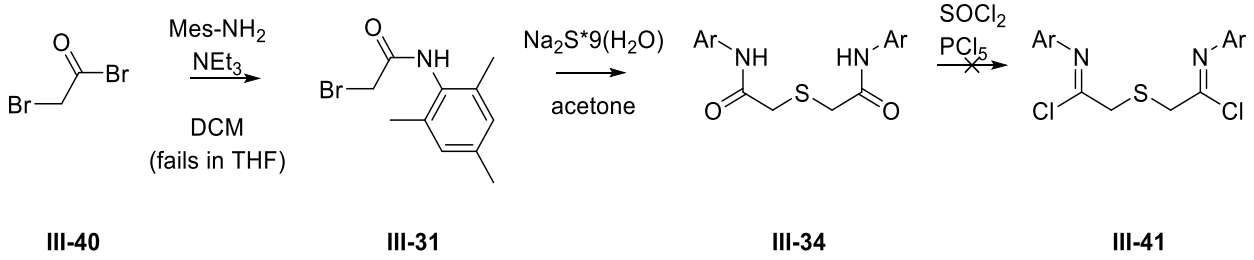

Scheme 45. Attempted route via sulfur-diester.

In 2012, Charette reported a chemoselective pathway for conversion of amides to imines in which one can introduce a new group at the carbonyl carbon by activation of an amide with triflic anhydride, followed by a reaction with Grignard or organozinc reagent.[133,134] This inspired an analogous set of reactions for introducing aryl groups at the carbonyl carbon, either with phenyllithium or an aryl Grignard. When monitored at low temperature, reaction of **III-34** occurred with triflic anhydride to produce a single species noted by a broad peak at 3.3ppm which grew in intensity sharpness until the reaction was warmed to zero degrees and more signals began to appear. The signals attributed to the assumed methylene at 3.87 ppm decreased to a ratio of 0.19:1 with the new signal, while confusingly signals attributed to aromatic protons and more so the N-H amide did not exhibit noticeable change with reaction progress. (Figure 14) While the exact nature of the species formed at low temperature was not unambiguously characterized, the reaction was assumed to proceed as expected, but further reaction with the Grignard was

unsuccessful for nucleophilic addition, and the reaction with phenyllithium was also unclear after multiple attempts. Unfortunately, the phenyllithium used for these experiments was a dark red/brown colour, and NMR of the stock phenyllithium solution revealed an unclean mixture of species. Titration of this solution also proved to be a problem as no colour change to blue could be observed when added to a cold solution of N-benzylamide.[135] The failure of the reaction with phenyllithium may be attributed to impurities and decomposition of the reagent. (Scheme 46)

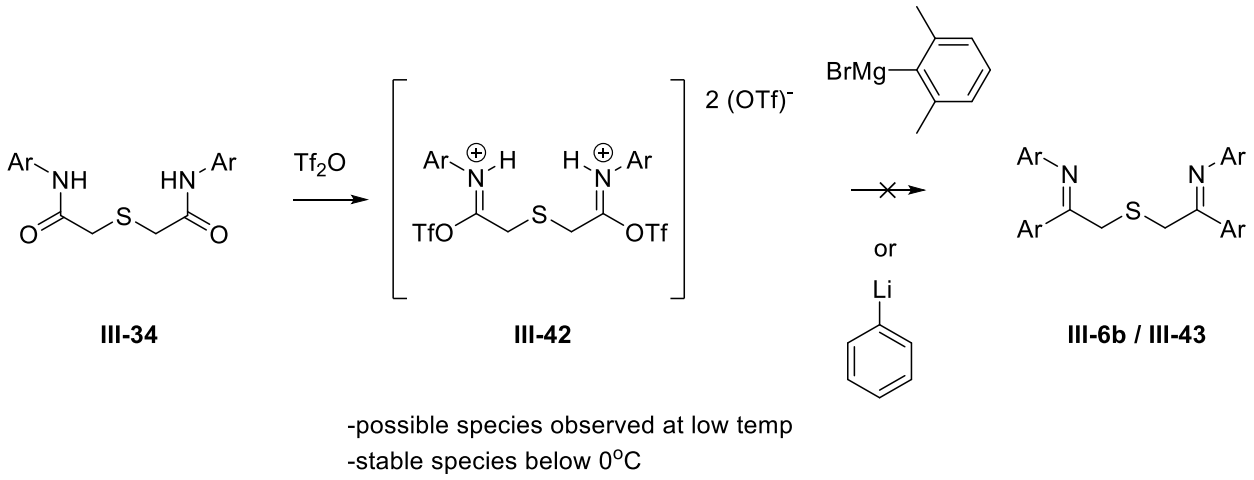

Scheme 46. Attempted conversion of S-diamide to S-diimine via activation by Tf_2O followed by nucleophilic addition to iminium carbon.

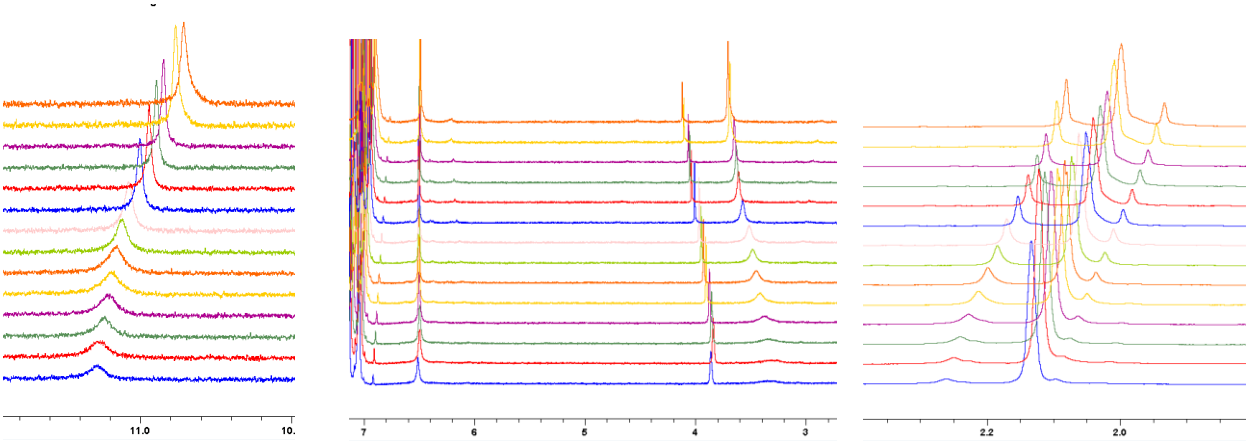

Figure 14. ^{1}H VT-NMR in toluene-d8 of III-34 reaction with triflic anhydride.

Attempts to react **III-34** with a metal to form a new complex were not performed, because although the amide functionality may act to stabilize charges, the backbone would largely be unutilized. There are already many examples of metal complexes with tridentate ligands containing bis(amido) functionalities, and this field has been reviewed. [136]

Finally, **III-15a** was prepared by a procedure adapted from a report by Kaplan, Li, and Byers.[137] These authors prepared DIPP-N=C(Me)CH_2Cl by using 0.5 eq $TiCl_4$ to generate the imine directly from bromoacetophenone, followed by a workup of extracting in DCM and removing some titanium species that are insoluble in hexane, concentration, purification by column chromatography and finally recrystallization from hexane at -30°C. Unfortunately, decomposition on silica was experienced during the chromatography, and compounds did not separate well (very close R_f's), thus multiple columns were used on occasion. An alternative workup was done to avoid hydrolysis on silica (well known for enolizable ketimines[138]) by performing vacuum distillation with a very careful temperature control, followed by multiple fractional crystallizations. Occasionally, an oily precipitate was decanted away. While its identity was unclear, NMR analysis largely showed the very deep-red oily substance contained diisopropylamine. Speculatively, it may be useful to filter off the sludge-like-aniline simply using

an alumina plug before recrystallization, which may help improve yield if multiple recrystallizations can be avoided. **III-15a** was collected as yellow crystals or presented with a slight red colour which may be attributed to co-crystallization with 2,6-diisopropylaniline.

Similarly, a small amount of mesityl-substituted α-bromoimine (**III-15b**) was successfully prepared by bromination of the mesityl imine in acetonitrile with bromine-dioxane adduct, as performed for the bromination of the ketone. Monitored by ^{1}H NMR, this reaction only gives about 40% α-bromination, but unfortunately excess bromine-dioxane seems to lead to impurities with aryl-brominations. Purification was performed by column chromatography to yield a dark red oil.

Successful attempts to generate a mono-α-brominated imine, characteristically demonstrate a roughly 4:1 ratio of isomers in chloroform, which show exchange. Singlets are observed at 4.08ppm and 4.21ppm, respectively. There is not significant magnetic inequivalence of the *i*Pr signals from the two isomers, as the signals are roughly isochronous and an aromatic multiplet is centred at 7.5ppm. Similarly, the doublets corresponding to the methyl signals are found unambiguously at 1.21ppm and 1.18ppm for the major and minor species respectively, and isochronous doublets at 1.14ppm.

As attempts to generate a ligand which is supported by a central amine had failed over multiple iterations, generation of **III-15a** was only mildly successful, and **III-6a** could be obtained after one more step, only this ligand was prepared from **III-15a**. Following a procedure adapted from reference [127], the mixture of DIPP-bromoimine isomers reacted with 0.5 eq Na_2S *$9H_2O$ in refluxing ethanol, filtered hot, then crystallized from ethanol solution. Bright yellow crystals were characterized by NMR and single-crystal X-ray diffraction (Figure 15). Unfortunately, while the crystal was suitable for assigning connectivity, the goodness of fit was only 0.719, thus not suitable for measuring distances reliably.

Similarly, other solvent conditions were attempted. The first preparation of **III-6a** was performed in DMF and required arduous multiple purifications by column chromatography, in low yield and relative purity, but was sufficiently pure to carry out some initial reactions by monitoring characteristic signals. As an aside, the synthesis failed when performed in acetone, as the major component was 4-hydroxy-4-methyl-2-pentanone likely formed by competitive deprotonation by sodium sulfide.

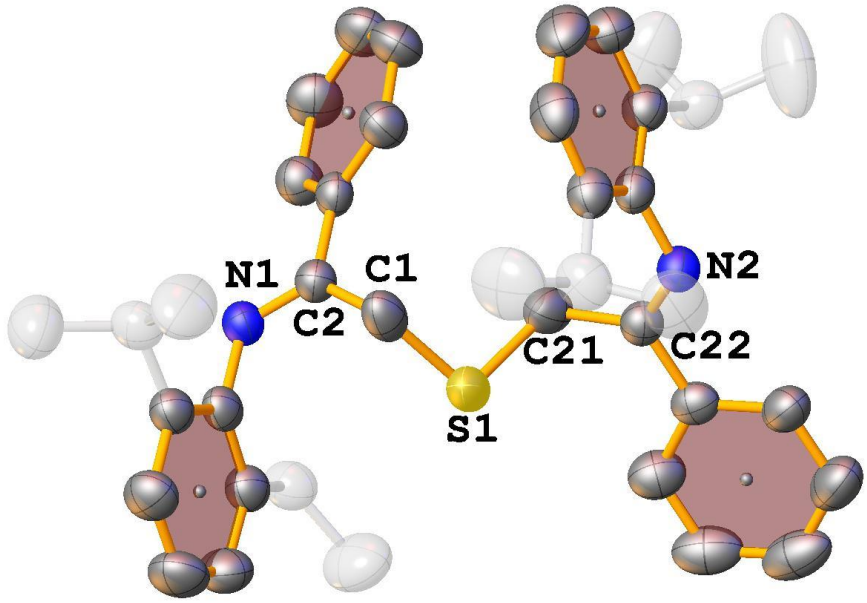

*Figure 15. X-ray molecular structure in the crystal of NSN ligand (**III-6a**) crystallized from Et_2O solution at -30°C. Crystallography and structure analysis performed by Anton Dmitrienko.*

III.2 Main Group Compounds Supported by NSN Ligand

For many metal complexes bearing donor ligands with α-hydrogens, deprotonation/lithiation followed by substitution at a MCl_x is a common procedure. Deprotonation of NSN (**III-6a**) was attempted by using KHMDS at room temperature. Initial efforts showed a reaction of KHMDS, indicated by a colour change and change in the ^{1}H NMR spectrum. It was not clear why two equivalents of base did not yield one clean species, but would later be shown to be solely due to a sub-stoichiometric amount of base, which led to mixtures of Li_2NSN (**III-43a**) (two conformers, symmetric and asymmetric), as well as a mono-lithiated NSN (**III-42a**) (potentially four isomers could exist – see Chart 1).

LDA was also used at room temperature and appeared to yield a relatively cleaner reaction. At room temperature, colour change from yellow to orange was rapid, and complete consumption of LDA was evidenced by the first set of spectra obtained, approximately 10 minutes post dropwise addition to the solution containing **III-6a**. This was also supported by both ^{1}H and ^{7}Li NMR, which lacked signals corresponding to unreacted LDA. While expectations were that the formation a single species should occur from this reaction, a series of unidentified peaks led us to believe the **III-43a** must be unstable over a short time at room temperature, but such a conclusion was possibly incorrect. A THF solution of the reaction mixture after 15 minutes and 1.5 hours revealed five peaks in ^{7}Li NMR. (Figure 16) While three of them were expected due to the known fluxional nature of the framework, the remaining two were presumed to come from decomposition of an unknown species. The identities of these elusive species remain unknown, but speculatively they are likely mono-lithiated **III-42a** isomers whose fluxionality led to their broadness (Chart 1 & Figure 16). Furthermore, as attempts to isolate clean **III-43a** were unsuccessful, it was then

decided to proceed via *in-situ* generation and utilization of the di-lithium salt in reactions with metal chlorides.

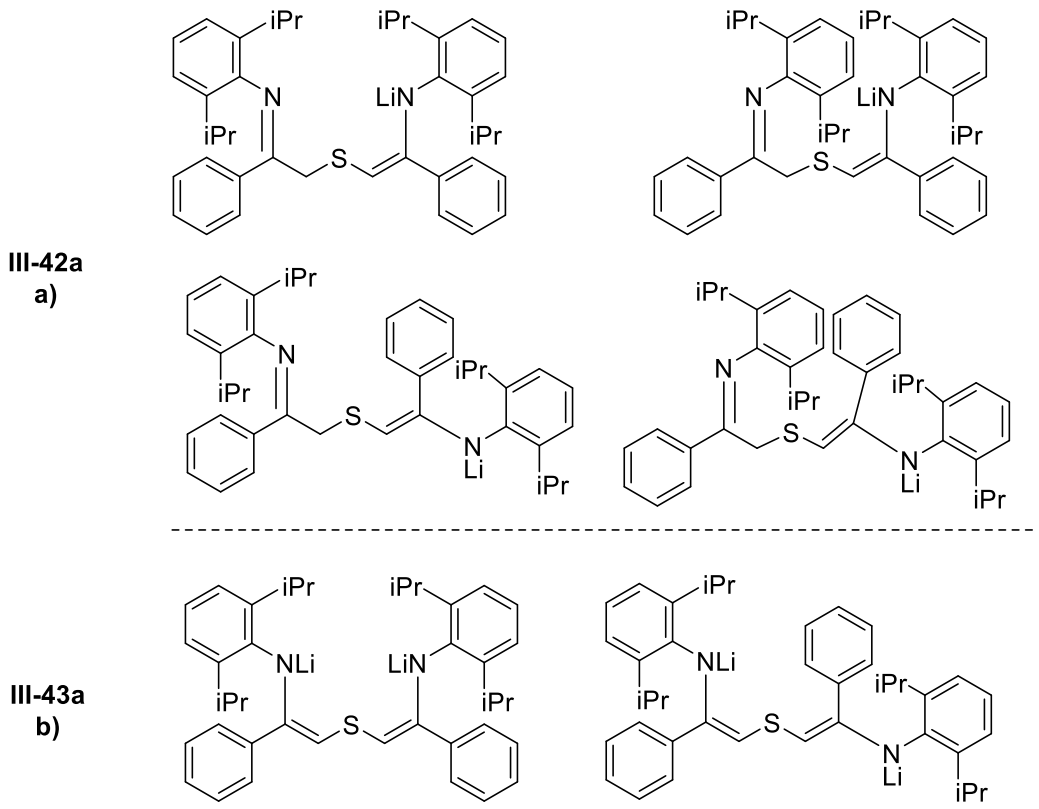

Chart 1. Isomers of mono[a)] and di-lithiated[b)] NSN.

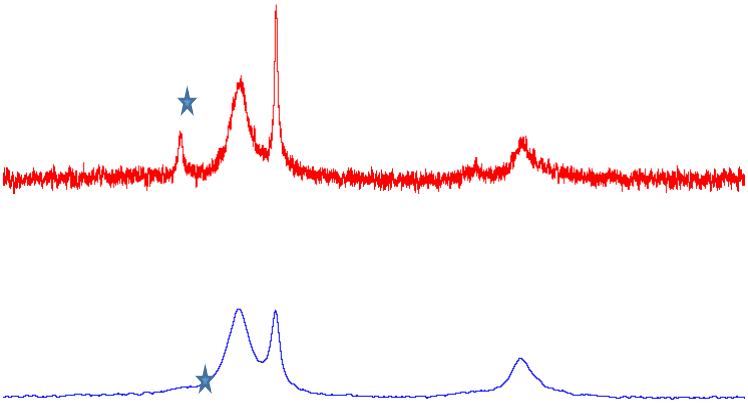

Figure 16. ^{7}Li NMR spectra of the lithiation of **III-6a** with two equivalents of LDA post 15 minutes (bottom) and 1.5 hours (top). Indicated broad peak was overlooked in the first spectrum.

III.2.1 Synthesis of Zinc Compounds Supported by NSN Ligand

Complexes of zinc supported by bulky donor ligands have been shown to catalyze various reductions of unsaturated substrates. Driess reported Zn-O,S,O (**III-27**/**III-28**) complexes coordinated by various amine ligands which were shown to catalyze hydrosilylation of ketones. Increasing the donor strength of the tridentate ligand by replacing oxygens with nitrogens may improve catalytic activity.

The first attempt to generate a ZnNSN (**III-44**) complex was to react $ZnMe_2$ directly with **III-6a**, but unfortunately no reaction was observed even when the mixture was heated. Next, $ZnCl_2$ was reacted with an *in-situ* generated **III-43a** in Et_2O, which again was not very clean, but addition of DMAP to the reaction mixture proved to be fruitful in generating ZnNSN(DMAP) (**III-45a**). Repeating the reaction of $ZnCl_2$ with **III-43a** in THF quickly led to the formation of a complex presumably coordinated by THF and demonstrating C_S symmetry in the ^{1}H NMR spectrum (ZnNSN(THF), **III-46a**). This symmetry is noted by one singlet for the two methylene groups at 4.58ppm ($^{13}C_{methylene}$: 83.8ppm), as well as four doublets for the methyl groups of the iso-propyl substituents at 1.12, 0.81, 0.51 and 0.66ppm ($^{13}C_{methyl}$: 25.7, 25.0, 23.7 and 23.3ppm respectively). Only one *i*Pr septet could be identified at 3.33ppm, while the second likely remains buried under the signal from proteo THF. Attempting to remove excess THF and the diisopropylamine by-product, led to decomposition of the zinc complex as seen when the mixture was re-dissolved in C_6D_6. Unfortunately, the identity of the decomposition species remains elusive and because THF was not removed completely, and it is still unclear whether THF remains bound to zinc in a solution of benzene. However, when benzene was removed from the same reaction and the residue was re-dissolved in THF along with the addition of one equivalent of DMAP, two species could be now clearly observed. 1-D EXSY showed exchange of the methyl signals **III-45a** with **III-46a**.

VT 1-D EXSY with variable mixing times allowed for the measurement of $\Delta H^{\ddagger}$ and $\Delta S^{\ddagger}$ of this exchange via an Eyring plot (Figure 17) according to equation (1). An approximation of $\kappa = 1$ in this equation assumes that upon formation of the transition state, the reaction only proceeds to the product (according to transition state theory). Measuring the formation of **III-46a** from 275K to 295K showed an activation enthalpy of 59.9 kJ/mol and an activation entropy of -60 J/molK. This clearly demonstrates that the formation of **III-46a** from **III-45a** occurs via an associative mechanism. This is also rationalized by the fact that the zinc atom is relatively accessible in this complex. $^{13}C\{^{1}H\}$ NMR spectrum of **III-45a** obtained had a low signal to noise ratio, but the majority of carbon signals could be assigned with the help of HSQC-edited and HMBC spectra (see Figure 38 in Supporting Information).

$$ln\frac{k}{T} = \frac{-\Delta H^{\ddagger}}{R} * \frac{1}{T} + ln\frac{\kappa k_B}{h} + \frac{\Delta S^{\ddagger}}{R} \qquad (1)$$

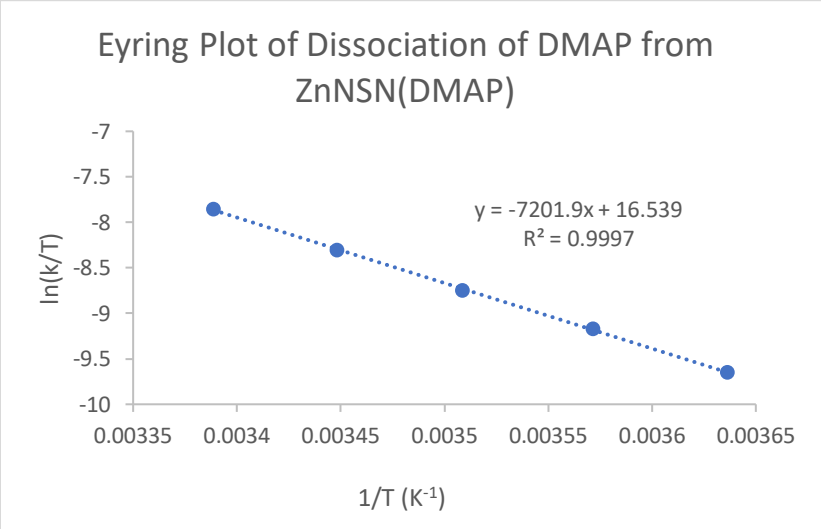

Figure 17. Eyring plot for measuring dissociation of DMAP from ZnNSN(DMAP).

Organozinc reagents are common and have shown utility in coupling reactions in the presence of a suitable metal catalyst, such as Co[139] and Ni[140]. From **III-45a**, we targeted

preparation of its hydrido-zincate derivative **III-48a** (Scheme 47). We believed that a zincate derivative with NSN should be nucleophilic enough to activate sp^2 C-X bonds, such as in bromobenzene, which could then potentially be used for cross coupling reactions.

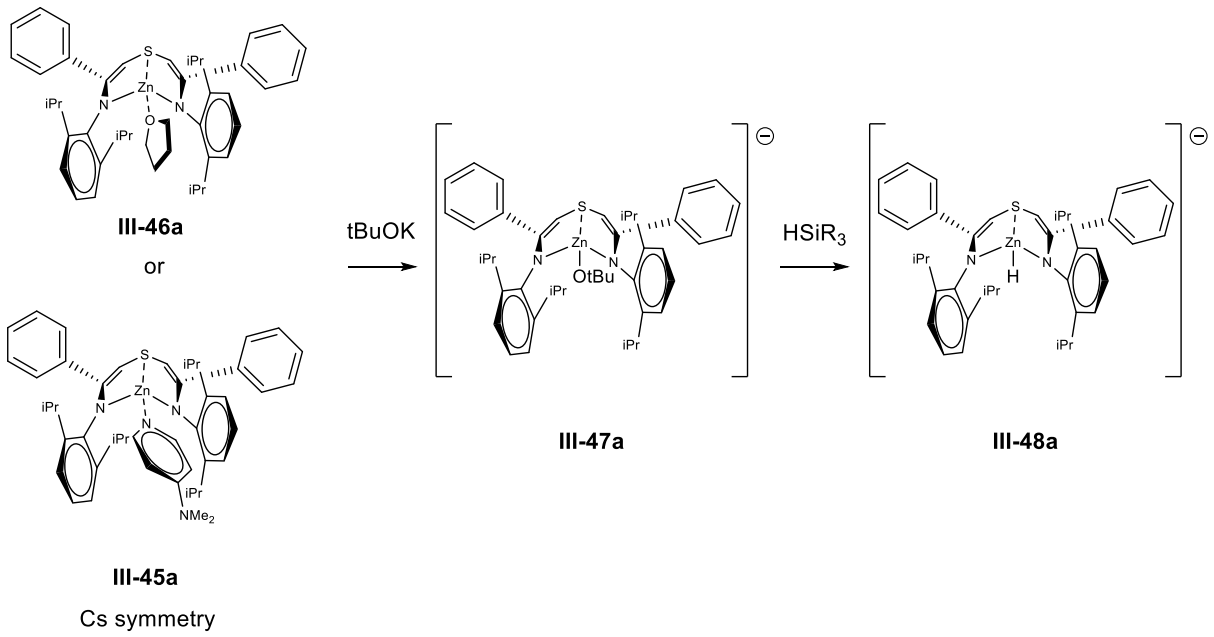

Scheme 47. Potential pathway for hydrido-zincate formation.

Unfortunately, attempts to generate and identify -O*t*Bu (**III-47a**) or hydrido (**III-48a**) zincate species were inconclusive. Addition of *t*BuOK to **III-45a** led to slow generation of a species having a downfield shifted singlet, assumed to be a methylene (6.7ppm from 5.4ppm), which may be a decomposition species which has been observed as a minor impurity in other preparations of ZnNSN species.

In summary, novel neutral zinc compounds **III-45a** and **III-46b** bearing a tridentate NSN-ligand were prepared and characterized by NMR spectroscopy. Coordinated DMAP was found to

be labile, as exchange was observed with free DMAP by 1-D EXSY. The activation parameters calculated suggest an associative mechanism for the exchange of DMAP in THF solution.

III.2.2 Synthesis and Reactivity of Germanium Compounds Stabilized by NSN Ligand

Germanium complexes have also been successful for bond activations. Applying the same procedure used for generation of **III-45a** and **III-46a**, the *in situ* generated **III-43a** was added into a suspension of $GeCl_2$. While the reaction progress was difficult to monitor visually due to $GeCl_2$ being transparent in ethereal solvents, complete consumption of **III-43a** was confirmed after approximately 1h at room temperature by ^1H NMR. A slightly scaled up synthesis was done using a scale of 50 mg of starting **III-6a** in Et_2O, which was filtered via filter pipette, then subsequently placed in a -30°C freezer until crystals were observed approximately 2 weeks later. The yield after recrystallization was very low, an estimated 3mg, but X-ray crystallography was able to reveal the structure. Confirmation of ^1H NMR was performed using 0.6 mg in C_6D_6. A higher concentration was later attained and used for $^{13}C\{^1H\}$ NMR analysis. Crystallizations were also attempted from a concentrated toluene solution (unsuccessful), but easily performed in Et_2O using a slow evaporation method at RT. (Figure 18)

The molecular structure of **III-47a** obtained from x-ray diffraction did not exhibit exact C2 symmetry, noted by the difference of N-Ge bond lengths (Δ=0.07Å) and the difference in ∠N-Ge-S angles (Δ=2.99°), as well as asymmetry of the *i*Pr groups. This suggests that in solution there is a rapid isomerization which gives rise to an apparent *Cs* symmetric molecule. When comparing **III-28** reported by Driess to **III-47a**, the olefinic C=C bonds in the backbone are quite similar but

do show a greater asymmetry than the zinc species with a bound DMEDA. (**III-28**: 1.359Å and 1.358Å; **III-47a**: 1.356Å and 1.373Å).[128]

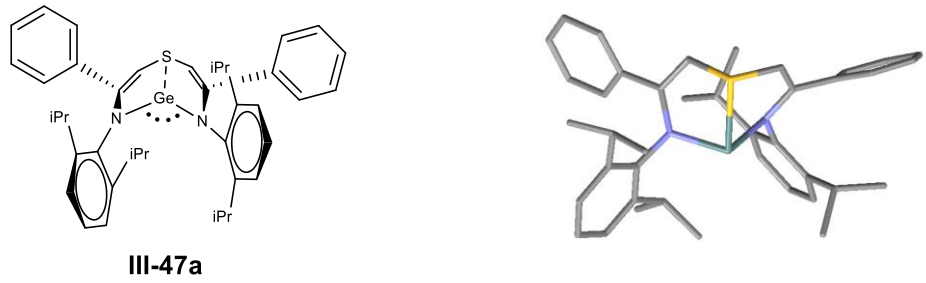

III-47a

*Figure 18. Molecular structure of GeNSN **III-47a** from X-ray diffraction. N_1-Ge=1.938Å, N_1-C_1=1.390Å, C_1-C_2=1.356Å, C_2-S=1.775Å, N_2-Ge=2.008Å, N_2-C_4=1.359Å, C_4-C_3=1.373Å, C_3-S=1.749Å, Ge-S=2.456Å, ∠N_1-Ge-S=83.79°, ∠N_2-Ge-S=80.80°, ∠N_1-Ge-N_2=101.58°, ∠C_2-S-Ge=91.07°, ∠C_3-S-Ge=91.23°.*

Interestingly, there was difficulty detecting the methine carbon chemical shift, possibly due to the quadrupolar moment of germanium (^{73}Ge, 7.8% natural abundance, electric quadrupolar moment of -0.17Q/m), ^{33}S to a lesser extent (0.76%, -0.055Q/m), as well as the low natural abundance of ^{13}C. Increasing the number of scans allowed for observation of a cross-peak of a broad signal in the expected region, but the shape of the peak could not be defined (see Figure 42). Similarly, as the broadening of one septet in the ^{1}H NMR spectra for both **III-45a** and **III-47a** are observed, it is possible that sulfur can be contributing factor in addition to rapid isomerization. Furthermore, if a library of similar compounds bearing this ligand can be crystallized and examined by X-ray crystallography in the future, it may be possible to correlate the internuclear distances to sulfur based on the signal's half-height width.

To begin the reactivity studies of **III-47a**, oxidative addition of methyliodide was attempted, but unfortunately, heating overnight at 70°C did not show any conversion. Since o-

benzoquinone are well-established trapping reagents for carbenoids and given the availability of catecholates of germanium, we decided to study the reaction of **III-47a** with 3,5-di-*tert*-butyl-o-benzoquinone (**III-48**). Previously, germanium catecholates were accessed from **III-48** with 3,5-di-*tert*-butyl-o-benzoquinone or sodium catecholate, and from reactions of Ge(IV) with disodium salts of the corresponding catecholate.[141] Therefore, we expected that oxidative cyclization with benzoquinones would yield GeNSN(catechol) (**III-51 and III-51'**). Indeed, addition of **III-48** to **III-47a** led, after 15 minutes at room temperature, to complete disappearance of the starting materials, but the identity of the products could not be established. Surprisingly, there was an appreciable amount of a species bearing signals resembling **III-6a** in solution, and these signals grew in intensity over time. This may be due to water present in the deuterated benzene solvent, or reaction with another equivalent of metal complex or ligand leading to decomposition. Similarly, the two singlets at 5.19ppm and 5.15ppm are roughly equal intensity after 15 minutes, but ratio diminished to approximately 5:1 after 40 hours (Figure 19). This may indicate there are two isomers which initially form but equilibrate over time (Figure 21). Surprisingly however, 1-D EXSY of the methylene singlet at 5.19ppm did not show exchange with the singlet at 5.15ppm, nor did exchange of the *t*Bu singlet at 1.75ppm for another. This could be because the barrier for the reverse reaction is too large for exchange at room temperature, and if performing this again in drier conditions may afford a single species if left for longer. We do however observe NOE of two of the singlets to doublets, likely of the *i*Pr methyl groups (see Figure 20). It is plausible that steric hinderance could be dictating the stability of the two isomers, thus the species with the least repulsion of the *t*Bu groups may be favoured (see Scheme 48).

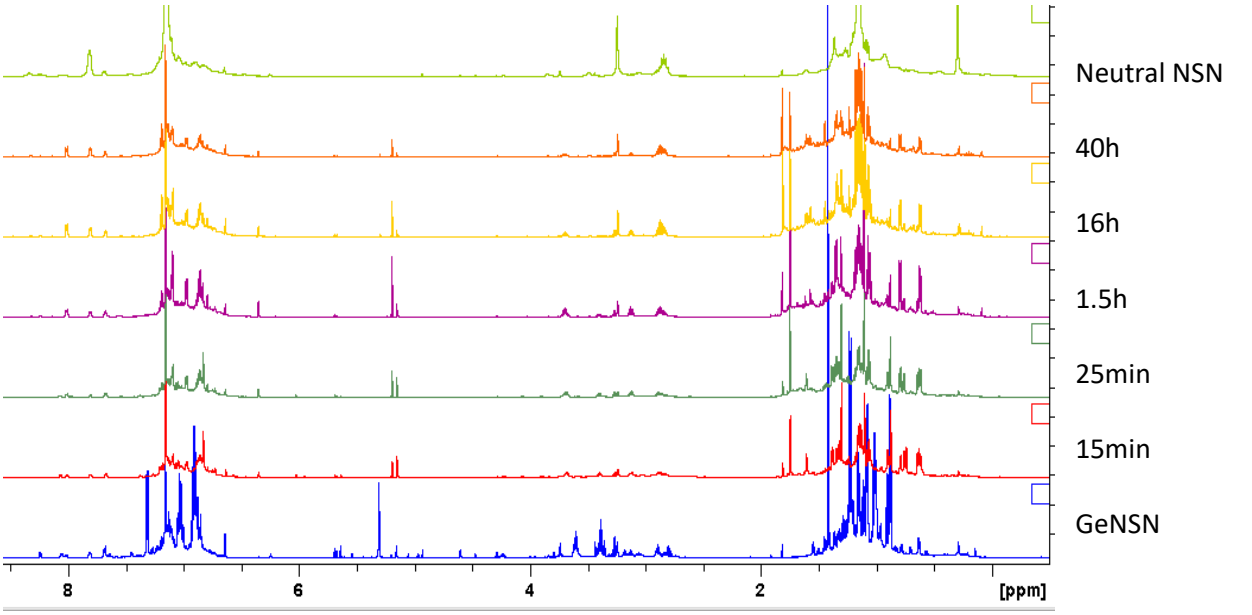

*Figure 19. Oxidative cyclization reaction progression of **III-47a** with **III-48**.*

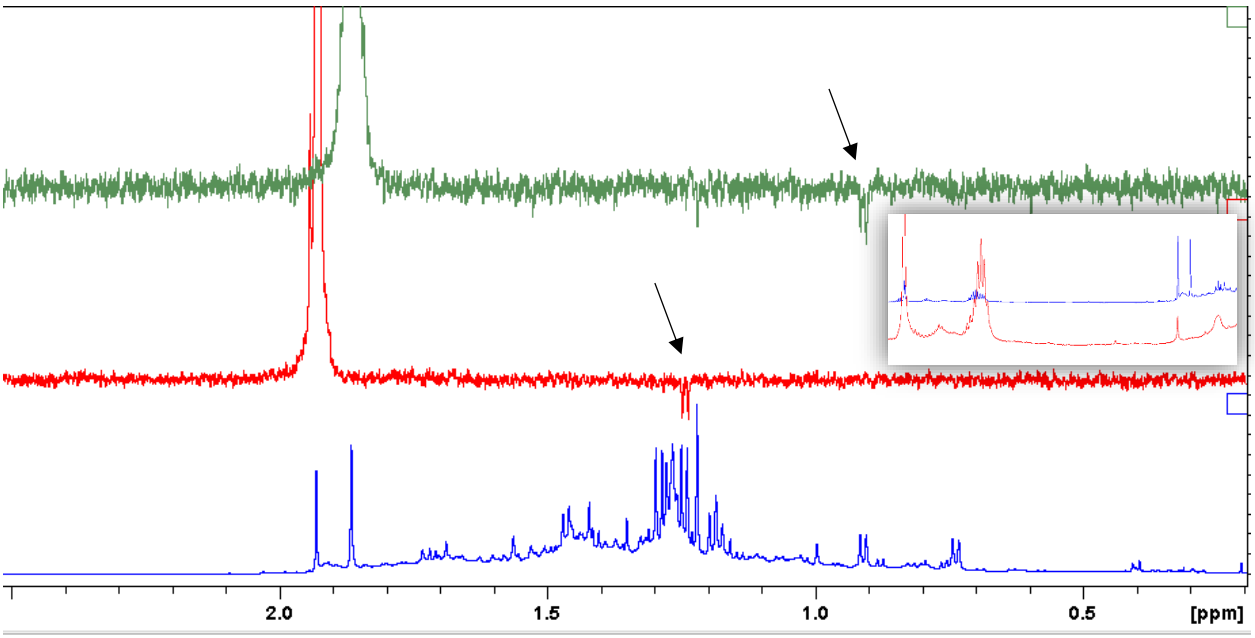

*Figure 20. 1-D NOE experiments of selected singlets. Green: more stable isomer of **III-51**. Red: impurity observed in unrelated NSN synthesis.*

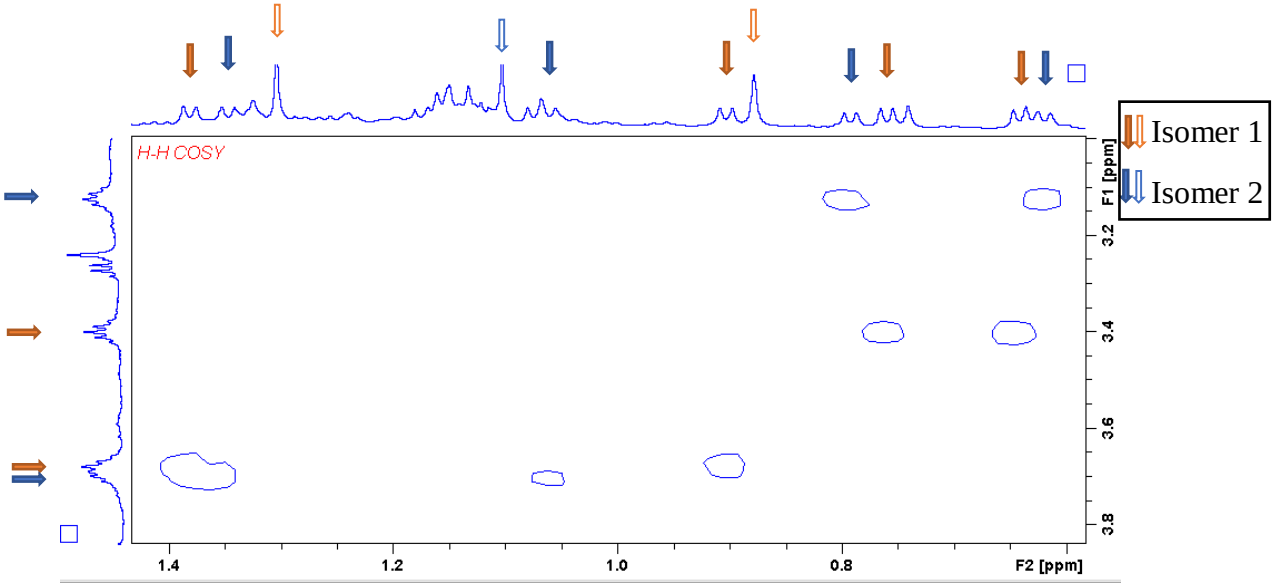

Figure 21. ^{1}H COSY to identify pairs of methyl/iPr signals for the two isomers.

Regardless of the identity of the quinone adduct of Ge, it is clear that the quinone starting material had reacted, and based on other literature precedents for generation of bis(catechols) and mono(catechol) of germanium along with the few diagnostic signals observed (5.19ppm, singlet, 2H, CH; 1.75ppm and 1.10ppm both singlets, 9H, $C(CH_3)_3$), it seems plausible that C_S symmetric species with inequivalent *t*Bu groups may have been formed of **III-51**/**III-51'**. A plausible explanation is that both species are formed initially, but one product (bottom-right, **III-51'**, Scheme 48) is believed to be more stable at room temperature due to presumably less repulsion *of t*Bu with DIPP groups, and increased ratio of CH signals at 5.19ppm to 5.15ppm over time.

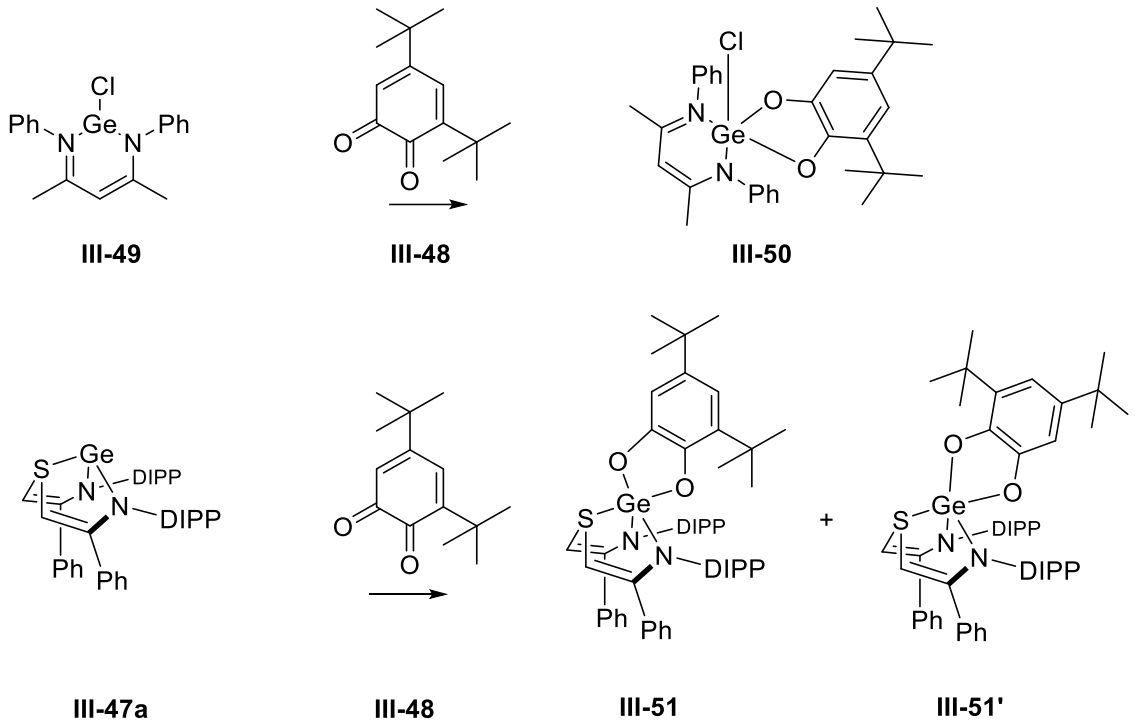

Scheme 48. Ge(II) reactions to Ge(IV) Top: from reference [84]; bottom: proposed products of GeNSN reaction with 3,6-di-tert-butyl-o-benzoquinone.

III.2.3 Synthesis and Reactivity of Phosphorus Compounds Supported by NSN Ligand

Another project envisioned was the formation of a phosphorus-hydride compound (NSN)PH (**III-52**) via NSNPCl (**III-53**). We reckoned that the P-bond hydride can exhibit some hydride character due to stabilization of a positive charge on phosphorus by a donating sulfur atom (Scheme 49). The situation is thus reminiscent of the well-studied Gudat's diazaphospholene hydrides (**III-54**) which show hydridic activity because of aromatic stabilization of the diazaphospholenium ring and were successfully used in catalysis. (Scheme 50). [142–145]

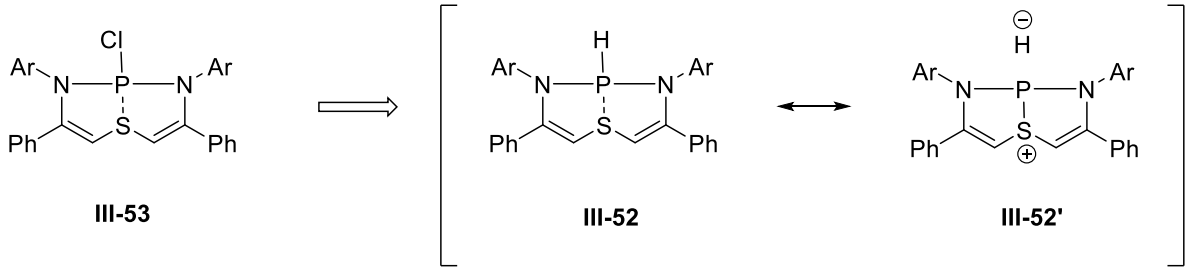

Scheme 49. Possible resonance structures for plausible hydridic character.

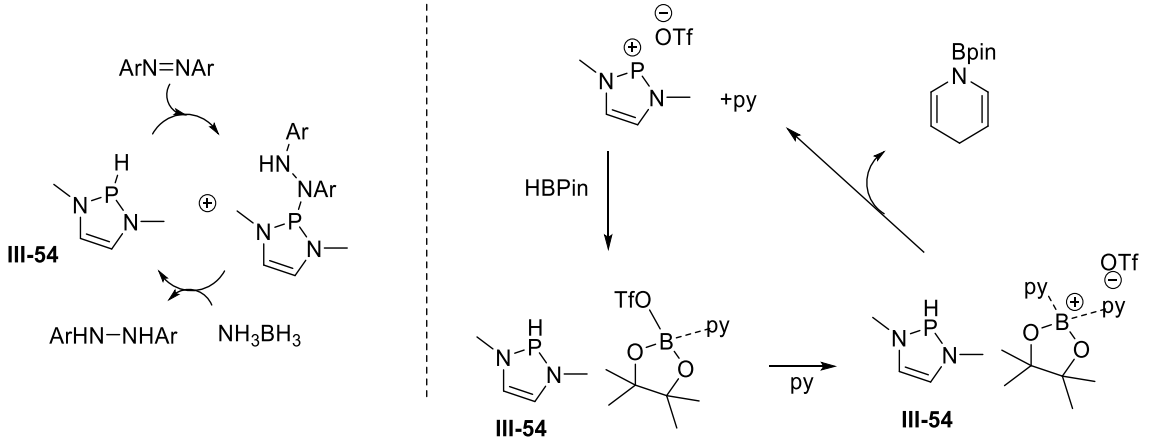

Scheme 50. Examples of catalysis employing hydridic character of diazaphospholene.[142]

To prepare the target **III-53**, we initially applied the same *in situ* protocol used for preparing the **III-47**. Thus, lithiated NSN was generated by the treatment of **III-6a** with two equivalents of LDA, followed by addition of PCl_3. Unfortunately, PCl_3 reacted with the diisopropylamine by-product instead of **III-6a**. There were at least four phosphorus species observed, thus a new route was required. **III-46a** prepared *in situ* was chosen as the starting material for transmetallation in THF. Approximately 30 minutes after the addition of PCl_3 to a solution of **III-46a**, the formation of a new species was noted. After a few days at room temperature, the reaction settled upon largely three main phosphorus species according to $^{31}P\{^{1}H\}$ NMR. In the proton spectrum, there were presumably two species, one with symmetric olefinic methines and one with a potentially protonated arm. The former likely was ClPNSN, while the latter species was presumed to be formed after due to the ligand-assisted N-H activation of unremoved residual diisopropylamine. The identity of this latter species is still unclear. More convincing evidence for this species could potentially be found if THF-d^8 were use instead.

An alternative method for preparing ClPNSN (**III-53**) was carried out, using MeLi for deprotonation of **III-6a** at low temperature in Et_2O, followed by low temperature addition of PCl_3. NMR spectra of the reaction mixture revealed formation of *C*s symmetric species, where only one singlet for backbone methines and only one *i*Pr septet (approximately 6.28ppm and 2.63ppm respectively) were observed. Oddly, reproduction of the ^{31}P NMR shift for the believed-to-be **III-53** at was inconsistent: a shift was observed at approximately 17.5ppm twice in ethereal solvent, and once at 36.7ppm (when the proton NMR matched). This may be due to the lack of a deuterium lock when in proteo solvent. However, the broadness in the aromatic region and in the methyl region suggest fluxionality in the compound. The reason for this exchange was hinted by the known structure of **III-47**, where the coordination of sulfur to Ge leads to a bent, envelope

structure, resulting in asymmetry. As an aside, a geometry optimization calculation of HPNSN by ORCA using the def2-SVP basis set, auxiliary basis def2/J, and BP86 functional there was no formal bond between the phosphorus and sulfur atoms, leading to a non-rigid backbone which may have the potential to invert rapidly. This should lead to averaging of signals and an apparent C_2 symmetry.

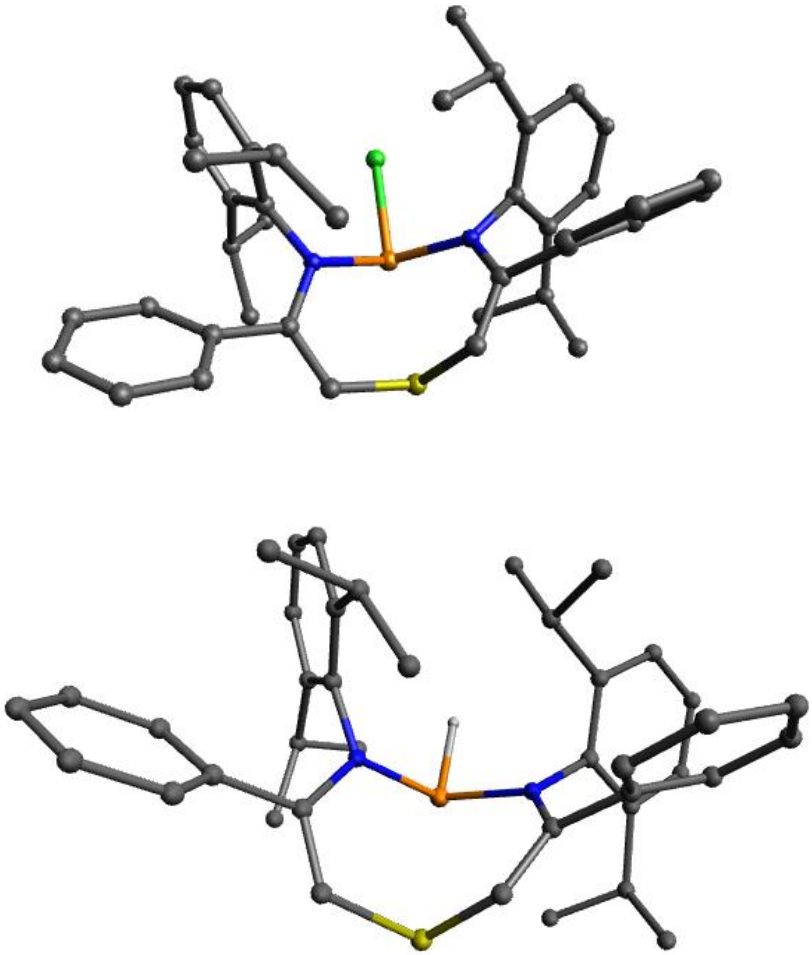

Figure 22. Geometry optimized structure of ClPNSN and HPNSN, using the def2-SVP basis set, auxiliary basis def2/J, and BP86 functional.

To test this hypothesis, variable temperature studies in Et_2O were performed. At room temperature, 1-D NOE reveals the presence an asymmetric species via exchange of the methine signals into a well-defined AB system of two coupled doublets, as well as the symmetric *i*Pr septet exchange into two signals (Figure 23). Exchange of methine protons was frozen out at 5°C, but the broadness of the aromatic region persisted even at -90°C. Interestingly, we could not identify the ^{31}P NMR signal for this compound even when the spectra window was increased to include the region down to +500 pm and up to -500 ppm. However, the presence of phosphorus was evident from the derivatization chemistry discussed below.

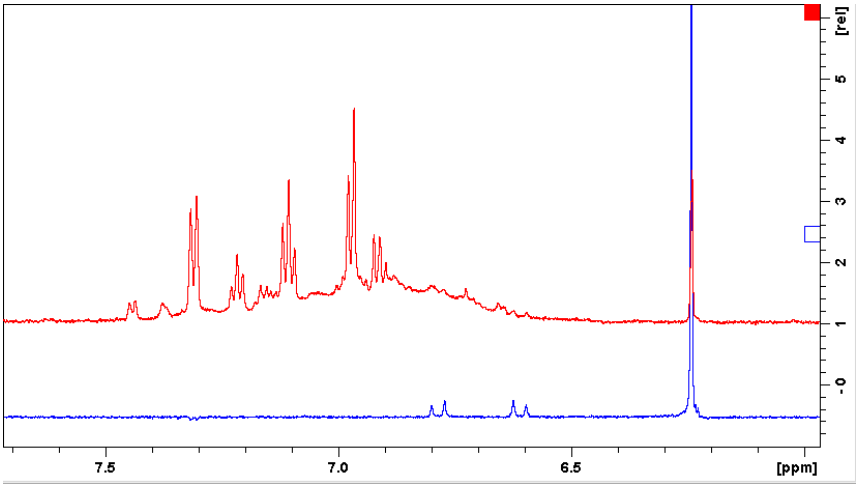

Figure 23. 1-D EXSY of ClPNSN in Et_2O (and ^1H NMR for reference) methine signal at RT and 600MHz.

As the goal was to generate a phosphorus compound bearing a P-H bond for application in bond activations and catalysis, **III-53** was reacted with a solution of L-selectride in THF. The ^1H NMR spectrum of the product in Et_2O did not give evidence of a phosphorus bound hydrogen. Comparing the ^{31}P and $^{31}P\{^1H\}$ spectra however clearly shows phosphorus has a coupled proton.

Thus, in Et_2O the ^{31}P NMR signal at 35.8ppm shows the ^{1}J(P-H) coupling of 163.6 Hz. Both the **III-53** and **III-52** phosphorus shifts were significantly upfield from PCl_3. (Figure 24)

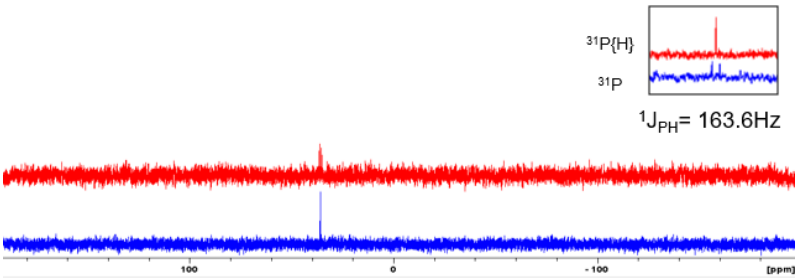

Figure 24. 31P and 31P{1H} spectra of III-52, with close-up in-set image.

It is also worth mentioning that Arduengo *et al*. reported difficulty in isolating the diphenyl-substituted P(ONO) system, due to an instability of the compound. Even the quite sterically demanding adamantyl substituted phosphorus species was isolated in only 29% yield upon treatment with PCl_3 and NEt_3. The species was observed by NMR but isolation was not successful for phosphorus, albeit its arsenic analogue was characterised. [99]

IV. Conclusions and Future Work

While the preparation of a tridentate ligand with a central nitrogen was not achieved due to complications of unselective brominations of ketimines, the bromo-imine PhC(=N-DIPP)CH_2Br (**III-15a**) was eventually prepared, albeit in very low yields, which allowed for the synthesis of the title NSN ligand (**III-6a**). Methods for deprotonating the ligand in-situ were developed and were applied to reactions with metal-chloride compounds of zinc, germanium, and phosphorus. Stabilization of ZnNSN compounds was achieved by THF or N,N-dimethylaminopyridine (DMAP). NMR spectroscopic evidence for ZnNSN(THF) (**III-46a**) and ZnNSN(DMAP) (**III-45a**) was obtained, and the activation parameters of the exchange of DMAP were measured. Similarly, NMR evidence for ClPNSN (**III-53**) and the product of halogen-hydrogen exchange, HPNSN (**III-52**), was obtained. Unfortunately, replication of the synthesis of ClPNSN (**III-53**) was inconsistent. Methods of isolation and crystallization for the zinc and phosphorus compounds remain elusive, thus reactivity studies were not investigated. In contrast, synthesis of GeNSN (**III-47**) could be repeated and crystals suitable for X-ray were obtained from Et_2O. The structure resembled two fused five-membered rings in an envelope-like geometry. Reaction of GeNSN (**III-47**)with 3,6-di-*tert*-butyl-o-benzoquinone (**III-48**) produced two species which exist in an equilibrium (**III-51**/**III-51'**), possibly due to weak interaction of Ge-S leading to fluxionality in the geometry of the NSN ligand (**III-6a**).

With the discovery of a route for PhC(=N-DIPP)CH_2Br (**III-15a**), it may still be possible to proceed via the originally planned pathway to the flexible ligand with a central nitrogen (**III-4a**). However, due to the poor scalability and very low yield of the titanium-mediated imination reaction to prepare PhC(=N-DIPP)CH_2Br (**III-15a**), coupled with the number of envisioned subsequent steps, renders the NNN ligand impractical.

V. Experimental

Unless otherwise noted, all reactions were carried out in dry, degassed solvents in a glovebox under N_2 or using Schlenk techniques. NMR spectra were obtained on either 300, 400, or 600 MHz spectrometers and referenced solvent signals according Fulmer *et al*. 2010[146].

Bromine-dioxane adduct: To a capped round-bottom flask containing 1,4-dioxane (8.0mL, 0.094mol)), bromine (3.0mL, 0.058mol) was added dropwise via an addition funnel over 25 minutes. The solution quickly darkened, and a precipitate is formed quickly. A magnetic stirring bar fails to continue to stir the product after about half of the bromine has been added. Allowing the addition to occur in a cooled, sealed flask, the crystals lighten to a bright orange. Once the gaseous bromine has appeared to dissipate, the crystals were filtered and rinsed with 12mL dioxane via a Buchner funnel for approximately 5 minutes, as the product is quite volatile. The bright orange crystals were quickly weighed (9.430g, 0.038mol, 66% yield) and placed in the freezer(-30°C) for storage.

α-Bromoacetophenone: To an open round bottom flask containing bromine-dioxane adduct (16.010g, 0.064mol), 100mL acetonitrile was quickly added to yield a dark red solution. The solution was stirred for 10 minutes in an ice bath, followed by the addition of acetophenone (7.10mL, 0.061mol). The flask was then capped and stirred while slowly warming to room temperature over two hours. Mixture went bright orange and was poured into 100mL ice water, then washed with 3x50mL DCM. Volatiles removed and recrystallization was done in EtOH, and 6.82g (0.034mol, 56% yield) collected after filtration.

DIPP-N=C(Ph)CH_2Br: To a cooled solution (0°C) of α-Bromoacetophenone (10.02g, 0.050mol) and 2,6-diisopropylaniline (10mL, 0.053mol) in 30mL DCM, a solution of $TiCl_4$ (2.76mL, 0.025mol) in DCM (10mL) was added dropwise over a period of 30 minutes. The solution quickly

darkened from a clear pinkish solution to a slightly brownish-red upon addition, and orange precipitate was formed after approximately 5 minutes while stirring in the ice bath. After 20 minutes of stirring, NEt_3(28mL, 0.2mol) was added via a dropping funnel, dropwise over 10 minutes. The mixture darkens very quickly to a dark brown-red mixture after a few drops were added. The brown mixture was stirred overnight while slowly warming to room temperature. Unreacted $TiCl_4$ was quenched with ice-water ~20mL, then filtered over Celite with copious amounts DCM 9 (~150mL) until rinsing was clear. Purification was performed by either column chromatography (2:1 hexane: toluene or 9:1 hexane: ethyl acetate) or vacuum distillation while closely monitoring the heat, followed by multiple fractional crystallizations in hexanes (crude product: 4.198g, ~70% purity, ~8% yield; recrystallized 0.36g, 0.001mol, 2% yield). ^{1}H: 8.06 (m, 4H, Ph-*o* (both isomers)), 7.54-7.50 (m, 6H, Ph-*m* and *p*, (both isomers)), 7.17 (d, 4H, N-Ar-*m* (both isomers)), 7.13-7.10 (m, 2H, N-Ar-*p* (both isomers)), 4.21 (s, 2H, C=C(H)-S (minor)), 4.08 (s, 2H, C=C(H)-S (major)), 2.80-2.68 (m, 4H, *i*Pr (both isomers)), 1.21 (d, 6H, 2x C*H*$_3$ (major)), 1.18 (d, 6H, 2x C*H*$_3$(minor)), 1.14 (d, 6H, 2x CH_3(both isomers)). ^{13}C{^{1}H} NMR peaks for minor species which are not overlapped N-Ar(ipso) 145.2ppm; Ar-*i*Pr(ipso) 135.8ppm; C=N 161.2ppm; Ph(ispo) 135.6ppm; Ph(ortho) 128.1ppm; CH_2Br 35.9ppm; CH_3 23.5ppm & 22.6ppm.

(DIPP-N=C(Ph)CH_2)$_2$S: synthesis A: to a refluxing solution of bromoimine (1.50g (93% purity), 0.004mol) in 30mL ethanol, 0.5 equivalents of Na_2S*9H_2O (0.485g, 0.002mol) in 1mL H_2O were added dropwise over approximately 20 minutes, then stirred at 100°C for an hour. Solution was filtered hot through a fine glass filter. Bright yellow fluffy solids collected (0.632g, 53% yield) Synthesis B: a solution of bromoimine (2.001g, 0.0056mol) in 50mL DMF was cooled to zero degrees and a 5mL aqueous solution of 0.5 equivalents of Na_2S*9H_2O (600mg, 0.0025mol) was added dropwise. When addition was completed the mixture was heated overnight at 60°C. Solvent

was removed by high vacuum with heating. The resulting oil was taken up in a small amount of hexane: ethyl acetate 40:1 and purified by flash chromatography. The fractions containing the compound were combined and volatiles removed, resulting in a sticky solid. (0.916g, 0.0016mol, 64%). ^{1}H: 8.08 (br-s, 4H, Ph-*o* (minor)), 7.69 (d, 4H, Ph-*o* (major)), 7.47-7.36 (m, 6H, Ph-*m* and *p*), 7.18-6.98 (m, N-Ar(*m* and *p*)), 3.69 (dd, 4H, N=C-C*H*$_2$-S (minor, asymmetric)), 3.28 (s, 4H, N=C-C*H*$_2$-S (major, symmetric)), 2.78 (br-s, 4H, *i*Pr (minor)), 2.66 (septet, 4H, *i*Pr (major)), 1.3-0.7 (m, 24H, C*H*$_3$ (both isomers)). ^{13}C:163.4 (N=*C*), 145.8, 137.5, 135.9, 130.6, 128.6, 127.8, 123.9, 123.0, 31.7 (CH_2-S), 28.5 (CH_3), 23.5 (CH_3), 22.3 (CH_3).

(DIPP-NLi-C(Ph)CH)$_2$S: The di-lithiated salt was not isolated successfully due to instability over time and to vacuum. A general small-scale procedure involves preparing solutions (~1mL) of NSN (20mg, 0.000034mol) and LDA (7.3mg, 0.000068mol), followed by dropwise addition of the LDA solution at room temperature. This species must be used quickly for subsequent substitution reactions. Alternatively, an ether solution of MeLi(1.6M) was added to the solution of NSN in either THF or Et_2O. ^{7}Li (THF, 600MHz): symmetric: 2.1ppm. Asymmetric: 2.0 & 0.0ppm.

[(DIPP-N=C(Ph)CH)$_2$S]Zn(THF): In the glovebox, a clear, colourless solution of LDA (7.3mg, 0.000068mol) in THF was added to a clear, yellow solution of (DIPP-N=C(Ph)CH_2)$_2$S (20mg, 0.000034mol) in THF. The solution quickly darkened to red, was stirred for ~2 minutes, then was added dropwise to a solution of $ZnCl_2$ (5.4mg, 0.000034mol) with concurrently lightening and precipitation. ^{1}H: 7.18(m, 4H, Ph-*o*), 6.83 (m, 6H, Ph-*m* and *p*), 6.64 (d, 4H, N-Ar(*m*)), 6.56 (t, 2H, N-Ar(*p*)), 4.54 (s, 2H, N-C=C(*H*)-S), 3.33 (sept, 2H, *i*Pr), 1.12 (d, 6H, 2x C*H*$_3$), 0.86 (d, 6H, 2x C*H*$_3$), 0.81 (d, 6H, 2x C*H*$_3$), 0.65 (d, 6H, 2x C*H*$_3$). ^{13}C: 163.4 (N-*C*(Ph)), 148.4, 143.9, 143.5, 141.6, 129.24, 125.8, 122.2, 122.0, 120.9, 83.8 (N-C=C-S), 25.7 (*C*H_3), 25.0 (*C*H_3), 23.7 (*C*H_3), 23.3 (*C*H_3)

[(DIPP-N=C(Ph)CH)$_2$S]Zn(DMAP): procedure A) In the glovebox, a clear, colourless solution of LDA (7.3mg, 0.000068mol) in Et_2O was added to a clear, yellow solution of (DIPP-N=C(Ph)CH_2)$_2$S (20mg, 0.000034mol) in Et_2O. The solution quickly darkened to red and stirred at RT for 30 minutes. After 30 minutes, a clear and colourless solution of $ZnCl_2$ (20mg, 0.000034mol) was added and the precipitate was filtered. A solution of 1 equivalent of N,N-dimethylaminopyridine (0.0083mg, 0.000068mol) was added to the NMR tube. Procedure b) analogous to formation in Et_2O, apart from THF as the solvent and addition of $ZnCl_2$ solution after 1 minute, followed by quick addition of DMAP. ^{1}H: 7.67(d, 4H, Ph-*o*), 7.52 (br-s, 2H, DMAP-Ar), 7.15 (m, 4H, Ph-*m*), 7.1-6.9 (m, Ph-*p* and Ar-*m* and *p)*, 5.57 (br-s, 2H, DMAP-Ar), 5.41 (s, 2H, N-C=C(*H*)-S), 3.92 (sept, 2H, *i*Pr), 3.78 (sept, 2H, *i*Pr), 1.81 (br-s, 6H, DMAP-C*H*$_3$), 1.21 (d, 6H, 2x C*H*$_3$), 1.16-1.12 (dd, 16H, 4x C*H*$_3$), 0.79 (d, 6H, 2x C*H*$_3$).

[(DIPP-N=C(Ph)CH)$_2$S]Ge: In the glovebox, to a stirred solution of NSN (20mg, 0.000034mol) in Et_2O, two equivalents of a solution of LDA (7.3mg, 0.000068mol) in Et_2O was added dropwise. After 5 minutes of stirring, solution was added dropwise to a stirred mixture of $GeCl_2$*dioxane (7.8mg, 0.000034mol) in Et_2O and filtered. ^{1}H NMR (600 MHz, C_6D_6) 7.32 (m, 4H, Ph-*o*), 7.00-7.06 (m, 6H, Ph-*m* and *p)*, 6.92-6.87 (m, 6H, N-*Ar (m* and *p))*, 5.31 (s, 2H, N-C=C(*H*)-S), 3.61 (septet, 2H, iPr), 3.39 (septet, 2H, iPr), 1.23 (d, 6H, 2x CH_3), 1.09 (d, 6H, 2x CH_3), 1.01 (d, 6H, 2x CH_3), 0.88(d, 6H, 2xCH_3). Elemental Analysis: Theoretical %: C:72.8; H:7.0; N:4.2; Theoretical + 1eq Et_2O: C:72.0; H:7.7; N:3.8; Measured %: C:71.4; H:7.6; N:4.3.

[(DIPP-N=C(Ph)CH)$_2$S]Ge(catechol): GeNSN was dissolved in C_6D_6 and an equivalent of methyl iodide added to the solution. The mixture was heated to 70°C overnight, then after no reaction with MeI, volatiles were removed under vacuum and compound was re-dissolved. To this solution, an equivalent of 3,5-di-*tert*-butyl-o-benzoquinone was added and monitored at room temperature.

Major isomer after 1.5h ^{1}H NMR (600 MHz, C_6D_6): δ 6.97 (multiplet, Ar), 5.20 (singlet, 2H, methine), 3.70 (septet, 2H, *i*Pr), 3.1 (septet, 2H, *i*Pr), 1.75 (singlet, 9H, *t*Bu), 1.11 (singlet, 9H, *t*Bu), 0.80 (doublet, 6H, methyl), 0.62 (doublet, 6H, methyl).

[(DIPP-N=C(Ph)CH)$_2$S]PCl: In the glovebox, 40.0mg of NSN was dissolved in 2-3mL of Et_2O and cooled to -30°C in the freezer. The pale-yellow solution was placed on a stir plate and 2 equivalents of cold MeLi (84μL of 1.6M solution in Et_2O) was added slowly over 1 minute, with instant colour change. The solution was stirred for 3 minutes, then 1 equivalent (6μL) of PCl_3 was added slowly in 1μL portions over ~30 seconds, also with instant darkening to dark orange/red, followed by gradual change back to yellow/orange and producing colourless solids. The mixture was filtered via pipette filter and rinsed with an extra 1mL Et_2O. The clear orange solution was concentrated and transferred to an NMR tube. 7.65 (d, Ph-*o*), 7.55 (t, Ph-*p*), 7.40 (t, Ph-*m*), 7.28 (d, N-Ar-*m*), 7.2(t, N-Ar-*p)*, 6.55 (s, C=C(H)-S), 2.9 (septet, *i*Pr), 1.1 (d, CH_3).

[(DIPP-N=C(Ph)CH)$_2$S]PH: In the glovebox, to the reaction which produced one phosphorus signal, a solution of 1M L-selectride (68uL) was added to the NMR tube at room temperature. Full characterization was not possible as species decomposed and synthesis of parent ClPNSN was inconsistent. ^{1}H (C_6D_6): 6.6 (N-C=C(*H*)-S), 2.9 (septet, 4H, *i*Pr), 1.1 (d, CH_3), 1.0 (d, CH_3)

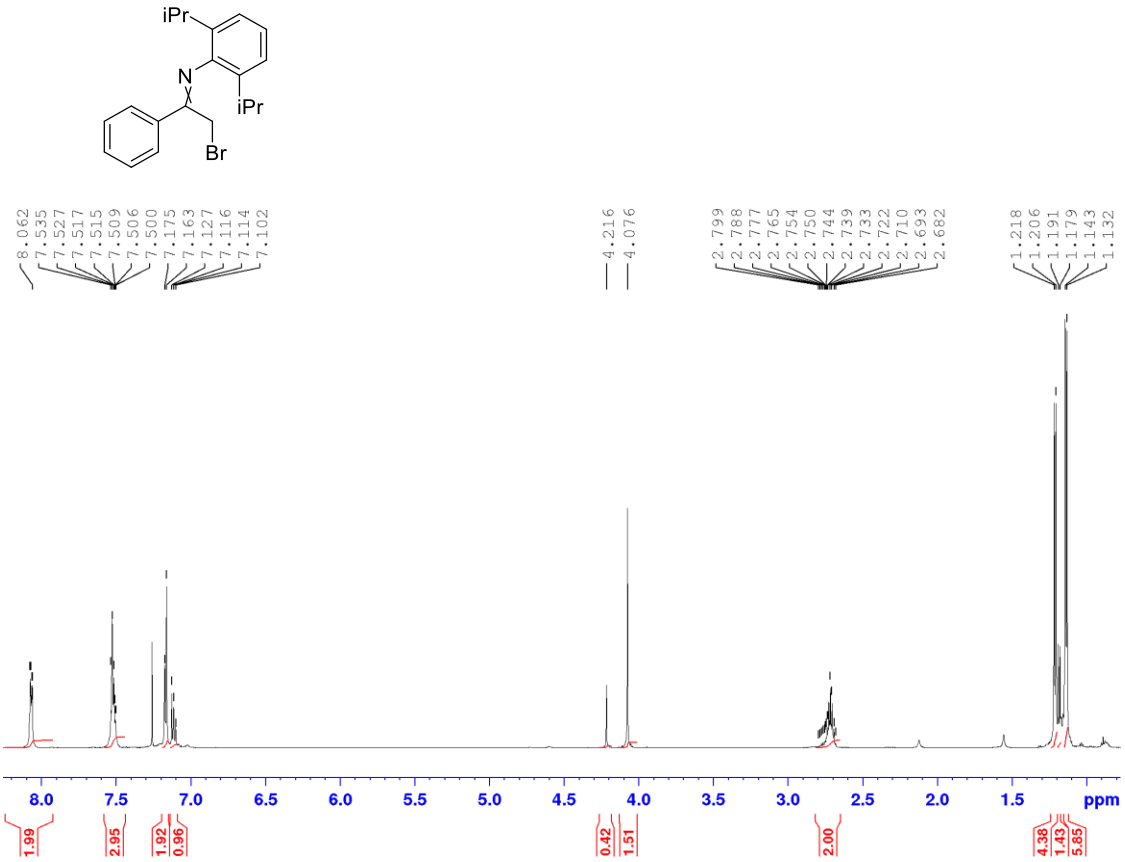

Figure 25. ^{1}H NMR of mixture of DIPP-(bromo)imine isomers in $CDCl_3$ at 600MHz, ratio of 3.6:1.

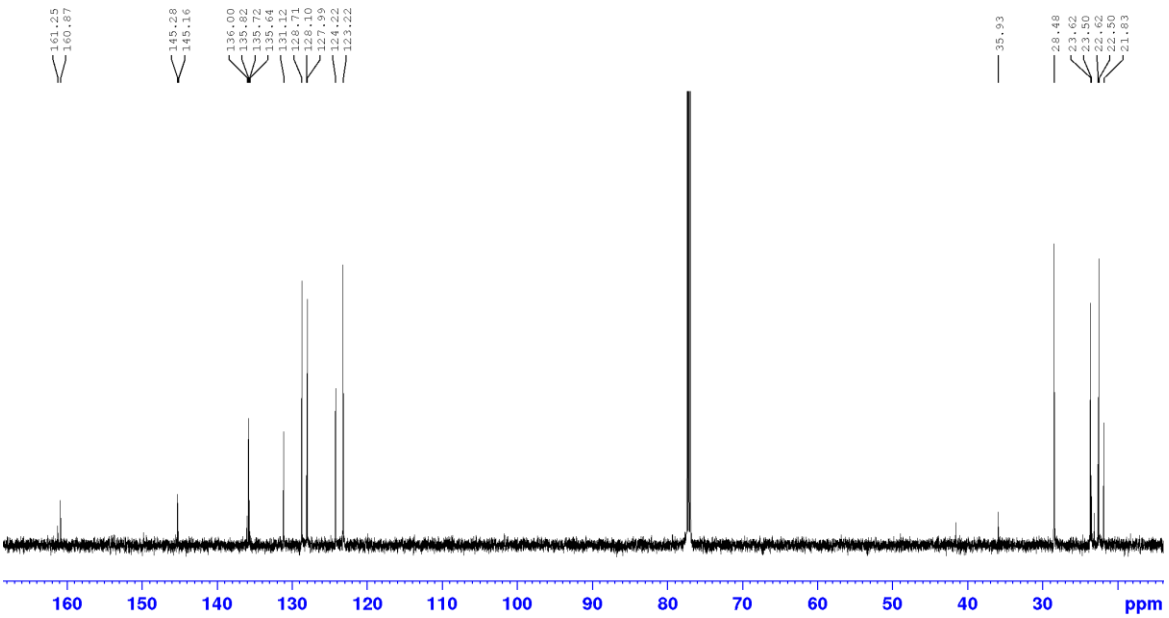

Figure 26. $^{13}C\{^{1}H\}$ NMR of DIPP-bromoimine mixture of isomers.

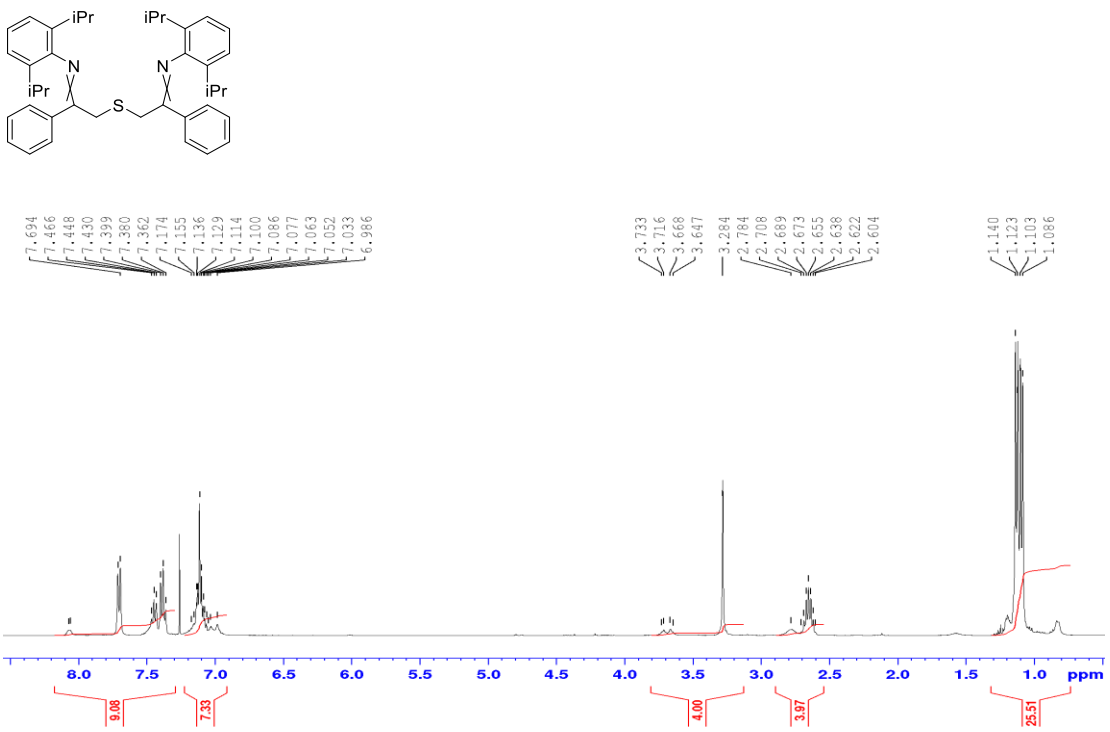

Figure 27. ^{1}H NMR of NSN in $CDCl_3$ at 400MHz. To demonstrate all signals for the equilibrium species are accounted for, aromatics are integrated to 16, methylenes to 4, iPr to 4, and methyls to 24.

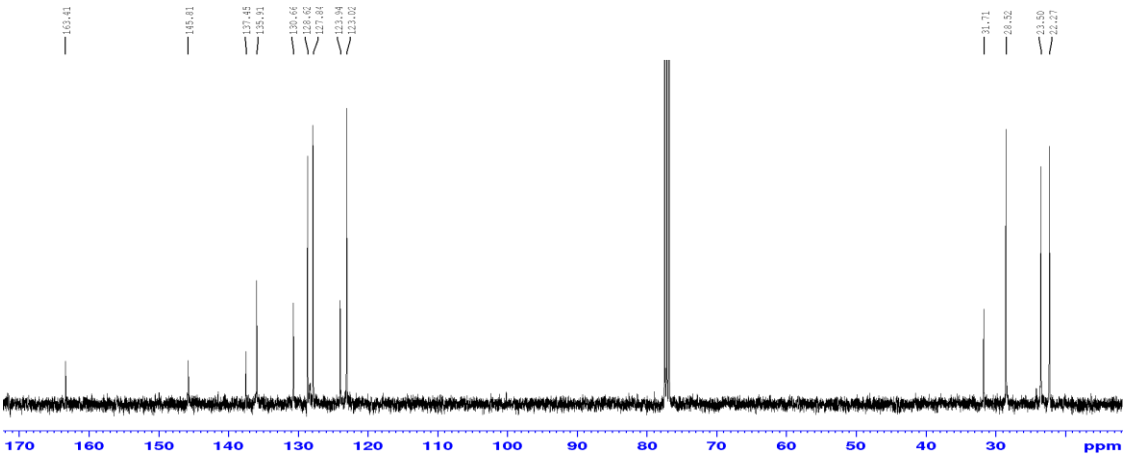

Figure 28. $^{13}C\{^{1}H\}$ NMR of NSN in $CDCl_3$ at 400MHz. Only symmetric species observed at room temperature. (See 2-D spectra, Figure 29, for rough assignment of select signals of asymmetric species)

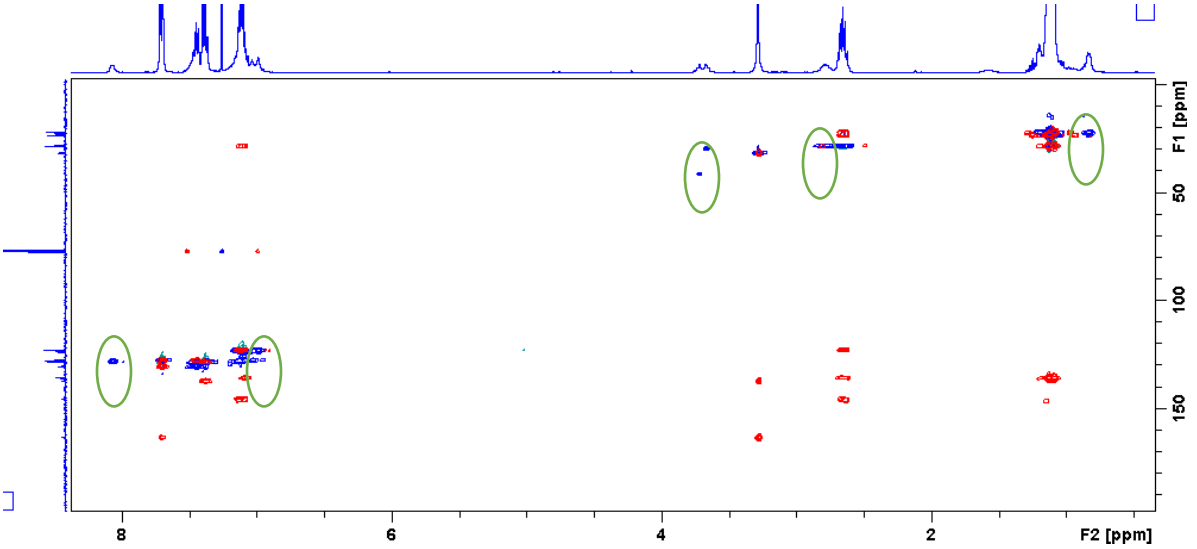

Figure 29. 2-D HSQC (blue) and HMBC (red) of NSN in $CDCl_3$ at 400 MHz. Highlighted discernable minor species (asymmetric) circled.

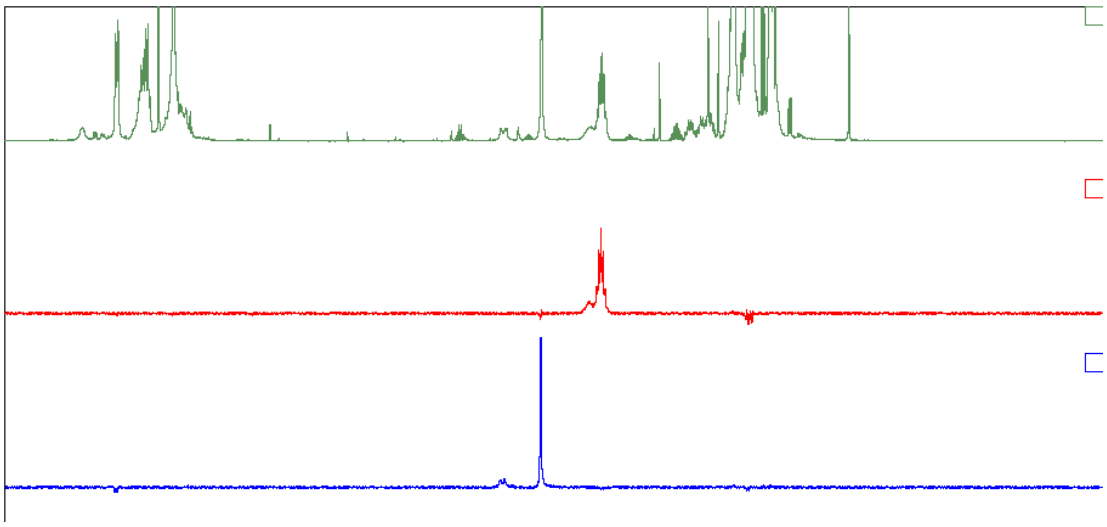

Figure 30. 1-D ^1H EXSY/NOE experiments of NSN in $CDCl_3$ at 300MHz. Green=^1H NMR ; Red =exchange of iPr upon excitation of symmetric iPr; Blue=exchange of methylenes upon excitation of symmetric species.

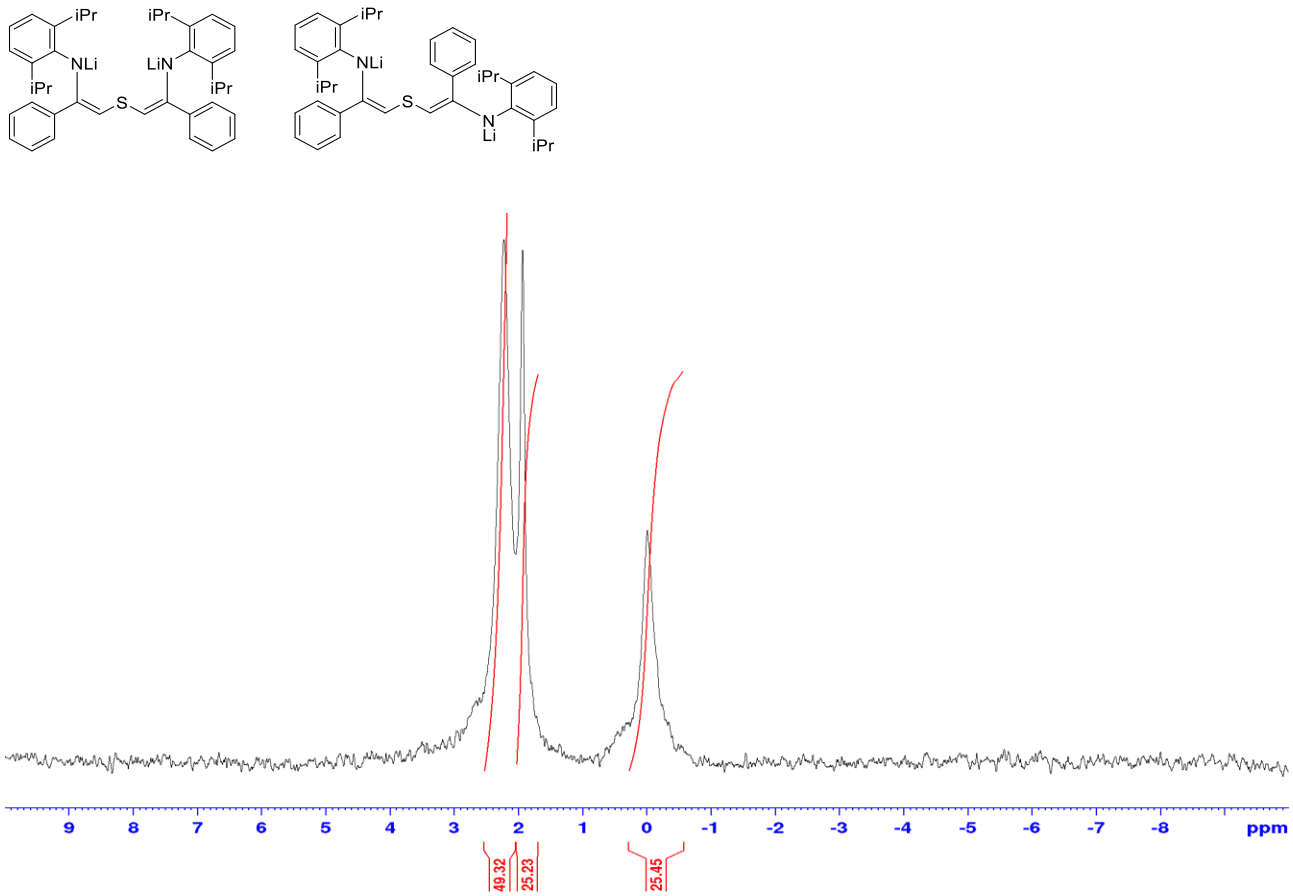

Figure 31. ^{7}Li NMR at 600 MHz spectrum of mixture of Li_2NSN symmetric and asymmetric species after 15 minutes at RT since mixing in THF.

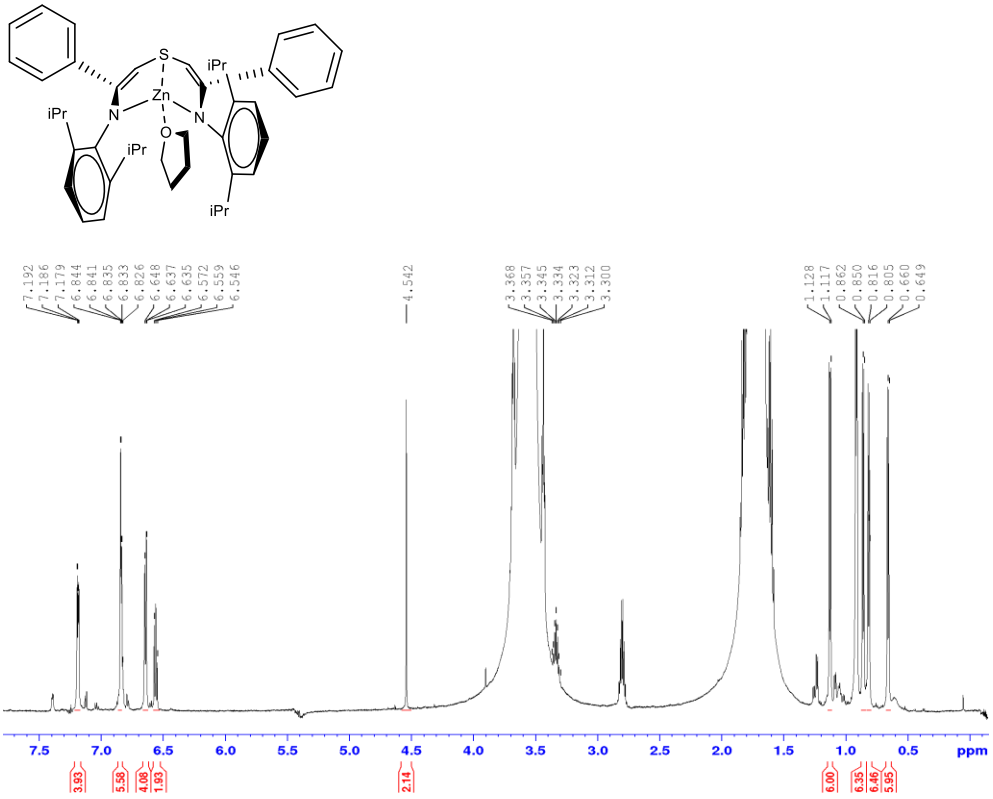

Figure 32.[1]H NMR of in-situ generated ZnNSN(THF) in THF at RT at 600 MHz. Sample contains residual diisopropylamine, and resonances for iPr signal overlapped by THF at ~3.4ppm and ~3.7ppm.

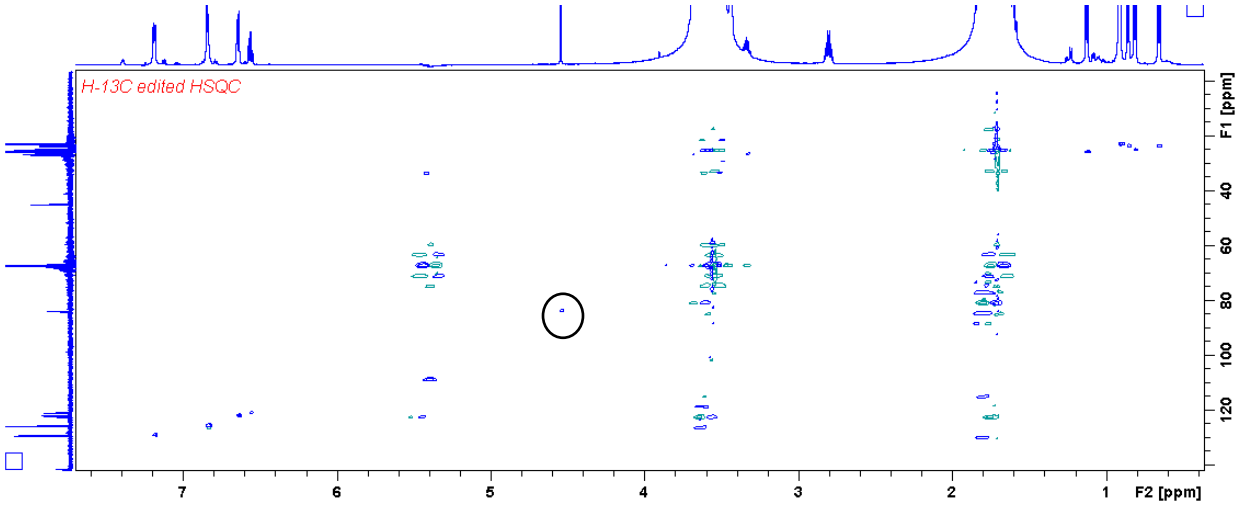

Figure 33. 2-D HSQC-ed of ZnNSN in THF. Blue cross peaks represent carbons bearing H or C-H_3. Methine peak circled. Contains residual diisopropylamine.

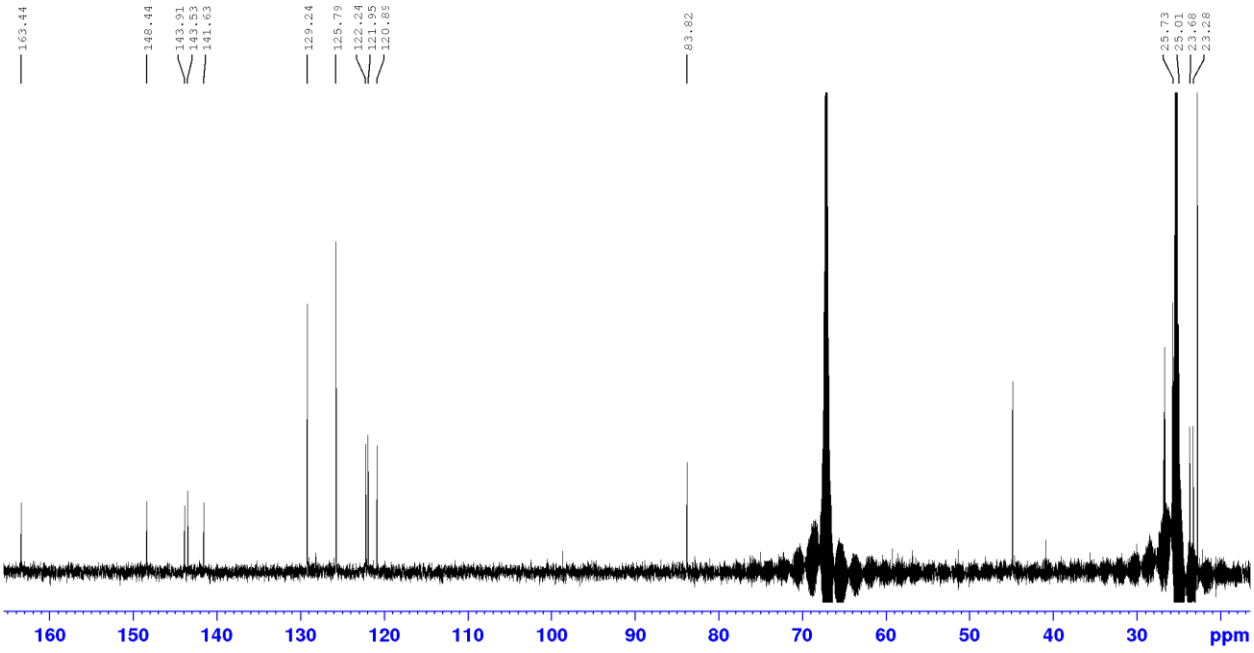

Figure 34. $^{13}C\{^{1}H\}$ NMR of ZnNSN in THF. Cannot identify iPr signals due to overlap with THF, and m-*Ph and* p-*Ph are isochronous (contains residual diisopropylamine).*

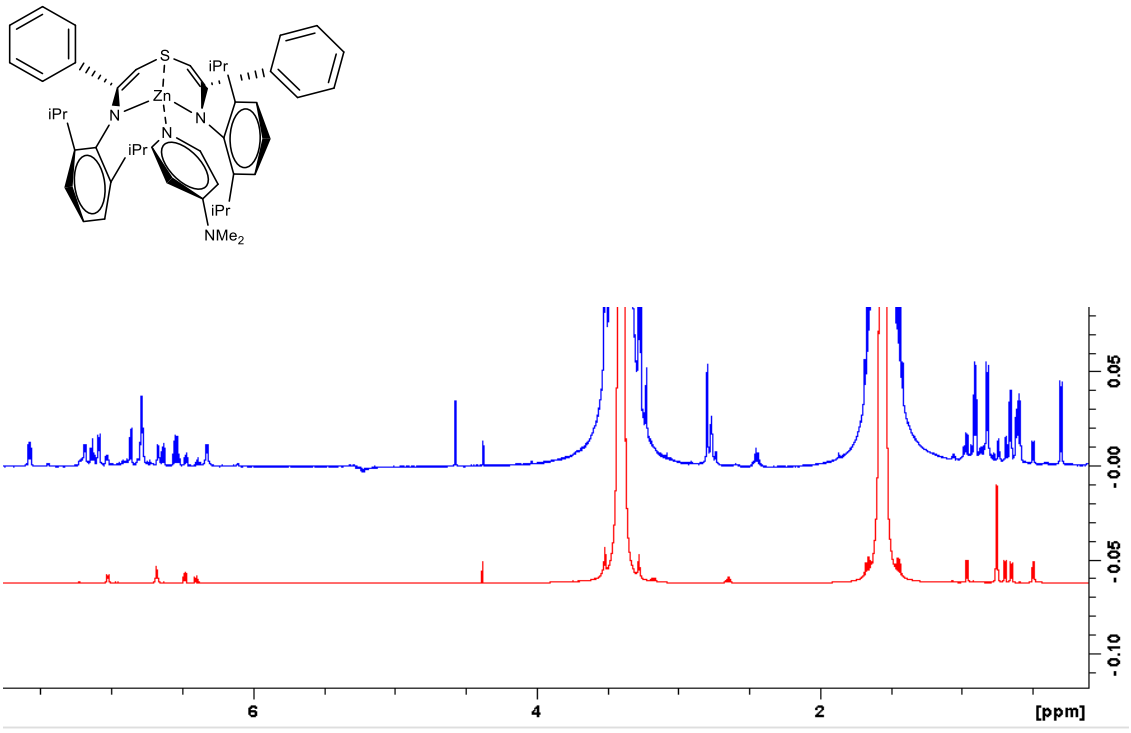

Figure 35. Room temperature spectra demonstrating ZnNSN(DMAP) & ZnNSN(THF) are present at the time of exchange parameters calculations via variable EXSY measurements at 600MHz.

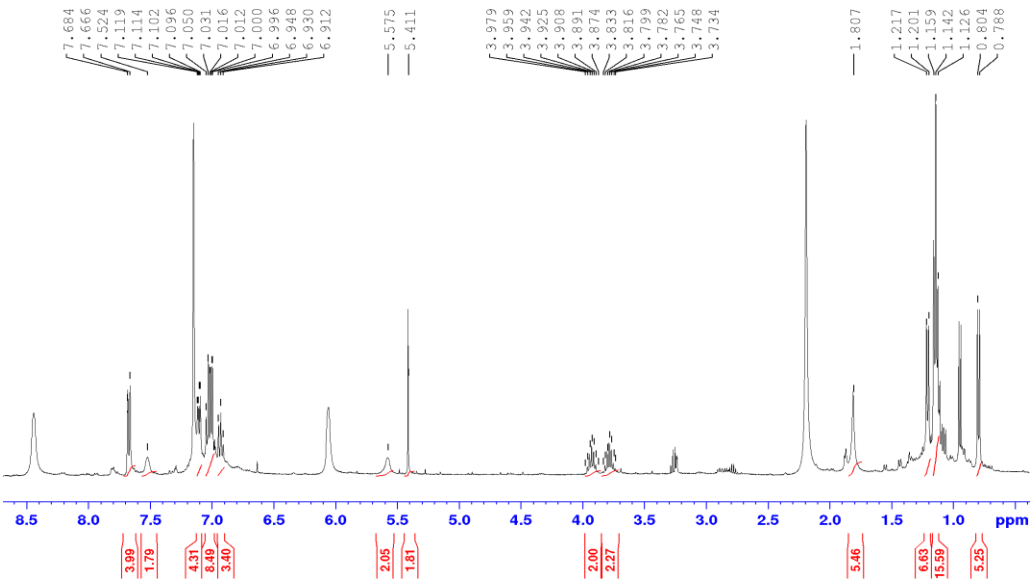

Figure 36. ^{1}H NMR of ZnNSN(DMAP) in C_6D_6 at 400MHz. Contains free DMAP which is in exchange with the coordinated DMAP fragment.

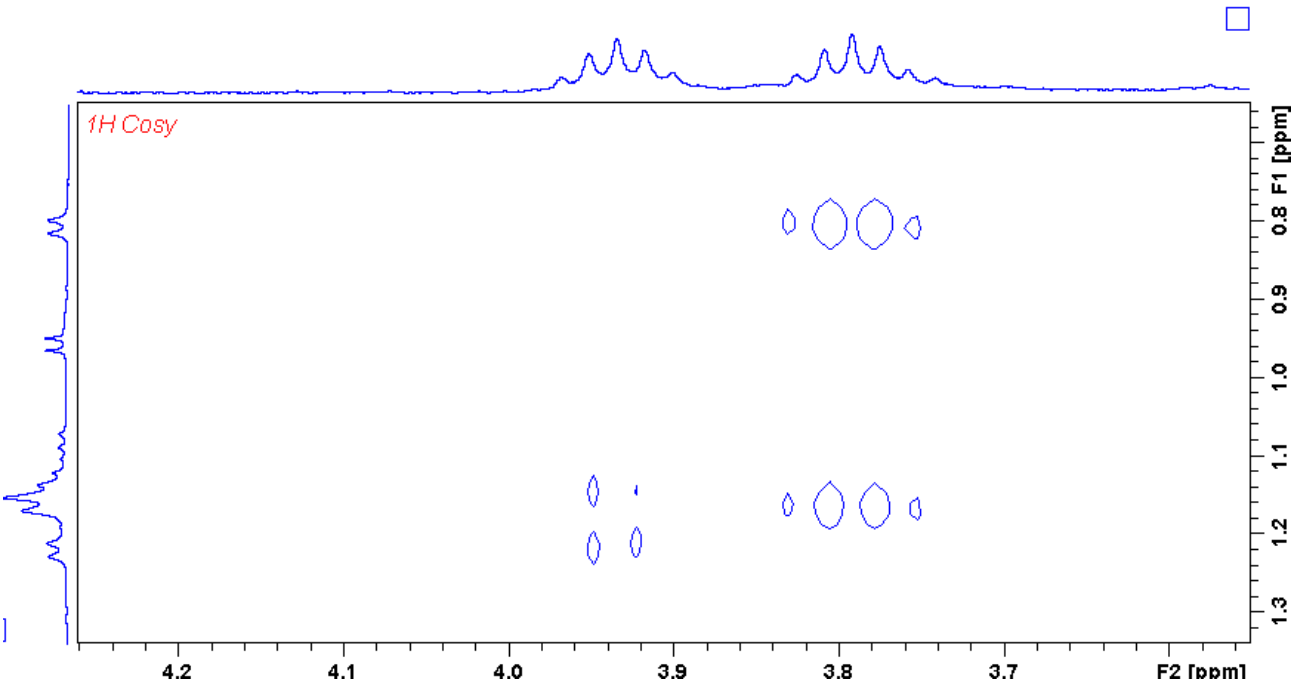

Figure 37. Support for assignment of peaks for ZnNSN(DMAP) in C_6D_6 via ^1H-^1H COSY @ 400MHz.

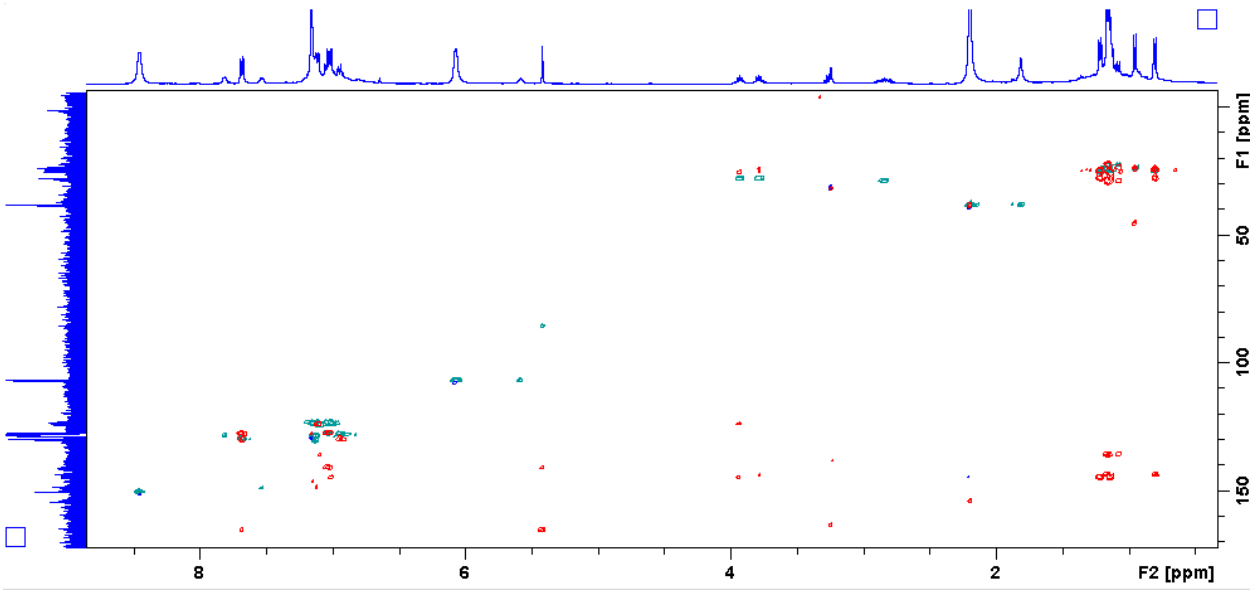

Figure 38. 2-D ^1H-$^{13}C\{^1H\}$ correlation spectra of ZnNSN(DMAP) of HSQCed(blue/green) & HMBC (red).

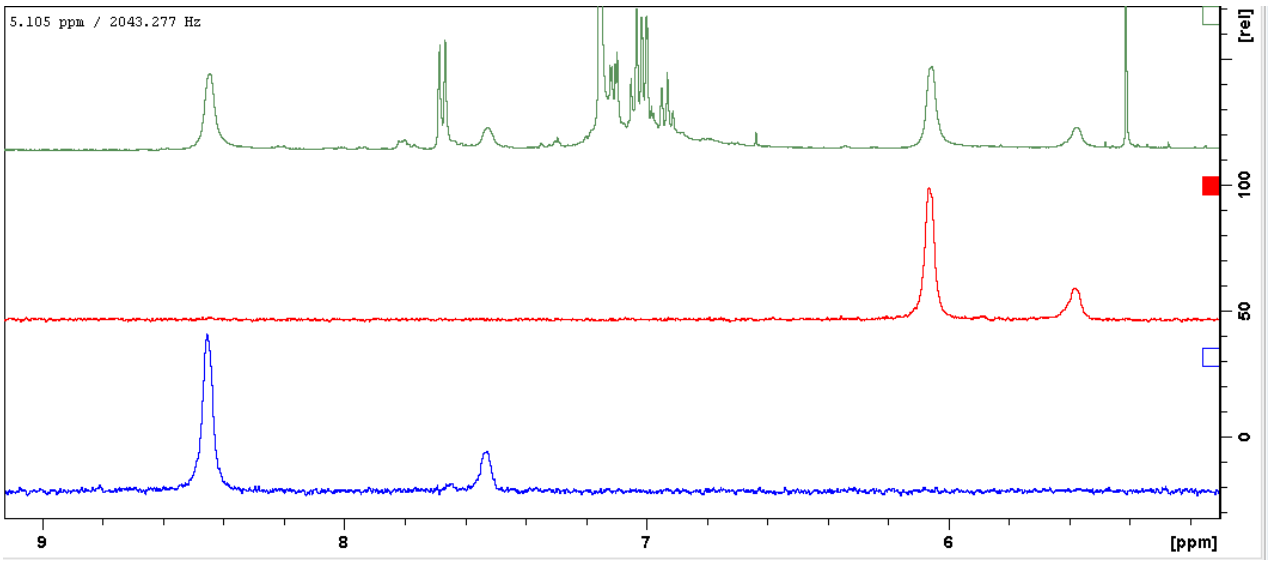

Figure 39. Evidence of exchange of free and coordinated DMAP fragments via 1-D ^{1}H NOE/EXSY spectra of excited free DMAP resonances.

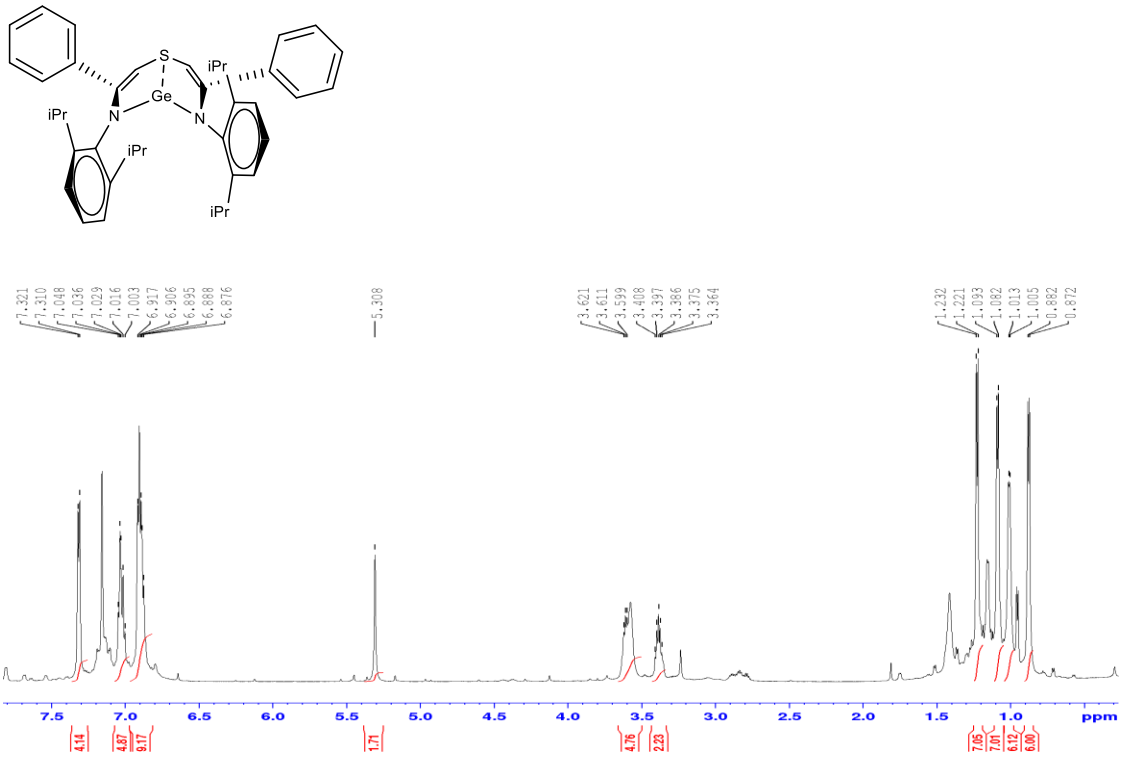

Figure 40. GeNSN in C_6D_6 after removal of (most) volatiles [contains some residual Et_2O and overlaps with iPr signal]

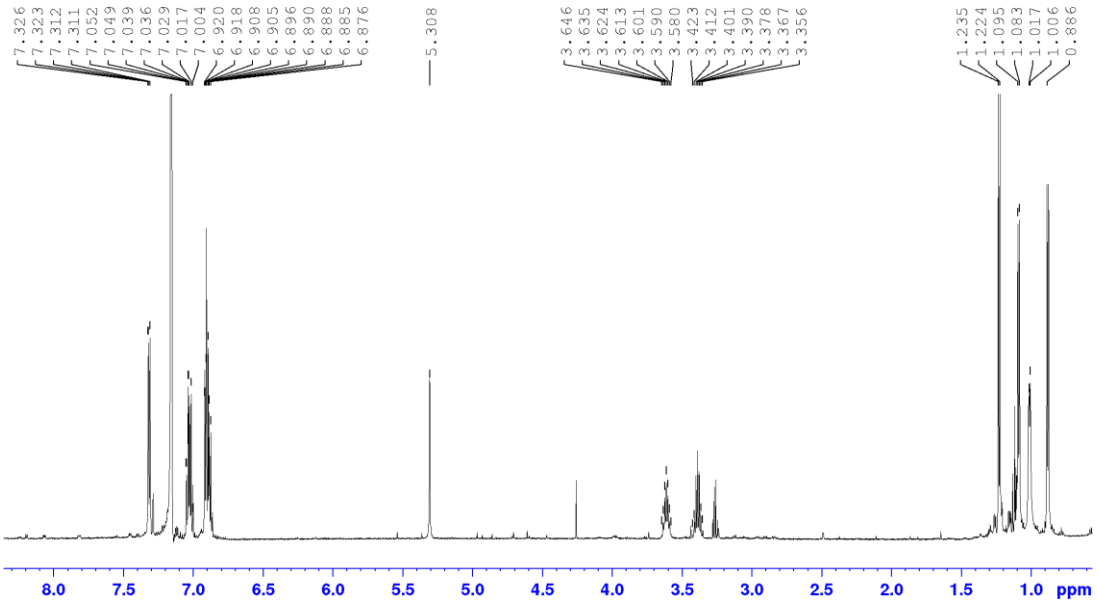

Figure 41. Higher resolution ^{1}H NMR using dilute sample of GeNSN crystals dissolved in C_6D_6

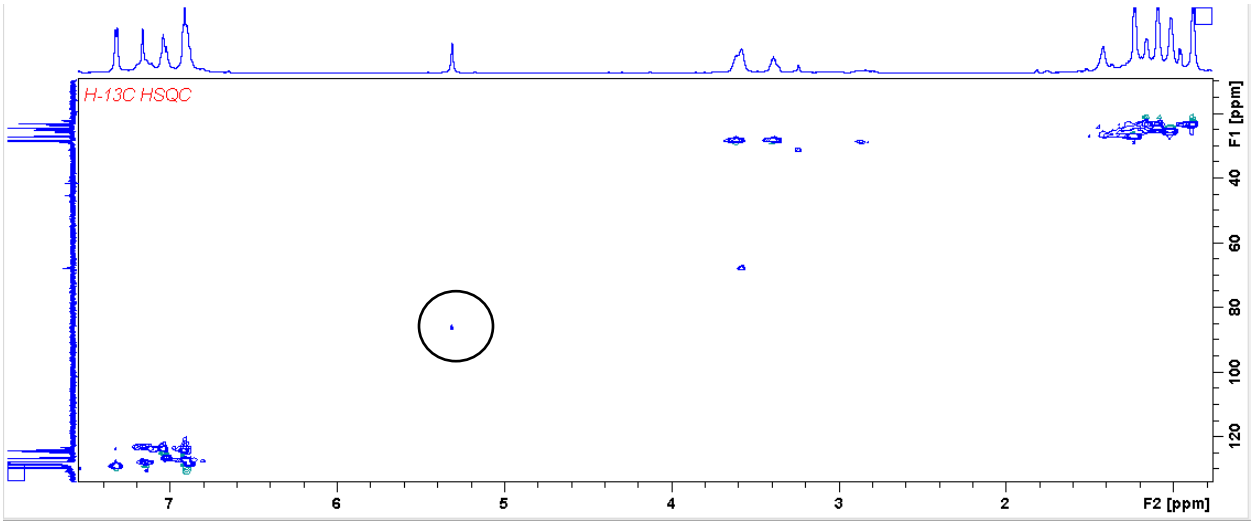

Figure 42. HSQC of GeNSN in C_6D_6 at 400MHz. Cross peak for methine signal is circled.

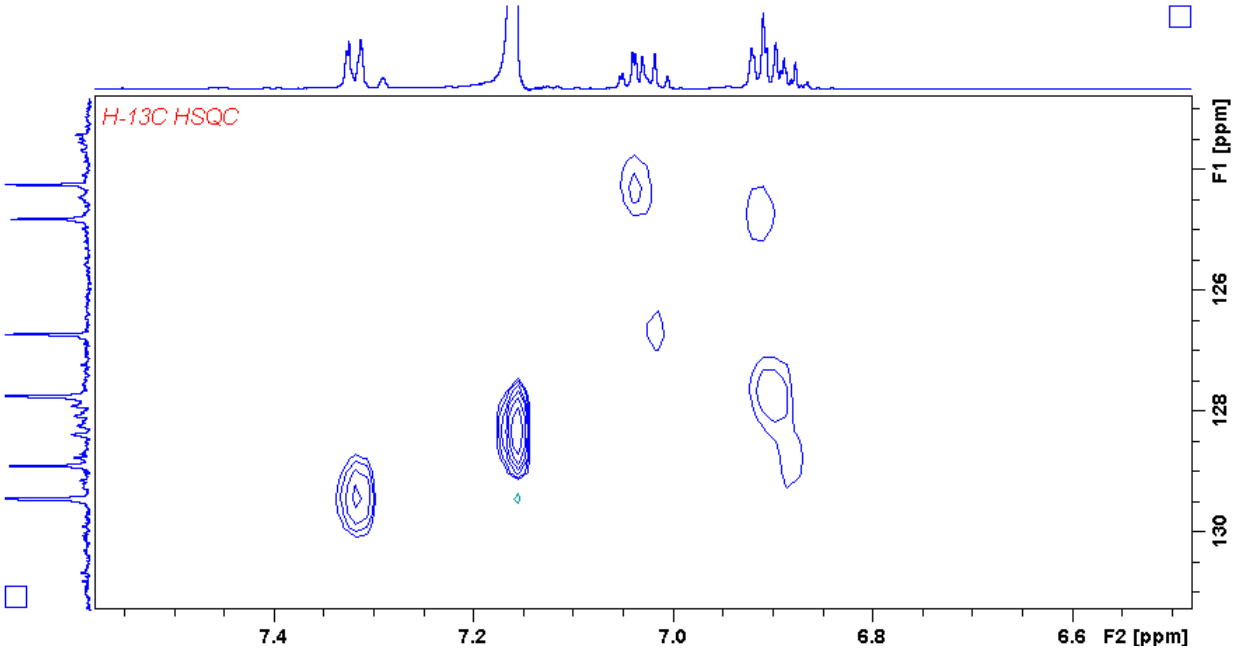

Figure 43. Combined support of assignment via HSQC of aromatic signals in multiplets for GeNSN in C_6D_6, using resolved ^1H from crystals with crude reaction mixture DEPT-135 y-axis overlay.

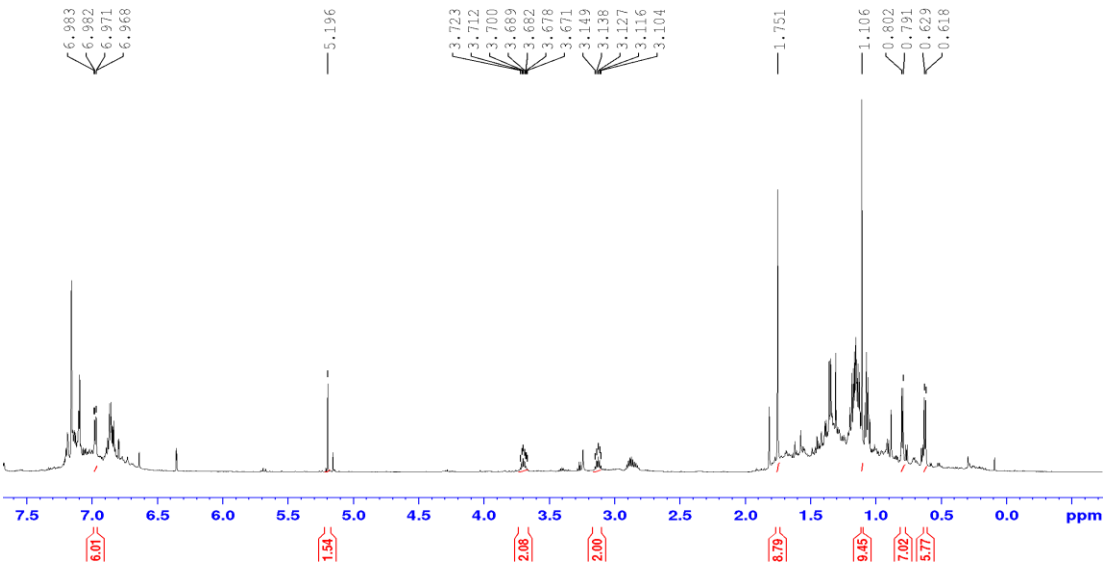

Figure 44. ^1H NMR spectrum 1.5h after addition of 3,5-di-tert-butyl-orthoquinone to GeNSN in C_6D_6, with unambiguous peaks assigned to a single isomer.

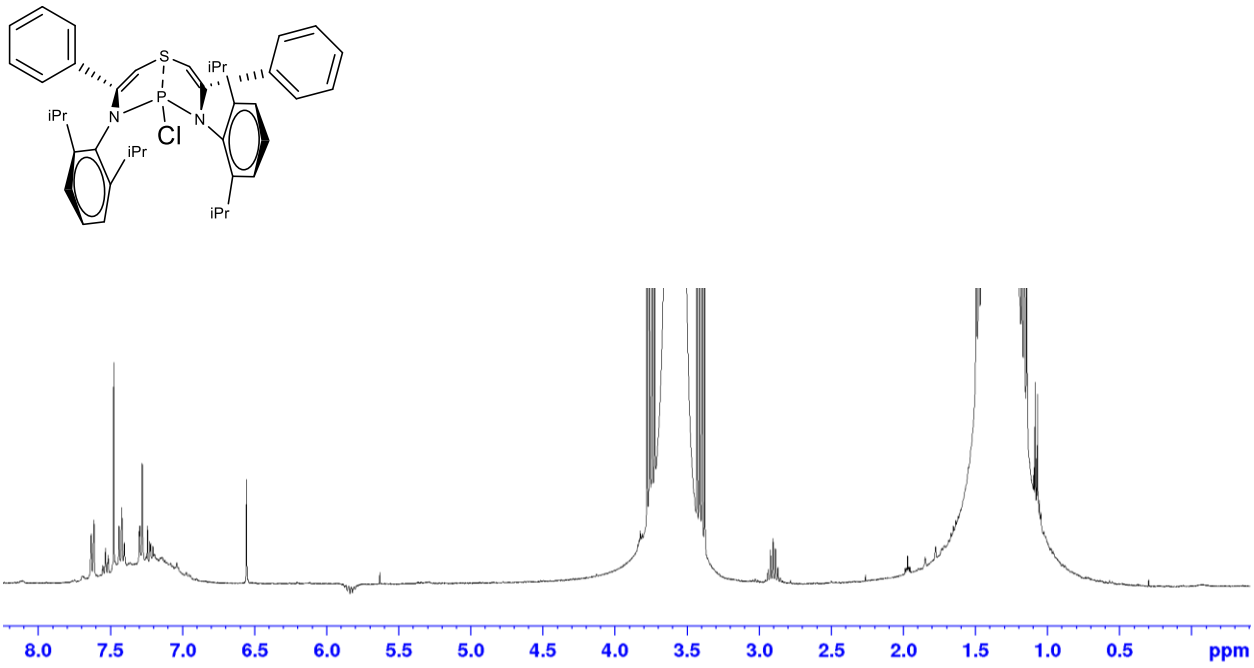

Figure 45. ^{1}H NMR of ClPNSN in Et_2O at 400MHz. Obvious splitting patterns for an expected symmetric species are present, yet there is broadness in the aromatic region which may indicate fluxionality.

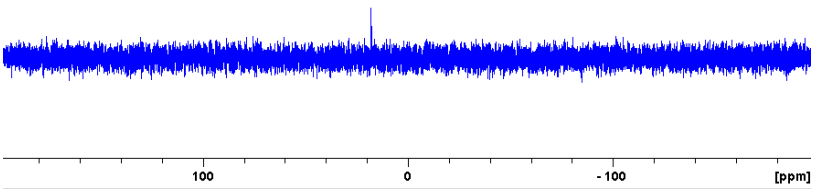

Figure 46. $^{31}P\{^{1}H\}$ NMR of ClPNSN at 400MHz in Et_2O after decanting from insoluble LiCl salt, generated from low temperature addition of MeLi to NSN, followed by low temperature addition of PCl_3.

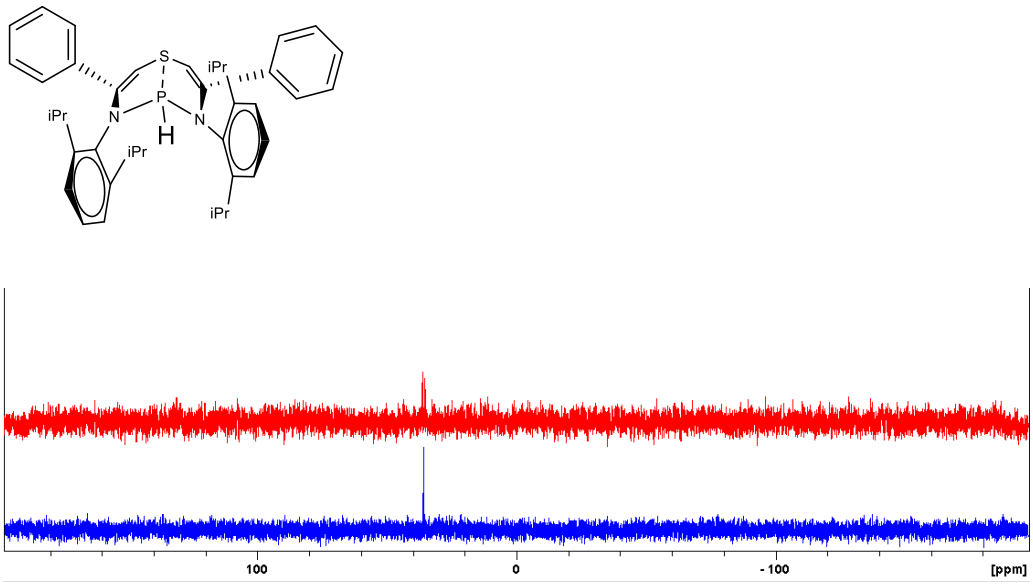

Figure 47. Top: ^{31}P NMR of HPNSN. Bottom: $^{31}P\{^{1}H\}$ NMR of HPNSN in Et_2O. ^{1}J P-H coupling constant measured to be 163.6Hz.

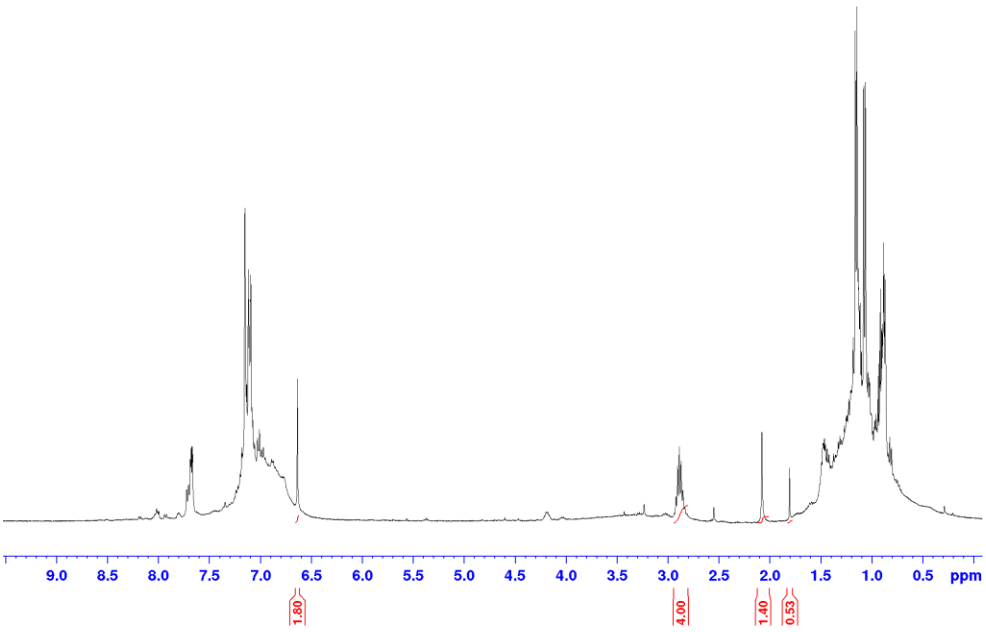

Figure 48. ^{1}H NMR of HPNSN re-dissolved in C_6D_6 at 400MHz. Multiplicity of aromatic signals are not as resolved as in ethereal solvent, but maintains symmetric iPr protons.

VI. References

[1] K. S. Egorova, V. P. Ananikov, *Organometallics* **2017**, *36*, 4071–4090.

[2] G. H. Spikes, J. C. Fettinger, P. P. Power, *J. Am. Chem. Soc.* **2005**, *127*, 12232–12233.

[3] P. P. Power, *Nature* **2010**, *463*, 171–177.

[4] P. P. Power, *Chem. Rec.* **2012**, *12*, 238–255.

[5] T. Chu, G. I. Nikonov, *Chem. Rev.* **2018**, *118*, 3608–3680.

[6] A. Freund, *Justus Liebigs Ann. Chem.* **1861**, *118*, 1–21.

[7] D. Pawlow, *Justus Liebigs Ann. Chem.* **1877**, *188*, 104–143.

[8] C. Mu-Chieh, A. J. McNeece, E. A. Hill, A. S. Filatov, J. S. Anderson, *Chem. – A Eur. J.* **2018**, *24*, 8001–8008.

[9] V. Lyaskovskyy, B. De Bruin, *ACS Catal.* **2012**, *2*, 270–279.

[10] J. R. Khusnutdinova, D. Milstein, *Angew. Chemie Int. Ed.* **2015**, *54*, 12236–12273.

[11] A. Brand, W. Uhl, *Chem. – A Eur. J.* **2019**, *25*, 1391–1404.

[12] Y. Segawa, M. Yamashita, K. Nozaki, *Science (80-.).* **2006**, *314*, 113 LP-115.

[13] A. Hinz, F. Breher, *Angew. Chemie Int. Ed.* **2018**, *57*, 8818–8820.

[14] T. Chu, L. Belding, A. van der Est, T. Dudding, I. Korobkov, G. I. Nikonov, *Angew. Chemie Int. Ed.* **2014**, *53*, 2711–2715.

[15] H. Grützmacher, *Angew. Chemie Int. Ed.* **2008**, *47*, 1814–1818.

[16] G. D. Frey, V. Lavallo, B. Donnadieu, W. W. Schoeller, G. Bertrand, *Science (80-.).*

2007, *316*, 439 LP-441.

[17] D. Martin, M. Soleilhavoup, G. Bertrand, *Chem. Sci.* **2011**, *2*, 389–399.

[18] C. Cui, H. W. Roesky, H.-G. Schmidt, M. Noltemeyer, H. Hao, F. Cimpoesu, *Angew. Chemie Int. Ed.* **2000**, *39*, 4274–4276.

[19] E. S. Schmidt, A. Jockisch, H. Schmidbaur, *J. Am. Chem. Soc.* **1999**, *121*, 9758–9759.

[20] M. Denk, R. Lennon, R. Hayashi, R. West, A. V. Belyakov, H. P. Verne, A. Haaland, M. Wagner, N. Metzler, *J. Am. Chem. Soc.* **1994**, *116*, 2691–2692.

[21] Y. Peng, J.-D. D. Guo, B. D. Ellis, Z. Zhu, J. C. Fettinger, S. Nagase, P. P. Power, *J. Am. Chem. Soc.* **2009**, *131*, 16272–16282.

[22] L. Horner, A. Christmann, *Angew. Chemie Int. Ed.* **1963**, *2*, 599–608.

[23] H. Aktaş, J. C. Slootweg, K. Lammertsma, *Angew. Chemie Int. Ed.* **2010**, *49*, 2102–2113.

[24] D. W. Stephan, G. Erker, *Angew. Chemie Int. Ed.* **2015**, *54*, 6400–6441.

[25] D. W. Stephan, *Dalt. Trans.* **2009**, 3129–3136.

[26] C. Jiang, O. Blacque, T. Fox, H. Berke, *Organometallics* **2011**, *30*, 2117–2124.

[27] G. C. Welch, R. R. San Juan, J. D. Masuda, D. W. Stephan, *Science* **2006**, *314*, 1124–6.

[28] D. J. Parks, J. M. Blackwell, W. E. Piers, *J. Org. Chem.* **2000**, *65*, 3090–3098.

[29] V. Fasano, M. J. Ingleson, *Chem. - A Eur. J.* **2017**, *23*, 2217–2224.

[30] T. Mahdi, D. W. Stephan, *J. Am. Chem. Soc.* **2014**, *136*, 15809–15812.

[31] T. Chu, I. Korobkov, G. I. Nikonov, *J. Am. Chem. Soc.* **2014**, *136*, 9195–9202.

[32] T. Chu, Y. Boyko, I. Korobkov, G. I. Nikonov, *Organometallics* **2015**, *34*, 5363–5365.

[33] M. R. Crimmin, M. J. Butler, A. J. P. White, *Chem. Commun.* **2015**, *51*, 15994–15996.

[34] *International Union of Pure and Applied Chemistry: Compendium of Chemical Terminology Gold Book*, **2014**.

[35] D. M. P. Mingos, *J. Organomet. Chem.* **2014**, *751*, 153–173.

[36] W. Kaim, B. Schwederski, *Coord. Chem. Rev.* **2010**, *254*, 1580–1588.

[37] Y. Wang, Y. Xie, P. Wei, R. B. King, H. F. Schaefer, P. v. R. Schleyer, G. H. Robinson, *J. Am. Chem. Soc.* **2008**, *130*, 14970–14971.

[38] C. Boone, I. Korobkov, G. I. Nikonov, *ACS Catal.* **2013**, *3*, 2336–2340.

[39] L. Bourget-Merle, M. F. Lappert, J. R. Severn, *Chem. Rev.* **2002**, *102*, 3031–3066.

[40] F. Bonnet, M. Visseaux, D. Barbier-Baudry, E. Vigier, M. M. Kubicki, *Chem. – A Eur. J.* **2004**, *10*, 2428–2434.

[41] S. Yao, Y. Xiong, X. Zhang, M. Schlangen, H. Schwarz, C. Milsmann, M. Driess, *Angew. Chemie Int. Ed.* **2009**, *48*, 4551–4554.

[42] D. J. Mindiola, *Angew. Chemie Int. Ed.* **2009**, *48*, 6198–6200.

[43] S. Pfirrmann, C. Limberg, C. Herwig, R. Stößer, B. Ziemer, *Angew. Chemie Int. Ed.* **2009**, *48*, 3357–3361.

[44] M. M. Khusniyarov, E. Bill, T. Weyhermüller, E. Bothe, K. Wieghardt, *Angew. Chemie* **2011**, *123*, 1690–1693.

[45] P. Ghosh, R. Naastepad, C. F. Riemersma, M. Lutz, M. E. Moret, R. J. M. Klein Gebbink,

Chem. - A Eur. J. **2017**, *23*, 10732–10737.

[46] S. K. Russell, E. Lobkovsky, P. J. Chirik, *J. Am. Chem. Soc.* **2011**, *133*, 8858–8861.

[47] S. C. Bart, K. Chłopek, E. Bill, M. W. Bouwkamp, E. Lobkovsky, F. Neese, K. Wieghardt, P. J. Chirik, *J. Am. Chem. Soc.* **2006**, *128*, 13901–13912.

[48] T. Chu, L. Belding, P. K. Poddutoori, A. van der Est, T. Dudding, I. Korobkov, G. I. Nikonov, *Dalt. Trans.* **2016**, *45*, 13440–13448.

[49] D. Zhu, I. Thapa, I. Korobkov, S. Gambarotta, P. H. M. Budzelaar, *Inorg. Chem.* **2011**, *50*, 9879–9887.

[50] B. Butschke, K. L. Fillman, T. Bendikov, L. J. W. W. Shimon, Y. Diskin-Posner, G. Leitus, S. I. Gorelsky, M. L. Neidig, D. Milstein, *Inorg. Chem.* **2015**, *54*, 4909–4926.

[51] Y. Li, K. Junge, M. Beller, *Zinc Catal.* **2015**.

[52] G. Parkin, *Chem. Rev.* **2004**, *104*, 699–767.

[53] T. Li, J. Wiecko, P. W. Roesky, *Zinc Catal.* **2015**.

[54] S. Marks, T. K. Panda, P. W. Roesky, *Dalt. Trans.* **2010**, *39*, 7230–7235.

[55] R. G. Cavell, R. P. Kamalesh Babu, K. Aparna, *J. Organomet. Chem.* **2001**, *617–618*, 158–169.

[56] P. Jochmann, D. W. Stephan, *Angew. Chemie - Int. Ed.* **2013**, *52*, 9831–9835.

[57] J. B. Gilroy, M. J. Ferguson, R. McDonald, B. O. Patrick, R. G. Hicks, *Chem. Commun.* **2007**, 126–128.

[58] R. Mondol, E. Otten, *Inorg. Chem.* **2018**, *57*, 9720–9727.

[59] M.-C. Chang, E. Otten, *Chem. Commun.* **2014**, *50*, 7431–7433.

[60] M. Asay, C. Jones, M. Driess, T. Universita, *Chem. Rev.* **2011**, *111*, 354–396.

[61] A. Caise, D. Jones, E. L. Kolychev, J. Hicks, J. M. Goicoechea, S. Aldridge, *Chem. – A Eur. J.* **2018**, *0*, 1–13.

[62] A. Tarasewicz, D. Ensan, R. A. Batey, *Chem. – A Eur. J.* **2018**, *24*, 6071–6074.

[63] W. W. Schoeller, G. D. Frey, *J. Organomet. Chem.* **2013**, *744*, 172–177.

[64] A. Seifert, D. Scheid, G. Linti, T. Zessin, *Chem. - A Eur. J.* **2009**, *15*, 12114–12120.

[65] J. A. B. Abdalla, I. M. Riddlestone, R. Tirfoin, S. Aldridge, *Angew. Chemie Int. Ed.* **2015**, *54*, 5098–5102.

[66] P. H. Liu, F. J. Chuang, C. Y. Tu, C. H. Hu, T. W. Lin, Y. T. Wang, C. H. Lin, A. Datta, J. H. Huang, *Dalt. Trans.* **2013**, *42*, 13754–13764.

[67] Y.-L. Lien, Y.-C. Change, N.-T. Chuang, A. Datta, S.-J. Chen, C.-H. Hu, W.-Y. Huang, C.-H. Lin, J.-H. Huang, *Inorg. Chem.* **2010**, *49*, 136–143.

[68] J. Hicks, P. Vasko, J. M. Goicoechea, S. Aldridge, *Nature* **2018**, *557*, 92–95.

[69] H. Lind, J. Deutschman Archie, *J. Org. Chem.* **1967**, *32*, 326–329.

[70] A. Igau, H. Grutzmacher, A. Baceiredo, G. Bertrand, *J. Am. Chem. Soc.* **1988**, *110*, 6463–6466.

[71] A. J. Arduengo, R. L. Harlow, M. Kline, *J. Am. Chem. Soc.* **1991**, *113*, 361–363.

[72] R. Hoffmann, G. D. Zeiss, G. W. Van Dine, *J. Am. Chem. Soc.* **1968**, *90*, 1485–1499.

[73] H. V. Huynh, *Organomet. Chem. N-heterocyclic Carbenes* **2017**.

[74] D. A. Dixon, A. J. Arduengo, K. D. Dobbs, D. V Khasnis, *Tetrahedron Lett.* **1995**, *36*, 645–648.

[75] D. Schmidt, J. H. J. Berthel, S. Pietsch, U. Radius, *Angew. Chemie Int. Ed.* **2012**, *51*, 8881–8885.

[76] G. D. Frey, J. D. Masuda, B. Donnadieu, G. Bertrand, *Angew. Chemie Int. Ed.* **2010**, *49*, 9444–9447.

[77] D. M. Flanigan, F. Romanov-Michailidis, N. A. White, T. Rovis, *Chem. Rev.* **2015**, *115*, 9307–9387.

[78] T. Krachko, J. C. Slootweg, *Eur. J. Inorg. Chem.* **2018**, *2018*, 2734–2754.

[79] S. Roy, K. C. Mondal, S. Kundu, B. Li, C. J. Schürmann, S. Dutta, D. Koley, R. Herbst-Irmer, D. Stalke, H. W. Roesky, *Chem. - A Eur. J.* **2017**, *23*, 12153–12157.

[80] M.-D. Su, S.-Y. Chu, *Inorg. Chem.* **1999**, *38*, 4819–4823.

[81] J. D. Erickson, R. D. Riparetti, J. C. Fettinger, P. P. Power, *Organometallics* **2016**, *35*, 2124–2128.

[82] J. Pfeiffer, W. Maringgele, M. Noltemeyer, A. Meller, *Chem. Ber.* **1989**, *122*, 245–252.

[83] S. Nagendran, H. W. Roesky, *Organometallics* **2008**, *27*, 457–492.

[84] A. Akkari, J. J. Byrne, I. Saur, G. Rima, H. Gornitzka, J. Barrau, *J. Organomet. Chem.* **2001**, *622*, 190–198.

[85] A. Jana, I. Objartel, H. W. Roesky, D. Stalke, *Inorg. Chem.* **2009**, *48*, 798–800.

[86] M. Driess, S. Yao, M. Brym, C. van Wüllen, *Angew. Chemie Int. Ed.* **2006**, *45*, 4349–4352.

[87] S. L. Choong, W. D. Woodul, C. Schenk, A. Stasch, A. F. Richards, C. Jones, *Organometallics* **2011**, *30*, 5543–5550.

[88] A. Burchert, R. Müller, S. Yao, C. Schattenberg, Y. Xiong, M. Kaupp, M. Driess, *Angew. Chemie Int. Ed.* **2017**, *56*, 6298–6301.

[89] Y. Zhou, M. Karni, S. Yao, Y. Apeloig, M. Driess, *Angew. Chemie Int. Ed.* **2016**, *55*, 15096–15099.

[90] S. Yao, Y. Xiong, M. Driess, *Acc. Chem. Res.* **2017**, *50*, 2026–2037.

[91] S. A. Culley, A. J. Arduengo, *J. Am. Chem. Soc.* **1984**, *106*, 1164–1165.

[92] A. J. Arduengo, C. A. Stewart, *Chem. Rev.* **1994**, *94*, 1215–1237.

[93] D. Houalla, F. H. Osman, M. Sanchez, R. Wolf, *Tetrahedron Lett.* **1977**, *18*, 3041–3044.

[94] C. Bonningue, D. Houalla, M. Sanchez, R. Wolf, F. H. Osman, *J. Chem. Soc. Perkin Trans. 2* **1981**, 19–25.

[95] C. Bonningue, D. Houalla, R. Wolf, J. Jaud, *J. Chem. Soc. Perkin Trans. 2* **1983**, 773–776.

[96] N. L. Dunn, M. Ha, A. T. Radosevich, *J. Am. Chem. Soc.* **2012**, *134*, 11330–11333.

[97] S. M. McCarthy, Y. C. Lin, D. Devarajan, J. W. Chang, H. P. Yennawar, R. M. Rioux, D. H. Ess, A. T. Radosevich, *J. Am. Chem. Soc.* **2014**, *136*, 4640–4650.

[98] A. J. Arduengo III, J. Breker, F. Davidson, M. Kline, *Heteroat. Chem.* **1993**, *4*, 213–221.

[99] A. J. Arduengo, C. A. Stewart, F. Davidson, D. A. Dixon, J. Y. Becker, M. B. Mizen, *J. Am. Chem. Soc.* **1987**, *109*, 627–647.

[100] M. Driess, N. Muresan, K. Merz, M. Päch, *Angew. Chemie - Int. Ed.* **2005**, *44*, 6734–6737.

[101] A. J. Arduengo, H. V. R. Dias, J. C. Calabrese, *J. Am. Chem. Soc.* **1991**, *113*, 7071–7072.

[102] A. J. Arduengo, M. Lattman, H. V. R. Dias, J. C. Calabrese, M. Kline, *J. Am. Chem. Soc.* **1991**, *113*, 1799–1805.

[103] C. A. Stewart, J. C. Calabrese, A. J. Arduengo, *J. Am. Chem. Soc.* **1985**, *107*, 3397–3398.

[104] A. J. Arduengo, S. A. Culley, *J. Am. Chem. Soc.* **1985**, *107*, 1089–1090.

[105] W. Zhao, S. M. McCarthy, T. Y. Lai, H. P. Yennawar, A. T. Radosevich, *J. Am. Chem. Soc.* **2014**, *136*, 17634–17644.

[106] J. Cui, Y. Li, R. Ganguly, A. Inthirarajah, H. Hirao, R. Kinjo, *J. Am. Chem. Soc.* **2014**, *136*, 16764–16767.

[107] J. Cui, Y. Li, R. Ganguly, R. Kinjo, *Chem. - A Eur. J.* **2016**, *22*, 9976–9985.

[108] J. L. Wong, R. H. Sánchez, J. G. Logan, R. A. Zarkesh, J. W. Ziller, A. F. Heyduk, *Chem. Sci.* **2013**, *4*, 1906.

[109] T. P. Robinson, D. M. De Rosa, S. Aldridge, J. M. Goicoechea, *Angew. Chemie Int. Ed.* **2015**, *54*, 13758–13763.

[110] A. Hentschel, A. Brand, P. Wegener, W. Uhl, *Angew. Chemie Int. Ed.* **2018**, *57*, 832–835.

[111] A. D. Dilman, V. V Levin, *Tetrahedron Lett.* **2016**, *57*, 3986–3992.

[112] K. Keerthi Krishnan, S. M. Ujwaldev, S. Saranya, G. Anilkumar, M. Beller, *Adv. Synth. Catal.* **2019**, *361*, 382–404.

[113] X.-F. Wu, H. Neumann, *Adv. Synth. Catal.* **2012**, *354*, 3141–3160.

[114] W. Xuan, H. Keiichi, K. Daisuke, K. Hisano, T. Naoyuki, T. Ryo, U. Masanobu, *Chem. – A Eur. J.* **2015**, *21*, 10993–10996.

[115] K. Okura, H. Kawashima, F. Tamakuni, N. Nishida, E. Shirakawa, *Chem. Commun.* **2016**, *52*, 14019–14022.

[116] K. Okura, E. Shirakawa, *European J. Org. Chem.* **2016**, *2016*, 3043–3046.

[117] A. P. Thankachan, K. S. Sindhu, K. K. Krishnan, G. Anilkumar, *Tetrahedron Lett.* **2015**, *56*, 5525–5528.

[118] K. K. Krishnan, S. M. Ujwaldev, A. P. Thankachan, N. A. Harry, A. Gopinathan, *Mol. Catal.* **2017**, *440*, 140–147.

[119] A. P. Thankachan, K. S. Sindhu, S. M. Ujwaldev, G. Anilkumar, *Tetrahedron Lett.* **2017**, *58*, 536–540.

[120] K. K. Krishnan, N. A. Harry, S. M. Ujwaldev, G. Anilkumar, *ChemistrySelect* **2018**, *3*, 3984–3988.

[121] S. Roy, K. C. Mondal, H. W. Roesky, *Acc. Chem. Res.* **2016**, *49*, 357–369.

[122] H. Dumont, A. Marbeuf, J.-E. Bourée, O. Gorochov, *J. Mater. Chem.* **1993**, *3*, 1075–1079.

[123] Y. Tohi, S. Matsui, T. Fujita, *Catalyst for Olefin Polymerization and Method of Polymerizing Olefin*, **2001**.

[124] M. Driess, N. Muresan, K. Merz, *Angew. Chemie Int. Ed.* **2005**, *44*, 6738–6741.

[125] P. Natarajan, Manjeet, N. Kumar, S. Devi, K. Mer, *Tetrahedron Lett.* **2017**, *58*, 658–662.

[126] J. Nakayama, R. Hasemi, K. Yoshimura, Y. Sugihara, S. Yamaoka, N. Nakamura, *J. Org. Chem.* **1998**, *63*, 4912–4924.

[127] Y. Miyahara, *J. Heterocycl. Chem.* **1979**, *16*, 1147–1151.

[128] N. A. Marinos, S. Enthaler, M. Driess, *ChemCatChem* **2010**, *2*, 846–853.

[129] T. Schlöder, M. Kaupp, S. Riedel, *J. Am. Chem. Soc.* **2012**, *134*, 11977–11979.

[130] C. Eller, G. Kehr, C. G. Daniliuc, D. W. Stephan, G. Erker, *Chem. Commun.* **2015**, *51*, 7226–7229.

[131] P. Arthur, W. M. Haynes, L. P. Varga, *Anal. Chem.* **1966**, *38*, 1630–1631.

[132] S. R. Oakley, G. Nawn, K. M. Waldie, T. D. MacInnis, B. O. Patrick, R. G. Hicks, *Chem. Commun.* **2010**, *46*, 6753–6755.

[133] A. B. Charette, M. Grenon, *Can. J. Chem.* **2001**, *79*, 1694–1703.

[134] W. S. Bechara, G. Pelletier, A. B. Charette, *Nat. Chem.* **2012**, *4*, 228–234.

[135] A. F. Burchat, J. M. Chong, N. Nielsen, *J. Organomet. Chem.* **1997**, *542*, 281–283.

[136] M. A. W. Lawrence, K. A. Green, P. N. Nelson, S. C. Lorraine, *Polyhedron* **2018**, *143*, 11–27.

[137] H. Z. Kaplan, B. Li, J. A. Byers, *Organometallics* **2012**, *31*, 7343–7350.

[138] A. G. Steinig, D. M. Spero, *Org. Prep. Proced. Int.* **2000**, *32*, 205–234.

[139] J. Paul, M. Presset, E. Le Gall, E. Léonel, P. Retailleau, *Synthesis (Stuttg).* **2018**, *50*, 254–266.

[140] T. L. Andersen, A. S. Donslund, K. T. Neumann, T. Skrydstrup, *Angew. Chemie Int. Ed.* **2017**, *57*, 800–804.

[141] A. V Lado, A. V Piskunov, I. V Zhdanovich, G. K. Fukin, E. V Baranov, *Russ. J. Coord. Chem.* **2008**, *34*, 251–255.

[142] D. Gudat, *Encycl. Inorg. Bioinorg. Chem.* **2018**.

[143] C. C. Chong, H. Hirao, R. Kinjo, *Angew. Chemie Int. Ed.* **2014**, *53*, 3342–3346.

[144] B. Rao, C. C. Chong, R. Kinjo, *J. Am. Chem. Soc.* **2018**, *140*, 652–656.

[145] T. Hynes, E. N. Welsh, R. McDonald, M. J. Ferguson, A. W. H. Speed, *Organometallics* **2018**, *37*, 841–844.

[146] G. R. Fulmer, A. J. M. Miller, N. H. Sherden, H. E. Gottlieb, A. Nudelman, B. M. Stoltz, J. E. Bercaw, K. I. Goldberg, *Organometallics* **2010**, *29*, 2176–2179.